Design, synthesis and *in vitro* evaluation of novel SARS-CoV-2 3CL^{pro} covalent inhibitors

Julia K. Stille [a, 1], Jevgenijs Tjutrins [a, 1], Guanyu Wang [a, 1], Felipe A. Venegas [a, 1],
Christopher Hennecker [a], Andrés M. Rueda [a], Itai Sharon [b], Nicole Blaine [a],
Caitlin E. Miron [a], Sharon Pinus [a], Anne Labarre [a], Jessica Plescia [a], Mihai Burai Patrascu [a],
Xiaocong Zhang [a], Alexander S. Wahba [a], Danielle Vlaho [a], Mitchell J. Huot [a],
T. Martin Schmeing [b], Anthony K. Mittermaier [a, *], Nicolas Moitessier [a, *]

[a] Department of Chemistry, McGill University, 801 Sherbrooke St W, Montreal, QC, Canada, H3A 0B8
[b] Department of Biochemistry, McGill University, 3649 Promenade Sir William Osler Montreal, QC, Canada, H3G 0B1

ARTICLE INFO

ABSTRACT

Severe diseases such as the ongoing COVID-19 pandemic, as well as the previous SARS and MERS outbreaks, are the result of coronavirus infections and have demonstrated the urgent need for antiviral drugs to combat these deadly viruses. Due to its essential role in viral replication and function, 3CL^{pro} (main coronaviruses cysteine-protease) has been identified as a promising target for the development of antiviral drugs. Previously reported SARS-CoV 3CL^{pro} non-covalent inhibitors were used as a starting point for the development of covalent inhibitors of SARS-CoV-2 3CL^{pro}. We report herein our efforts in the design and synthesis of submicromolar covalent inhibitors when the enzymatic activity of the viral protease was used as a screening platform.

1. Introduction

Coronaviruses. Coronaviruses (CoV) are a large family of viruses associated with some forms of common colds (together with rhinoviruses, respiratory syncytial virus, adenoviruses and others), as well as far more serious diseases including Severe Acute Respiratory Syndrome (SARS, caused by SARS-CoV infection), which made headlines worldwide in 2002–2003 with over 700 deaths including 43 in Canada [1], and the Middle East Respiratory Syndrome (MERS, caused by MERS-CoV infection), which was reported in Saudi Arabia in 2012 and killed over 900 [2]. The current outbreak of novel coronavirus (COVID-19, caused by SARS-CoV-2 infection), its numerous variants, and the discovery of animal reservoirs provide significant motivation for the development of potent therapeutics against these viruses to prevent future outbreaks [3,4].

SARS, MERS, and COVID-19 are respiratory illnesses characterized by fever, cough, and shortness of breath, posing significant danger to patients. The case fatality rates for those infected with SARS-CoV and MERS-CoV were estimated at about 10% and 35%, respectively [1,2]. Estimates for SARS-CoV-2 are ranging anywhere from of 0.1–25% depending on the age group, the country and the stage of the pandemic, although this number could change substantially as more accurate information on the numbers of infections and deaths becomes available [5,6]. In contrast to SARS and MERS, COVID-19 has rapidly spread worldwide despite the severe restrictions imposed in many countries, and the official number of deaths now exceeds 5.0 million [7] (which is a well underestimated number as shown by excess mortality studies [8]).

Vaccines and therapeutics. While vaccines are a central pillar of our efforts to end our current deadly phase of the COVID-19 pandemic, therapeutics offer a complementary approach with many distinct advantages. For example, oral therapeutics tend to be easy to store and administer and need only be given to the small minority of patients suffering more serious symptoms. In contrast, a large proportion of the population must be inoculated for vaccines to be effective and mRNA-based vaccines require complex

---

* Corresponding authors.
E-mail addresses: anthony.mittermaier@mcgill.ca (A.K. Mittermaier), nicolas. moitessier@mcgill.ca (N. Moitessier).
[1] These authors contributed equally to this work.

logistics to maintain the cold chain, leading to enormous challenges in production, supply and administration. In addition, large vaccine campaigns require public compliance and amplifies the number of people suffering from adverse reactions to medication. To add to these difficulties, Pfizer recently announced that the immunity of their vaccine drops after about 6 months suggesting that regular injections would be needed, further amplifying the public compliance issue and burden to public health systems [9,10]. Importantly, vaccines primarily induce an immune response against the spike protein [11], while future variants of concern may have mutations in this protein that could allow them to evade immunity. In contrast, antiviral therapeutics can target a wide range of proteins including viral proteases (3CL^{pro}, PL^{pro}), the RNA-dependent RNA polymerase (RdRp) and RNA helicase. Therefore, they can be equally effective against strains of the virus with mutations that escape spike-based vaccination or herd immunity. Overall, it is clear that effective therapeutics would be complementary to mass vaccination. Finally, some groups (pregnant and breastfeeding women, people with allergies, young children, immunocompromised patients or people with other conditions) may be at risk or not responsive to vaccines and alternative treatments (e.g., oral therapeutics) must be available [12]. Consequently, major efforts from a large number of research groups focused on the development of small molecules as antivirals against SARS-CoV-2 which culminated in the recent approval of Molnupiravir in the United Kingdom [13].

Coronavirus (CoV) and 3-Chymotrypsin-like Protease Inhibition. Coronaviruses express 3-chymotrypsin-like cysteine proteases (3CL^{pro}), also referred to as the main proteases (Mpro) or nsp5 (non-structural protein 5), which feature a Cys-His catalytic dyad (Cys^{145}, His^{41}) and are required for viral replication and infection. 3CL^{pro} enzymes were identified early on as attractive targets for antiviral development, resulting in several inhibitors and structures of SARS-3CL^{pro}-inhibitor complexes (eg, PDB codes: 4TWY, 2ZU5, 2ALV [14]). The 3CL^{pro} enzymes from SARS-CoV and SARS-CoV-2 share nearly 80% sequence identity [15,16], suggesting that many of the lessons learned for developing SARS therapeutics can be applied to COVID-19. As a note, 3CL^{pro} is not limited to coronaviruses but is also a drug target for the development of antivirals against noroviruses (such as the one involved in gastroenteritis [17]) or antivirals against enteroviruses (e.g., antiviral drug 3CLpro-1 [18] targeting the hand, foot, and mouth disease enterovirus 71 and **Rupintrivir** — Fig. 1- originally developed to fight rhinoviruses [19]).

Covalent Inhibitors. The quest for novel antivirals against SARS-CoV and, more recently, SARS-CoV-2 has been intense, and several viral enzyme inhibitors and crystal structures of enzyme-inhibitor complexes have quickly been reported (e.g., PDB codes: 6LU7 [20], 6M2N [21], 6XQU [22], 6WQF [23]) [24–26]. The presence of a catalytic cysteine residue in the active site makes 3CL^{pro} amenable to covalent inhibition, a strategy that was successfully employed following the SARS-CoV pandemic (SARS). In fact, many of the reported SARS-CoV inhibitors feature an electrophilic group, such as an α-ketoamide, epoxide, aziridine, α,β-unsaturated ester (Michael acceptor), or α-fluoroketone, which forms a covalent bond with the catalytic cysteine residue (Cys^{145}), as confirmed by X-ray crystallography (e.g., PDB code: 5N19) [24]. A crystal structure of the SARS-CoV-2 3CL^{pro} with a covalent peptidic inhibitor bound to Cys^{145} was quickly elucidated (PDB code: 6LU7). This pseudo-peptidic inhibitor, an analogue of **Rupintrivir** (tested on SARS [28] and COVID-19 [29]), has been the starting point for a number of drug discovery campaigns [30–34]. 3CL^{pro} inhibitor (**PF-0730814**

and **PF-07321332** — Paxlovid -, Fig. 1) entered clinical trials [32,35,36] and some encouraging phase 2/3 results were reported [37]. Investigations from a group of Canadian researchers identified other warheads for this lead molecule with potential for further development [38,39]. The identification of a potent warhead was also the focus of Hilgenfeld and co-workers [40].

The structurally similar GC376 was originally identified as active against a feline coronavirus [41] and more recently confirmed as a SARS-CoV-2 3CL^{pro} inhibitor [26], and structure-activity relationship studies led to improved analogues [42]. Smaller, more drug-like inhibitors such as the isatin derivative **2** have been devised [43,44]. More recently, Jorgensen and co-workers converted Perampanel, a known antiepileptic drug that is also a weak 3CL^{pro} inhibitor, into potent inhibitors (**3**, Fig. 1) using a combination of computational and experimental investigation [45].

As described in our recent review [48], covalent drugs can be extremely effective and useful pharmaceuticals, yet they have been largely ignored in most drug design endeavours and particularly in those concerning structure-based drug design. Concerns about their potential off-target reactivity and toxicity have often been raised [49]. Despite these concerns, there are many examples of covalent drugs on the market, including two of the ten most widely prescribed medications in the U.S., as well as several other common drugs like aspirin and penicillin [48]. The advantages of covalent drugs are becoming increasingly recognized: they have extremely high potencies, long residence times, and high levels of specificity [50]. Although skepticism persists, many pharmaceutical companies are embracing covalent drugs as exemplified by **Neratinib** (Nerlynx®, Pfizer) and **Afatinib** (Gilotrif®, Boehringer-Ingelheim).

3CL^{pro} inhibitor design. Many of the structure-based studies related to COVID-19 to date have employed virtual screening and machine learning techniques. Several _**potential**_ 3CL^{pro} inhibitors have been identified, however experimental verification has lagged [51–53]. As of today, much of the research has focused on peptidic substrate-like inhibitors (Fig. 1). There is currently a need for the development of drug-like inhibitors with synthetically accessible scaffolds that will allow for more thorough investigations of structure-activity relationships. We thought to benefit from our team's expertise in covalent inhibition and from our software that enables automated docking and virtual screening of covalent inhibitors, which is not possible with most commercial packages. We present herein our efforts towards the development of novel potent covalent inhibitors of 3CL^{pro}.

2. Chemistry

Inhibitor design through covalent docking. In the past years, we have successfully applied covalent docking to the design and discovery of prolyl oligopeptidase inhibitors [54,55] and thought to apply a similar strategy to develop SARS-CoV-2 3CL^{pro} inhibitors. An investigation of the crystal structure of a non-covalent inhibitor (**X77**, Fig. 2) bound to 3CL^{pro} of SARS-CoV-2 (PDB code: 6W63) suggested that it might be possible to modify this inhibitor by incorporating a covalent warhead in proximity to the catalytic cysteine residue. As shown in Fig. 2, the sulphur atom of Cys^{145} is positioned at 3.2 Å from the imidazole moiety and at the same location as the covalent warhead of **PF-00835231**. Thus, replacement of the imidazole with a covalent warhead appeared to be a promising strategy to improve the inhibitory potency of this non-covalent inhibitor. Additionally, this scaffold could be prepared via a 4-component Ugi reaction [56], enabling a combinatorial approach that would provide an efficient synthetic method for
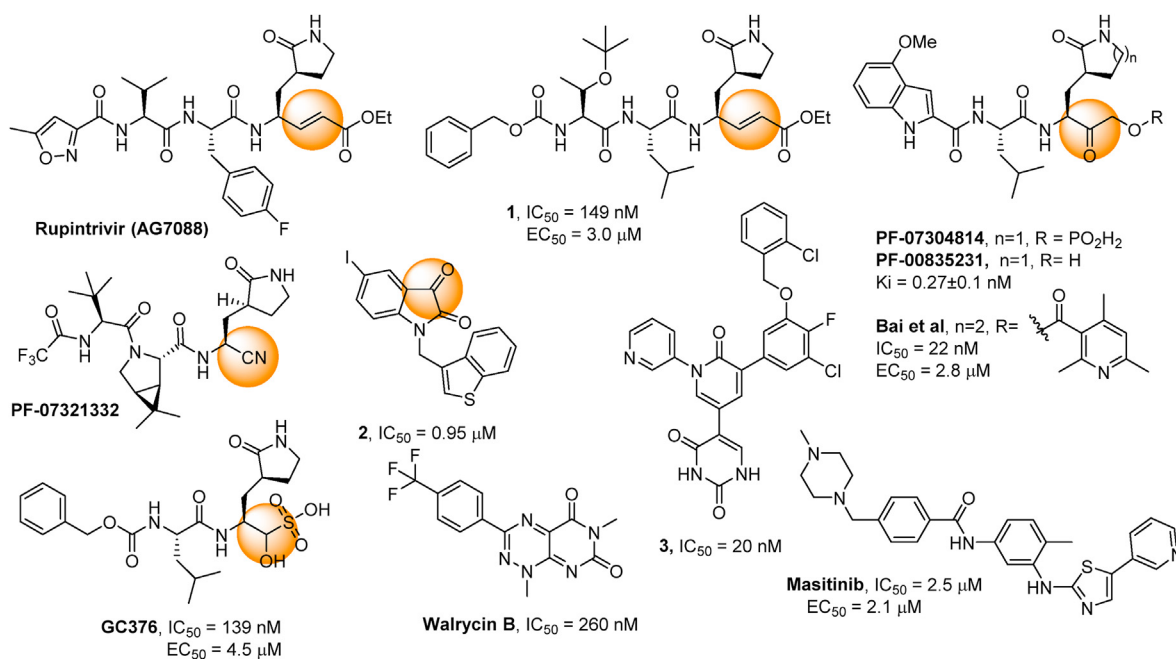
Fig. 1. Reported covalent SARS-CoV-2 3CL^{pro} inhibitors **1, GC376** [26], **PF-07321332, PF-0730814** [32,35,36] and an analogue [38], and reported non-covalent inhibitors **Masitinib** [46] and **Walcyrin B** [47]. Reported inhibitors of SARS-CoV 3CL^{pro} **2** [43] and **3** [45]. Orange spheres indicate the warheads for covalent binding.
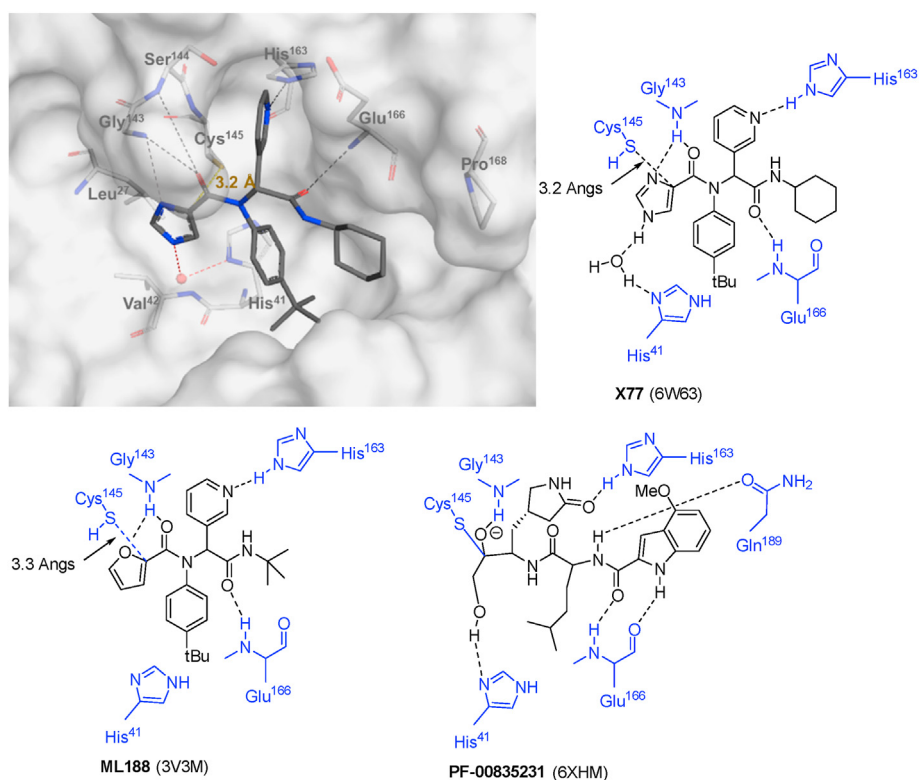
Fig. 2. Binding site interactions of inhibitors **X77**, **ML188** and **PF-00835213** (PDB codes: 6W63 [58], 3V3M [56], 6XHM [33]).

preparing diverse analogues. This would provide a significant advantage in exploring structure-activity relationships when compared to previously reported inhibitors, as a wide range of covalent warheads could be readily incorporated into the same inhibitor scaffold. As a note, a consortium of research groups including a group at the Weizmann Institute of Science in Rehovot

(Israel) took a very similar strategy although focusing primarily on non-covalent inhibitors [57].

To validate the design strategy, a virtual library of modified inhibitors was prepared based on incorporation of covalent warheads that could be accessed via a traditional or modified Ugi 4 component coupling (4CC) reaction (Fig. 3). These compounds were
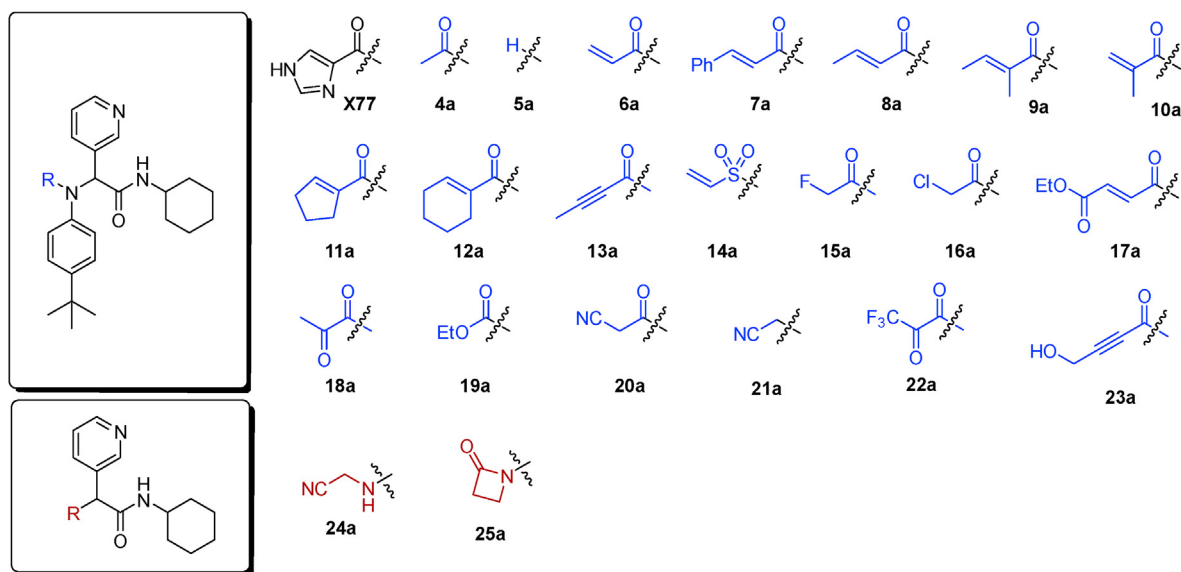
Fig. 3. Selected covalent 3CL^{pro} inhibitors for synthesis. Compound **X77** is the original non-covalent lead compound.
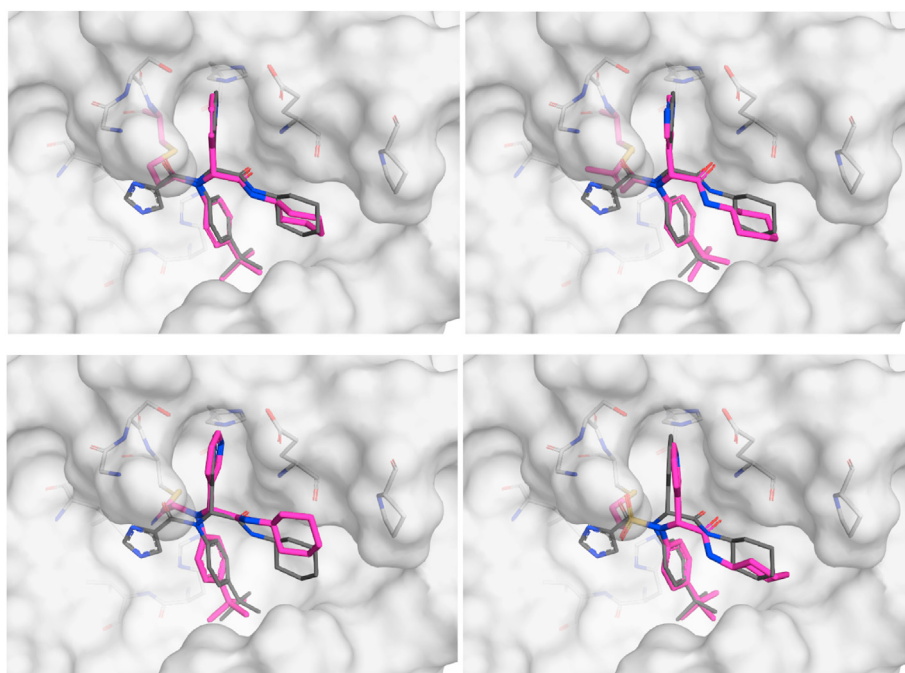

Fig. 4. Selected docked binding modes of design covalent inhibitors (pink) overlaid with the non-covalent inhibitor (co-crystallized) **X77** (grey). Top left: **6a**, top right: **13a**, bottom left: **16a** and bottom right: **14a**.

docked to 3CL^{pro} (PDB code: 6W63) using our docking program, FITTED [59]. The docked poses (Fig. 4) suggested that many of these modified inhibitors would be able to maintain the same non-covalent interactions as the original non-covalent inhibitor while also positioning the warhead close enough to Cys^{145} to facilitate the formation of a covalent bond. Based on the promising docking results with multiple warheads, a small library of analogues was synthesized for experimental testing.

Synthesis. Following a protocol reported by Jacobs et al. [56], a 4-component Ugi reaction was used to prepare analogues bearing four different classes of covalent warheads (alkene Michael acceptor, α-halo ketone, alkyne Michael acceptor, and α-ketoamide,

Scheme 1a). This synthetic strategy was later employed to probe some of the features of this class of inhibitors by modifying the R^2, R^3 and R^4 groups.

A 3-component Ugi reaction was used to prepare additional analogues bearing nitrile [60] and β-lactam [61] covalent warheads following reported procedures (Scheme 1b, c and d).

In order to complete the synthesis of the analogues featuring warheads not accessible through the 4-component Ugi, an intermediate was prepared and used to incorporate vinylsulfonamide and ethyl carbamate warheads (Scheme 2). This intermediate was also used to probe the importance of having a group at this position.

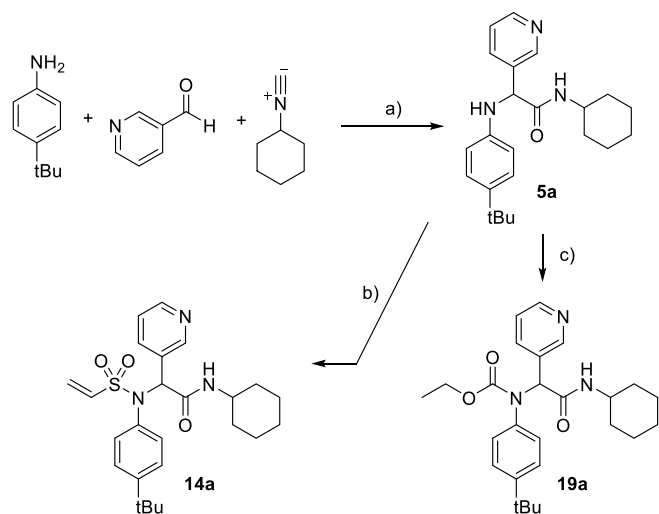In order to further probe the R^4 group of the potential inhibitors,
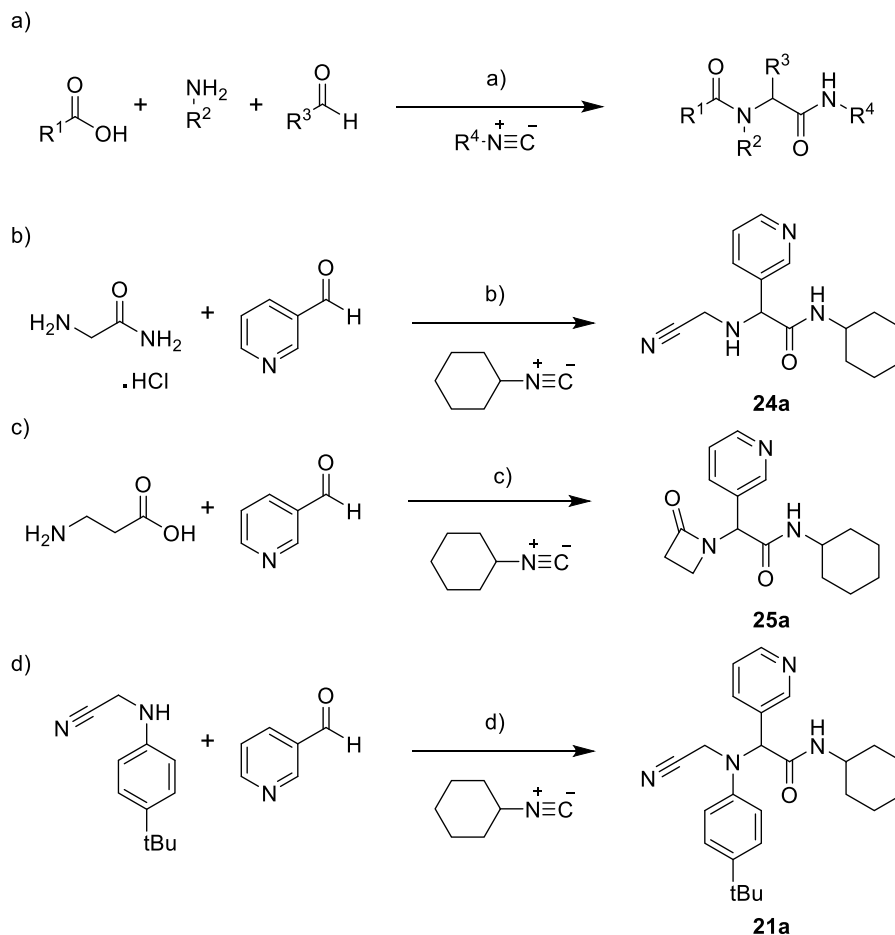
Scheme 1. a) carboxylic acid (1.0 mmol, 1.0 eq.), 4-*tert*-butylaniline (1.0 mmol, 1.0 eq.), 3-pyridinecarboxaldehyde (1.0 mmol, 1.0 eq.), cyclohexyl isocyanide (0.9 mmol, 0.9 eq.), MeOH (5 mL, 0.2 M), r.t., overnight, **X77** (30%), **ML188** (84%), **4a** (76%), **6a** (32%), **7a** (94%), **8a** (32%), **9a** (73%), **10a** (68%), **11a** (80%), **12a** (37%), **13a** (92%), **15a** (70%), **16a** (93%), **17a** (52%), **18a** (36%), **20a** (84%), **21a** (68%), **22a** (29%), **23a** (43%), **8b** (54%), **13b** (82%), **6b** (42%), **4b** (84%), **13c** (94%), **13d** (86%), **16b** (88%), **16c** (91%), **11b** (67%), **11c** (79%), **11d** (59%), **11e** (26%), **11f** (71%), **11g** (29%), **11h** (78%), **11i** (37%), **8c** (74%), **16d** (87%), **16f** (34%), **13e** (90%), **13f** (69%), **13g** (91%), **13h** (92%), **13i** (22%), **13j** (47%), **18b** (37%), **13k** (83%), **13l** (57%), **13m** (82%), **13n** (89%), **13o** (88%), **13p** (89%), **13q** (35%). b) 3-pyridinecarboxaldehyde (2.0 mmol, 2.0 eq.), glycinamide hydrochloride (2.0 mmol, 2.0 eq.), triethylamine (2.0 mmol, 2.0 eq.), acetic acid (2.0 mmol, 2.0 eq.), cyclohexyl isocyanide (2.0 mmol, 2.0 eq.), MeOH (5 mL, 0.2 M), r.t., overnight, **24a** (79%). c) 3-pyridinecarboxaldehyde (1.0 mmol, 1.0 eq.), β-alanine (1.0 mmol, 1.0 eq.), cyclohexyl isocyanide (1.0 mmol, 1.0 eq.), MeOH (5 mL, 0.2 M), r.t., overnight, **25a** (54%). D) phosphoric acid, MeOH, r.t., 68%.

Scheme 2. a) H₃PO₄, MeOH, rt, **5a** (96%); b) Cl−CH₂−CH₂−SO₂Cl, pyridine, DCM, 0 °C to rt, **14a** (35%); c) Cl−CO₂Et, pyridine, DCM, 0 °C to rt, **19a** (76%).

a recently reported strategy to make isocyanides [62,63] was employed (Scheme 3). The strategy illustrated in Scheme 2 was then used to prepare these analogues.
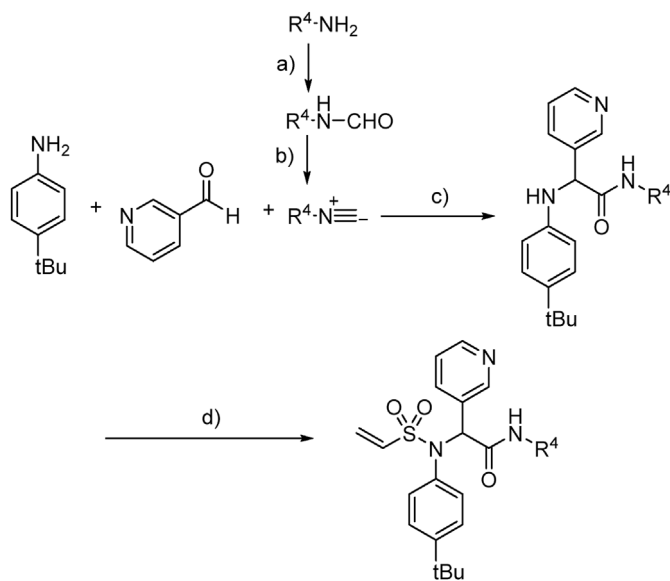
3. Results and discussions

3CL^pro inhibition − covalent warheads. Twenty potential warheads (compounds **6a-25a**, Fig. 3) and four non-covalent analogues (**X77**, **ML188**, **4a** and **5a**) were synthesized and evaluated for their inhibitory potency using a fluorescence inhibition assay. The compounds were initially screened at 50 μM and IC₅₀ values were subsequently determined for compounds displaying greater than 80% inhibition (Table 1).

Confirmation of covalent binding. To evaluate the covalent inhibition hypothesis, the time dependence of our most potent inhibitors, **16a** and **14a**, were measured (Fig. S4). The level of inhibition increased with incubation time, an observation that is consistent with the formation of a covalent adduct. Additionally, the presence of 3CL^pro -**16a** and -**14a** adducts were confirmed by LC-MS (Fig. S4a/b). As a definitive proof of covalent inhibition and binding mode, crystal structures of 3CL^pro co-crystallized with **16a** and **14a** were obtained (Fig. 5).

Scheme 3. a) HCO₂Et, 60 °C, **26b** (95%), **26c** (98%), **26d** (40%), **26e** (99%), **26f** (99%), **26g** (99%); b) POCl₃, Et₃N, DCM, **27b** (73%), **27c** (83%), **27d** (79%), **27e** (71%), **27f** (50%), **27g** (74%); c) H₃PO₄, MeOH, rt, **28b** (42%), **28c** (45%), **28d** (48%), **28e** (26%), **28f** (25%), **28g** (40%); c) Cl−CH₂−CH₂−SO₂Cl, pyridine, DCM, 0 °C, **14b** (66%), **14c** (45%), **14d** (73%), **14e** (80%), **14f** (42%), **14 g/h** (75%).

Analysis of covalent warheads. We observed that **GC376**, **X77** and **ML188**, previously reported SARS-CoV 3CL^{pro} inhibitors (**X77**: IC$_{50}$ = 3.4 μM [64] and **ML188**: IC$_{50}$ = 4.8 μM [56] respectively) and SARS-CoV2 inhibitor (**GC376**: 139 nM), also inhibit SARS-CoV-2 3CL^{pro} with similar potencies with our assay. (Table 1, entries 1 to 3). Gratifyingly, low micromolar to sub-micromolar potencies were also observed for the covalent analogues containing acrylamide (**6a**), alkynylamide (**13a**), vinyl sulfonamide (**14a**), α-chloroamide (**16a**) and α-ketoamide (**18a**) warheads. Interestingly, our two most potent inhibitors **16a** and **14a** (IC$_{50}$ = 0.4 and 0.5 μM) were an order of magnitude more potent than the original non-covalent hit molecule (**X77**: IC$_{50}$ = 4.1 μM).

An increase in potency was observed when increasing the electrophilicity of the warhead − the α-chloroamide (**16a**) was more active than the corresponding α-fluoroamide (**15a**), and the vinyl sulfonamide (**14a**) was more active than the corresponding acrylamide (**6a**). However, this trend was not observed when increasing the electrophilicity of the ketoamide (**18a**) with a CF₃ group (**22a**), potentially due to an increase in the steric bulk and/or electrostatic properties of the warhead that are not tolerated in the active site. Similarly, while acrylamides are typically more reactive with cysteine than the corresponding alkynylamides (when tested in glutathione or cysteine binding assays [65]), the aklynylamide warhead was more active against 3CL^{pro}. A possible explanation could be that the sp geometry of the aklynylamide warhead positions the electrophile more favorably to the cysteine residue to facilitate covalent bond formation.

The binding pocket also seems to favor smaller warheads − any steric bulk around the acrylamide warhead resulted in a decrease in potency, regardless of electronics. As mentioned previously, a similar effect was observed when comparing the activity of inhibitor **22a** and **18a**.

The position of the covalent bond formation also appears to influence inhibitor activity. Minimal inhibition was observed with compounds **19a** and **25a** which both require the formation of a covalent bond directly with the carbonyl carbon. This carbon is positioned slightly further from the cysteine residue (3.4 Å in PDB

6W63) and therefore covalent bond formation may result in the loss of other non-covalent interactions. Covalent bond formation appeared to be equally tolerated at either the alpha position (**16a** and **18a**) or beta position (**6a**, **13a**, and **14a**). However, the co-crystallized structure of **16a** (Fig. 5a) shows that covalent bond formation at the alpha position resulted in a slight shift of the inhibitor towards the cysteine residue that resulted in the loss of a hydrogen bond interaction with Glu^{166}. This interaction was maintained in the co-crystallized structure of **14a** (Fig. 5b), suggesting that covalent bond formation at the beta position is preferable for non-covalent binding affinity.

Another observation is the significant loss of potency when removing the heterocyclic ring of **X77** or **ML188** (**X77/ML188** vs. **4a**, Table 1). As illustrated in Fig. 2, the basic imidazole nitrogen of **X77** forms a hydrogen bond interaction with the backbone of Gly^{143}, an interaction that is also observed with the furan ring of **ML188** (PDB code: 3V3M) or other heterocycles of the same chemical series [56,66]. Gly^{143}, together with the backbone amides of Ser^{144} and Cys^{145}, forms an oxyanion hole that contributes to the catalytic activity of this enzyme. Substitution of this heterocycle with a carbocycle of similar size but no hydrogen bonding groups (compounds **11a** vs. **X77**) does not preserve the inhibitory potency even when this ring was converted to a warhead for covalent binding. Additionally, no difference in activity was observed when comparing the activity of compounds **4a** and **5a**, suggesting that the carbonyl group does not contribute significantly to the inhibitor's binding affinity.

As shown in Fig. 2, both **X77** and **PF-00835231** interact with the catalytic His^{41}, either through a direct hydrogen bond in the case of **PF-00835231**, or though a water-mediated hydrogen bond (**X77**) via a conserved water molecule. In an attempt to reproduce this interaction, longer covalent groups were designed by incorporating an ethyl ester to an acrylamide warhead (**17a**) and by incorporating a hydroxyl group to an alkynylamide warhead (**23a**). While **17a** resulted in a loss of potency, **23a** led to a nearly 10-fold improvement in potency over the alkynylamide analogue **13a**. Although our initial hypothesis was that the increase in potency was due to the formation of a hydrogen-bond interaction with His^{41}, docking suggests that the hydroxyl group of **23a** instead occupies the oxyanion hole and interacts with the backbone amides of Gly^{143}, Ser^{144} and Cys^{145} (Fig. S7).

Isothermal Titration Calorimetry (ITC). ITC was employed to validate the initial fluorescence inhibition assay and to gain information of the kinetics of covalent bond formation. ITC provides unique insights into the kinetics and thermodynamics of inhibitor binding that are not available in traditional enzyme assays [67]. ITC experiments measure the heat produced by catalysis in real time (Fig. 6, y- and x-axis, respectively), as one component is titrated into another. The power is proportional to the enzyme velocity, with larger deflections from the baseline corresponding to higher velocities, and exothermic and endothermic reactions giving downward and upward deflections of the ITC signal, respectively. Since the instrument detects the heat released by the native reaction, unlabeled substrates can be used in the experiments, unlike the fluorescence assay which requires substrates modified with hydrophobic dyes and quenchers.

We performed activity assays where 3CL^{pro} was titrated into the sample cell, which contained either substrate alone or a mixture of substrate and inhibitor. We then fit the resulting kinetic traces to determine both the kinetic parameters of the enzyme and the rate and mechanism of inhibitor binding. Fig. 6a shows the ITC trace obtained when 3CL^{pro} was injected into substrate alone, with the first (0.2 μL) and second (1.5 μL) injections shown in red and yellow. The signal was deflected downwards, indicating an exothermic reaction, and gradually returned to the baseline over about 1000 s

Table 1
Inhibitory potency against SARS-CoV-2 3CL^{pro}. Evaluation of warheads (R^1)[].
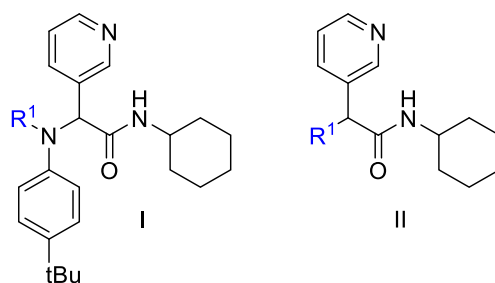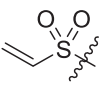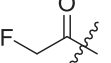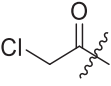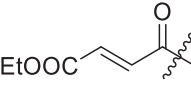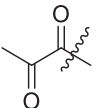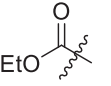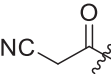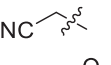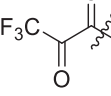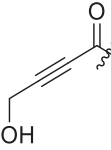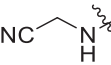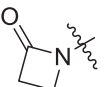
Entry	Scaffold	Cmpd	R^1	Inhibition (%)[a]	IC$_{50}$ (µM)
1	–	**GC376**	–	>95	0.11 ± 0.06
2	I	**X77**		>95	4.1 ± 1.2
3	I[c]	**ML188**		>95	1.4 ± 0.4
4	I	**4a**		25 ± 8	nd[b]
5	I	**5a**		28 ± 3	nd[b]
6	I	**6a**		84 ± 1	11.1 ± 1.5
7	I	**7a**		44 ± 6	nd[b]
8	I	**8a**		63 ± 5	nd[b]
9	I	**9a**		47 ± 2	nd[b]
10	I	**10a**		30 ± 1	nd[b]
11	I	**11a**		55 ± 10	nd[b]
12	I	**12a**		52 ± 1	nd[b]
13	I	**13a**		>95	5.3 ± 0.8

Table 1 (*continued*)

Entry	Scaffold	Cmpd	R^1	Inhibition (%)[a]	IC$_{50}$ (µM)
14	I	**14a**		>95	0.42 ± 0.11
15	I	**15a**		30 ± 7	nd[b]
16	I	**16a**		>95	0.41 ± 0.13
17	I	**17a**		59 ± 6	nd[b]
18	I	**18a**		92 ± 1	5.2 ± 1.2
19	I	**19a**		35 ± 3	nd[b]
20	I	**20a**		74 ± 1	7.0 ± 0.2
21	I	**21a**		<5	nd[b]
22	I	**22a**		77 ± 4	12.4 ± 5.2
23	I	**23a**		>95	0.85 ± 0.42
24	II	**24a**		25 ± 1	nd[b]
25	II	**25a**		<5	nd[b]

[a] The enzyme activity was measured with 150 nM 3CL^{pro} (114 nM after inhibitor addition) and 50 µM of each potential inhibitor with incubation time of 30 min [b] not determined. [c] cyclohexyl replaced by *tert*-butyl in scaffold I.
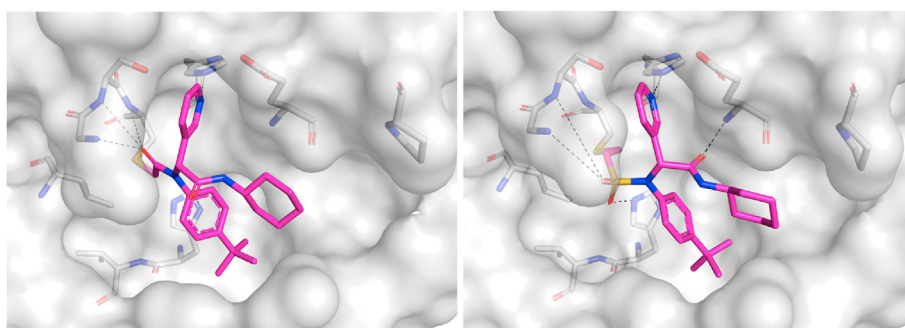
Fig. 5. a) Crystal structure of **16a** (PDB ID: 7MLF) bound to 3CL^{pro} and b) crystal structure of **14a** (PDB ID: 7MLG) bound to 3CL^{pro}.
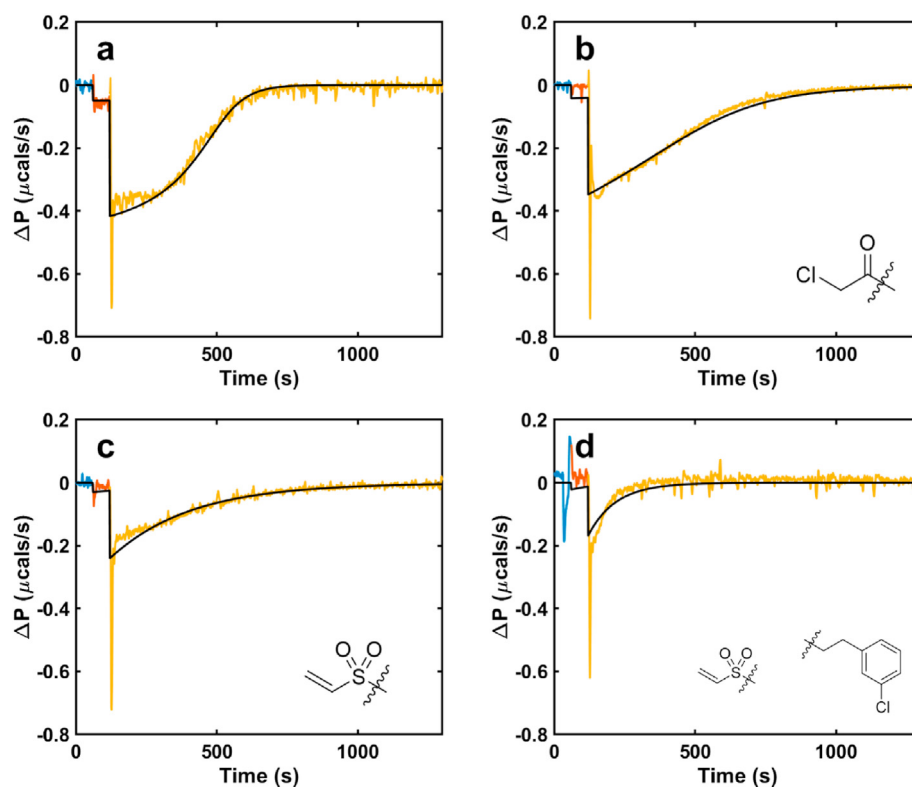
Fig. 6. ITC enzyme activity assay in the presence of a) no inhibitor, b) **16a**, c) **14a**, d) **14c**; each successive injection is shown in separate color. ITC simulations corresponding to the minimized kinetic parameters from fitting a covalent inhibition model are shown as black.

as all the substrate was cleaved. The data were fit to the Michaelis Menten equation to extract the turnover number, k_{cat}, and the Michaelis constant, K_m. Panels b−d show the ITC traces obtained when 3CL^{pro} was injected into a mixture of substrate and inhibitor. In all cases, the total amounts of heat (areas of the peaks) were less than that obtained in the absence of inhibitor (panel a), indicating that the enzyme was inactivated before all the substrate was cleaved. To obtain quantitative information on inhibition, the traces were fit to three different models: (i) a reversible (rapid equilibrium) mechanism, E↔EI characterized by an equilibrium affinity constant, K_i; (ii) an irreversible mechanism, E→EI characterized by a second order rate constant k_{inact}; and (iii) a two-step mechanism, E↔EI*→EI, consisting of a rapid pre-equilibrium described by K_i, followed by irreversible inhibition described by a first-order rate constant k_{inact}. In models (ii) and (iii), k_{inact} can be tentatively assigned to the rate of covalent bond formation with the enzyme. The Michaelis Menten enzymatic parameters were held fixed at the values obtained in (a) and the parameters of the inhibition models were varied to minimize the residual-sum-of-squared-deviations (RSS). In all cases, the pre-equilibrium irreversible model (iii) gave the best agreement with data. The improvements in RSS given by model (iii) compared to models (ii) and (i) were calculated using F-test statistics [68] and found to be significant at levels of $p \leq 10^{-2}$. The extracted values of K_i and k_{inact} are listed in Table S1. **14c** had both the fastest rate of covalent bond formation (largest k_{inact}) and tightest binding in the initial non-covalent step (smallest K_i) of the three inhibitors, tested. Both **14a** and **14c** have similar values of K_i to the parent non-covalent scaffold, which is consistent with the two-step binding model (iii), since the first step corresponds to non-covalent binding.

Structure-Activity Relationship. Following our search for an optimal warhead, several modifications were made to the core of
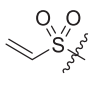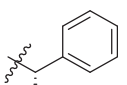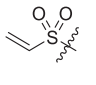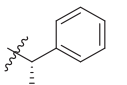
the molecule (Tables 2−4). Previously, it was shown that replacement of the *tert*-butylphenyl group (R^2) by smaller groups or differently substituted phenyl groups modulates the potency against SARS-CoV 3CL^{pro} with slight improvements in some cases, while various hydrophobic groups were tolerated as R^3 [64]. We thought this information could help further improve these inhibitors for the highly homologous SARS-CoV-2 3CL^{pro}. However, all of our attempts to replace the *tert*-butylphenyl and pyridyl groups have proven unsuccessful to date. More specifically, the use of a variety of aromatic heterocycles such as thiophene, benzothiazole, pyrimidine, pyrazine and benzothiophene led to loss of potency (Table 3). Additionally, replacement of the heterocyclic ring with a hydantoin moiety also led to a loss in potency. Similarly, diversely functionalized phenyl groups in place of the *tert*-butylphenyl group were detrimental for the activity and replacement of the phenyl group with a benzyl moiety led to a complete loss of activity (Table 4).

Replacement of the cyclohexyl group with groups of similar sizes did not improve the potency (Table 2, entries 1−7 and 9). However, we have found that substitution of the cyclohexyl (R^4 group in Table 2) for longer groups (**14b-l**) improved the inhibitory potency over that of **16a** and **14a**. The longer chains likely enable the inhibitor to form a hydrophobic interaction with Pro^{168}, while the amine nitrogen of analogue **14f** may facilitate a hydrogen-bond interaction with Gln^{189} or the carbonyl of Glu^{166}. Based on these optimizations, our current most potent compound (**14c**) has a potency similar to the previously reported inhibitor **GC376**. It is expected that one enantiomer is more potent that the other one. To confirm this hypothesis, we used a chiral isocyanide leading to easily separable diastereomers **14h** and **14g**. Diastereomer **14g** was found to be approximately 20 times more potent that **14h** in line with what has been observed previously [69].

Table 2
Inhibitory potency against SARS-CoV-2 3CL^{pro}. Optimization of R^4.
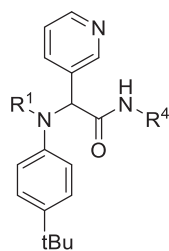
Entry	Cmpd	R^1	R^4	Inhibition (%)[a]	IC$_{50}$ (μM)
1	**8b**			33 ± 1	nd[b]
2	**13b**			93	15.0 ± 9.3
3	**6b**			68 ± 1	nd[b]
4	**4b**			<5	nd[b]
5	**13c**			88	9.7 ± 3.8
6	**13d**			69	>30
7	**16b**			>95	0.38 ± 0.09
8	**16c**			>95	0.92 ± 0.24
9	**11b**			16	nd[b]
9	**14b**			>95	0.28 ± 0.10
10	**14c**			>95	0.17 ± 0.07
11	**14d**			>95	0.24 ± 0.15
12	**14e**			>95	0.52 ± 0.16
13	**14f**			>95	0.22 ± 0.08

Table 2 (continued)

Entry	Cmpd	R^1	R^4	Inhibition (%)[a]	IC_{50} (μM)
14	**14g (R,S)**			>95	0.32 ± 0.10
15	**14h (S,S)**			>95	6.0 ± 2.7

[a] The enzyme activity was measured with 150 nM 3CL^{pro} (114 nM after inhibitor addition) and 50 μM of each potential inhibitor with incubation time of 30 min.
[b] Not determined.

aThe enzyme activity was measured with 150 nM 3CL^{pro} (114 nM after inhibitor addition) and 50 μM of each potential inhibitor with incubation time of 30 min [b] not determined. [c] IC$_{50}$ was not determined as poor solubility did not allow us to accurately measure activity beyond 50 μM.

aThe enzyme activity was measured with 150 nM 3CL^{pro} (114 nM after inhibitor addition) and 50 μM of each potential inhibitor with incubation time of 30 min [b] not determined.

Off-target Cathepsin L inhibition. Lysosomal ubication of cysteine proteases could have cross-reactivity with the potential viral inhibitors, decreasing the therapeutical effect against SARS-CoV-2. [70]. For example, the increase of the cathepsin L levels, a ubiquitous human protease, in plasma of patients with SARS-CoV-2 severe infections generates a target competence for the protease antiviral inhibitors [71]. To assess this potential undesired effect of our most potent 3CL^{pro} inhibitors, we measured the inhibitor effect against cathepsin L. The low inhibition of cathepsin L activity for our inhibitors at 50 μM (25% ± 2, 19% ± 1 and 15% ± 2 for **16a**, **14a** and **14c**, respectively, Figs. S3a and S3b) indicates an excellent selectivity of these inhibitors against 3CL^{pro} over cathepsin L.

4. Conclusion

Covalent inhibition of SARS-CoV-2 3CL^{pro} is a promising strategy for the treatment of COVID-19. Our strategy relied on a previously reported imidazole-containing inhibitor of the similar coronavirus SARS-CoV responsible for the epidemic of SARS in the early 2000's. We first used our docking program FITTED, specifically modified to accommodate covalent inhibitors, and screened a set of covalent warheads. The docked poses confirmed that replacing the imidazole ring by a reactive group should lead to potent covalent inhibition. Gratifyingly, while the imidazole of **X77** was known to be essential for the inhibitory potency, replacing it with many warheads maintained and even improved the potency, with our lead compounds **16a** and **14a** being an order of magnitude more potent. Both the inhibition pattern of enzymatic activity and the biophysical data first suggested that these inhibitors bind covalently to the viral protease, a binding mode later confirmed by crystallography; thus, the robustness of *in silico* rational-drug design was validated using *in vitro* detection of protein processing.

5. Experimental section

5.1. Synthesis and characterization

General Considerations. All other reagents were purchased from commercial suppliers and used without further purification. All ^{1}H, ^{13}C and ^{19}F NMR spectra were acquired Bruker Avance 500 MHz spectrometer. Chemical shifts are reported in ppm using the residual of deuterated solvents as an internal standard. Chromatography was performed on silica gel 60 (230-40 mesh) or using the Biotage One Isolera with ZIP cartridges. High resolution mass spectrometry was performed by ESI on a Bruker Maxis Impact API QqTOF mass spectrometer at McGill University. Reversed-phase HPLC (water and MeCN or MeOH gradient) was used to verify the purity of compounds on an Agilent 1100 series instrument equipped with VWD-detector, C18 reverse column (Agilent, Zorbax Eclipse XDBC18 150 mm 4.6 mm, 5 μm), and UV detection at 254 nm. Measured purities for all tested compounds are listed in Table S3 in the supporting information.

General Procedures A, B and C for 4-Component Ugi Reaction. In a 6-dram vial equipped with a stir bar aldehyde (1.0 mmol, 1.0 eq.), aniline (1.0 mmol, 1.0 eq.) and carboxylic acid (1.0 mmol, 1.0 eq.) were combined in MeOH (4 mL). The obtained reaction mixture was stirred for 30 min at room temperature. Afterwards cyclohexyl isocyanide (0.9 mmol, 0.9 eq.) was added to the reaction mixture and the walls of the vial were washed with 1 mL of MeOH. The reaction mixture was continued to stir at room temperature overnight. The crude reaction mixture was evaporated in vacuo. Purification procedure A) The crude product was triturated with hexanes (5 mL) and filtered. The obtained product was further washed with hexanes (3 x 3 mL). Purification procedure B) The crude product recrystallized from CHCl$_3$/hexanes mixture, filtered and the obtained product was further washed with hexanes (3 x 3 mL). Purification procedure C) The crude product was redissolved in DCM. The obtained crude solution was deposited on silica. It was then purified using flash column chromatography using DCM/MeOH (gradient 0 → 5%) as eluent.

General Procedure D to Prepare Formamides. The synthesis of formamides was derived from known literature [62]. In a 1-dram vial equipped with a stir bar, 5 mmol (1 eq.) of amine was mixed with 15 mmol (3 eq.) of ethyl formate and stirred at 60 °C until completion (monitored using TLC - 1:1 EtOAc:hexanes or 2:1 EtOAc:hexanes). Once the amine was fully converted, ethyl formate was removed in vacuo and the product was used in the next step without further purification.

General procedure E to Prepare Isocyanides. The synthesis of isocyanides was derived from known literature [63]. In a 6-dram vial equipped with a stir bar, 2 mmol (1 eq.) of formamide was dissolved in 1 mL DCM with 10 mmol (5 eq.) of Et$_3$N. The mixture was cooled to 0 °C and 2 mmol (1 eq.) of POCl$_3$ was added dropwise. The reaction mixture was stirred at 0 °C for 10 min then quickly purified through a silica pad (2 g of silica 230−400 mesh, washing with a gradient of mixture of Et$_2$O and DCM (100% Et$_2$O →, 100% DCM). The fractions containing the desired product were collected and concentrated in vacuo. This procedure (silica pad, washing and concentration) is repeated once.

General Procedures F for 3-Component Ugi Reaction. In a 6-dram vial equipped with a stir bar, 1 mmol (1.0 eq.) of 4-*tert*-butylaniline and 1 mmol (1.0 eq.) of 3-pyridinecarboxaldehyde were dissolved in 5 mL MeOH with 10 μL of 85% H$_3$PO$_4$. 1 mmol (1.0 eq.) of isocyanide was then added. The mixture was stirred at rt

Table 3
Inhibitory potency against SARS-CoV-2 3CL^{pro}. Optimization of R^3.
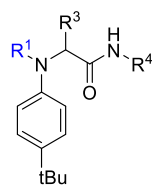
Entry	Cmpd	R^1	R^3	R^4	Inhibition (%)[a]	IC$_{50}$ (µM)
1	11c			cHex	22 ± 8	nd[b]
2	11d			cHex	18 ± 8	nd[b]
3	11e			cHex	<5	nd[b]
4	11f			cHex	19 ± 8	nd[b]
5	11g			cHex	38 ± 8	nd[b]
6	11h			cHex	<5	nd[b]
7	11i			cHex	24 ± 8	nd[b]
8	8c			tBu	24 ± 8	nd[b]
9	16d			cHex	22 ± 11	nd[b]
10	16e			cHex	>95	0.84 ± 0.30
11	16f			cHex	>95	0.98 ± 0.35
12	13e			cHex	>95	5.0 ± 2.3
13	13f			cHex	80 ± 10	nd[b,c]

Table 3 (*continued*)

Entry	Cmpd	R^1	R^3	R^4	Inhibition (%)[a]	IC$_{50}$ (μM)
14	**13g**			cHex	54 ± 15	nd[b]
15	**13h**			cHex	57 ± 6	nd[b]
16	**13i**			cHex	10 ± 10	nd[b]
17	**13j**			cHex	19 ± 5	nd[b]

overnight. The reaction mixture was then concentrated in vacuo. The crude product was purified using flash column chromatography using EtOAc/hexanes (33% → 80%) as eluent.

General Procedure G for Synthesis of Vinyl Sulfonamides. The synthesis of vinyl sulfonamides was derived from known literature [72]. In a 6-dram vial equipped with a stir bar, 0.2−0.3 mmol (1.0 eq.) of the previously made acetamide (see general procedure F) was dissolved in 5 mL of DCM with 0.7−3.5 mmol (from 0.5 eq. to 3 eq.) of Et$_3$N. The mixture was cooled to 0 °C and 0.3−0.45 mmol (1.5 eq.) of 2-chloroethanesulfonyl chloride was added dropwise. The solution was stirred at 0 °C for 2 h. The solution was then diluted with 5 mL DCM and washed with 10 mL sat. NaHCO$_3$. The aqueous layer was extracted with 10 mL DCM and the combined organic layer was washed with 10 mL sat. NaCl solution and further dried with anhydrous Na$_2$SO$_4$. The crude product was purified using flash column chromatography using DCM/EtOAc (gradient 0% → 50%) as eluent.

N-(4-(*tert*-butyl)phenyl)-N-(2-(cyclohexylamino)-2-oxo-1-(pyridin-3-yl)ethyl)-1H-imidazole-5-carboxamide (X77). Compound was made and purified using general procedure B, white solid 30% yield, 125 mg. ^{1}H NMR (500 MHz, MeOD) δ 8.37 (s, 1H), 8.33 (dd, J = 4.9, 1.5 Hz, 1H), 7.66−7.57 (m, 2H), 7.31 (d, J = 7.8 Hz, 2H), 7.22 (dd, J = 7.9, 4.9 Hz, 1H), 6.27 (s, 1H), 5.46 (s, 1H), 3.71 (td, J = 10.5, 9.3, 3.9 Hz, 1H), 1.93 (d, J = 12.3 Hz, 1H), 1.80−1.72 (m, 2H), 1.65 (ddt, J = 30.9, 12.9, 3.8 Hz, 2H), 1.27 (s, 12H). ^{13}C NMR (126 MHz, MeOD) δ 169.00, 152.54, 150.62, 148.24, 138.83, 136.36, 131.58, 131.07, 125.72, 123.31, 62.74, 34.16, 32.16, 32.12, 30.25, 25.22, 24.72, 24.64. HRMS (ESI/Q-TOF) *m/z*: [M + Na]$^+$ calculated for C$_{27}$H$_{33}$N$_5$NaO$_2$ 482.2526; found 482.2535.

N-(4-(*tert*-butyl)phenyl)-N-(2-(*tert*-butylamino)-2-oxo-1-(pyridin-3-yl)ethyl)furan-2-carboxamide (ML188). Compound was made and purified using general procedure A, white solid 84% yield, 290 mg. ^{1}H NMR (500 MHz, CDCl$_3$) δ 8.48 (d, J = 2.3 Hz, 1H), 8.46 (dd, J = 4.9, 1.7 Hz, 1H), 7.51 (d, J = 8.1 Hz, 1H), 7.39 (dd, J = 1.7, 0.7 Hz, 1H), 7.24 (d, J = 6.6 Hz, 2H), 7.06 (ddd, J = 8.0, 4.8, 0.8 Hz, 1H), 6.98 (s, 2H), 6.19−6.13 (m, 2H), 6.10 (s, 1H), 5.38 (dd, J = 3.6, 0.8 Hz, 1H), 1.37 (s, 9H), 1.28 (s, 9H). ^{13}C NMR (126 MHz, CDCl$_3$) δ 167.96, 159.80, 152.62, 151.59, 149.72, 146.36, 145.12, 138.32, 136.63, 130.56, 130.30, 126.22, 122.94, 117.26, 111.35, 63.83, 51.92, 34.84, 31.41, 28.80. HRMS (ESI/Q-TOF) *m/z*: [M + Na]$^+$ calculated for C$_{26}$H$_{31}$N$_3$NaO$_3$ 456.2258; found 456.2245.

2-(N-(4-(*tert*-butyl)phenyl)acetamido)-N-cyclohexyl-2-(pyridin-3-yl)acetamide (4a). Compound was made and purified using general procedure A, white solid 76% yield, 280 mg. ^{1}H NMR (500 MHz, CDCl$_3$) δ 8.46−8.43 (m, 1H), 8.42 (s, 1H), 7.41 (d, J = 8.1 Hz, 1H), 7.23 (d, J = 8.5 Hz, 2H), 7.03 (dd, J = 8.0, 4.8 Hz, 1H), 6.93 (s, 1H), 6.03 (s, 2H), 3.94−3.65 (m, 1H), 1.98 (d, J = 16.8 Hz, 1H), 1.89−1.81 (m, 4H), 1.75−1.63 (m, 2H), 1.59 (dt, J = 13.0, 4.3 Hz, 1H), 1.43−1.28 (m, 2H), 1.25 (s, 9H), 1.23−1.04 (m, 3H). ^{13}C NMR (126 MHz, CDCl$_3$) δ 171.83, 168.21, 151.89, 151.44, 149.66, 138.09, 137.42, 130.87, 129.60, 126.28, 122.92, 62.42, 48.88, 34.73, 32.95 (d, J = 10.4 Hz), 31.37, 25.61, 24.87 (d, J = 6.9 Hz), 23.34. HRMS (ESI/Q-TOF) *m/z*: [M + Na]$^+$ calculated for C$_{25}$H$_{33}$N$_3$NaO$_2$ 430.2465; found 430.2464.

N-cyclohexyl-2-(pyridin-3-yl)-2-(*p*-tolylamino)acetamide (5a). To a solution of 4-*t*Bu-aniline (1.01 mmol, 0.16 mL) and 3-pyridinecarboxaldehyde (1.01 mmol, 0.09 mL) in MeOH (5 mL) was added cyclohexyl isocyanide (1.01 mmol, 0.12 mL) and phosphoric acid (0.2 mmol, 0.01 mL, 85%), and the solution stirred at room temperature overnight. The solvent was evaporated under a stream of air, and the crude reaction mixture was suspended in a small amount of EtOAc. Hexanes was added and the precipitate was collected by filtration and rinsed with hexanes and acetone. The precipitate was dried over vacuum to afford the desired product (353 mg, 96% yield) as a white powder. ^{1}H NMR (500 MHz, DMSO) δ 8.69 (dd, J = 2.4, 0.9 Hz, 1H), 8.46 (dd, J = 4.8, 1.7 Hz, 1H), 8.19 (d, J = 7.9 Hz, 1H), 7.85 (dt, J = 7.9, 2.0 Hz, 1H), 7.35 (ddd, J = 7.8, 4.8, 0.9 Hz, 1H), 7.10−7.04 (m, 2H), 6.61−6.55 (m, 2H), 6.04 (d, J = 8.1 Hz, 1H), 5.02 (d, J = 8.0 Hz, 1H), 3.56−3.47 (m, 1H), 1.74 (dd, J = 10.5, 4.8 Hz, 1H), 1.70−1.63 (m, 1H), 1.62−1.48 (m, 3H), 1.31−1.19 (m, 2H), 1.18 (s, 10H), 1.17−1.03 (m, 1H). ^{13}C NMR (126 MHz, DMSO) δ 169.29, 148.65, 148.56, 144.47, 138.99, 135.44, 134.52, 125.39, 123.45, 112.89, 58.39, 47.58, 33.46, 32.24, 32.06, 31.38, 25.11, 24.37, 24.26. HRMS (ESI/Q-TOF) *m/z*: [M + Na]$^+$ calculated for C$_{23}$H$_{31}$N$_3$NaO 388.2359; found 388.2352.

N-(4-(*tert*-butyl)phenyl)-N-(2-(cyclohexylamino)-2-oxo-1-(pyridin-3-yl)ethyl) acrylamide (6a). Compound was made and purified using general procedure C, white solid 32% yield, 120 mg. ^{1}H NMR (500 MHz, CDCl$_3$) δ 8.41−8.39 (m, 1H), 8.38−8.37 (m, 1H), 7.42−7.35 (m, 1H), 7.19 (d, J = 8.1 Hz, 2H), 7.01 (dd, J = 8.0, 4.8 Hz, 1H), 6.91 (s, 1H), 6.49 (d, J = 8.0 Hz, 1H), 6.33 (dd, J = 16.8, 2.0 Hz, 1H), 6.11 (s, 1H), 5.93 (dd, J = 16.8, 10.3 Hz, 1H), 5.49 (dd, J = 10.4, 2.0 Hz, 1H), 3.84−3.73 (m, 1H), 1.93 (s, 1H), 1.81 (dd, J = 13.1, 4.1 Hz, 1H), 1.67−1.53 (m, 3H), 1.37−1.26 (m, 2H), 1.22 (s, 9H), 1.17−1.06 (m, 3H). ^{13}C NMR (126 MHz, CDCl$_3$) δ 168.04, 166.50, 151.79, 151.28, 149.45, 137.93, 136.14, 130.83, 129.93, 128.64, 128.52, 126.08, 122.85, 62.69, 48.76, 34.64, 32.86, 32.80, 31.27, 25.52, 24.83, 24.77. HRMS (ESI/Q-TOF) *m/z*: [M + Na]$^+$ calculated for C$_{26}$H$_{33}$N$_3$NaO$_2$ 442.2465; found 442.2456.

Table 4
Inhibitory potency against SARS-CoV-2 3CL^{pro}. Optimization of R^2.
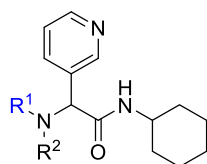
Entry	Cmpd	R^1	R^2	Inhibition (%)[a]	IC$_{50}$ (μM)
1	**18b**			< 5%	nd[b]
2	**13k**			39 ± 1	nd[b]
3	**13l**		-H	10 ± 15	nd[b]
4	**13m**			43 ± 3	nd[b]
5	**13n**			23 ± 13	nd[b]
6	**13o**			65 ± 3	nd[b]
7	**13p**			77 ± 2	45.1 ± 18.3
8	**13q**			< 5%	nd[b]

[a] The enzyme activity was measured with 150 nM 3CL^{pro} (114 nM after inhibitor addition) and 50 μM of each potential inhibitor with incubation time of 30 min.
[b] not determined.

N-(4-(tert-butyl)phenyl)-N-(2-(cyclohexylamino)-2-oxo-1-(pyridin-3-yl)ethyl) cinnamamide (7a). Compound was made and purified using general procedure A, pale white solid 94% yield, 420 mg. ^{1}H NMR (500 MHz, CDCl$_3$) δ 8.48 (d, J = 2.3 Hz, 1H), 8.47 (dd, J = 4.8, 1.7 Hz, 1H), 7.71 (d, J = 15.6 Hz, 1H), 7.50 (dt, J = 7.9, 2.0 Hz, 1H), 7.27 (s, 6H), 7.07 (dd, J = 8.0, 4.8 Hz, 1H), 6.98 (s, 1H), 6.33 (d, J = 8.1 Hz, 1H), 6.24 (d, J = 15.5 Hz, 1H), 6.14 (s, 1H), 3.91−3.80 (m, 1H), 1.94 (dd, J = 52.0, 13.0 Hz, 2H), 1.70 (ddd, J = 18.3, 11.4, 6.7 Hz, 2H), 1.59 (dd, J = 8.9, 4.1 Hz, 1H), 1.44−1.32 (m, 2H), 1.29 (s, 9H), 1.26−1.09 (m, 4H). ^{13}C NMR (126 MHz, CDCl$_3$) δ 168.16, 167.14, 151.97, 151.36, 149.60, 143.22, 138.03, 136.60, 135.07, 130.93,

129.91, 129.86, 128.82, 128.13, 126.35, 122.95, 118.61, 63.32, 48.85, 34.81, 33.02, 32.96, 31.38, 25.62, 24.90, 24.86. HRMS (ESI/Q-TOF) m/z: [M + Na]$^+$ calculated for C$_{32}$H$_{37}$N$_3$NaO$_2$ 518.2778; found 518.2790.

(E)-N-(4-(tert-butyl)phenyl)-N-(2-(cyclohexylamino)-2-oxo-1-(pyridin-3-yl)ethyl)but-2-enamide (8a). Compound was made and purified using general procedure B, pale white solid 32% yield, 126 mg. ^{1}H NMR (500 MHz, CDCl$_3$) δ 8.46−8.41 (m, 2H), 7.44 (dt, J = 7.9, 2.0 Hz, 1H), 7.24 (d, J = 8.2 Hz, 2H), 7.04 (ddd, J = 8.0, 4.8, 0.8 Hz, 1H), 6.99−6.91 (m, 3H), 6.36 (d, J = 8.1 Hz, 1H), 6.09 (s, 1H), 5.65 (dd, J = 15.0, 1.7 Hz, 1H), 3.87−3.76 (m, 1H), 1.97 (dd, J = 11.7,

4.6 Hz,1H), 1.92−1.82 (m, 1H), 1.72 (dd, *J* = 7.0, 1.7 Hz, 3H), 1.69−1.63 (m, 1H), 1.60−1.56 (m, 1H), 1.42−1.30 (m, 2H), 1.27 (s, 9H), 1.22−1.09 (m, 3H). ^{13}C NMR (126 MHz, CDCl₃) δ 168.25, 166.99, 151.78, 151.24, 149.41, 143.08, 138.09, 136.62, 131.00, 129.80, 126.22, 122.88, 122.71, 62.96, 48.78, 34.75, 32.97, 32.91, 31.37, 25.62, 24.88, 24.84, 18.21. HRMS (ESI/Q-TOF) *m/z*: [M + Na]⁺ calculated for C₂₇H₃₅N₃NaO₂ 456.2621; found 456.2630.

(*E*)-*N*-(4-(*tert*-butyl)phenyl)-*N*-(2-(cyclohexylamino)-2-oxo-1-(pyridin-3-yl)ethyl)-2-methylbut-2-enamide (9a). Compound was made and purified using general procedure A, white solid 73% yield, 294 mg. ^{1}H NMR (500 MHz, CDCl₃) δ 8.50 (d, *J* = 2.3 Hz, 1H), 8.49−8.45 (m, 1H), 7.55 (dt, *J* = 7.9, 2.0 Hz, 1H), 7.17 (d, *J* = 8.8 Hz, 2H), 7.10 (ddd, *J* = 7.9, 4.8, 0.8 Hz, 1H), 6.87 (d, *J* = 8.1 Hz, 2H), 6.29 (d, *J* = 8.2 Hz, 1H), 5.98 (s, 1H), 5.77 (dddd, *J* = 8.5, 6.9, 5.5, 1.6 Hz, 1H), 3.90−3.79 (m, 1H), 1.96 (d, *J* = 9.1 Hz, 1H), 1.92−1.87 (m, 1H), 1.74−1.55 (m, 3H), 1.51 (s, 3H), 1.45 (dd, *J* = 6.9, 1.2 Hz, 3H), 1.44−1.30 (m, 2H), 1.24 (s, 9H), 1.23−1.08 (m, 3H). ^{13}C NMR (126 MHz, CDCl₃) δ 174.17, 168.17, 151.06, 150.92, 149.49, 138.40, 137.72, 132.44, 131.30, 131.17, 128.98, 125.80, 123.03, 64.28, 34.67, 33.00, 32.98, 31.36, 25.63, 24.86, 24.81, 14.17, 13.46. HRMS (ESI/Q-TOF) *m/z*: [M + Na]⁺ calculated for C₂₈H₃₇N₃NaO₂ 470.2778; found 470.2766.

N-(4-(*tert*-butyl)phenyl)-*N*-(2-(cyclohexylamino)-2-oxo-1-(pyridin-3-yl)ethyl) methacrylamide (10a). Compound was made and purified using general procedure B, pale white solid 68% yield, 265 mg. ^{1}H NMR (500 MHz, MeOD) δ 8.33 (d, *J* = 2.3 Hz, 1H), 8.31 (dd, *J* = 4.9, 1.6 Hz, 1H), 7.56 (dt, *J* = 7.9, 2.0 Hz, 1H), 7.23−7.15 (m, 3H), 7.05 (s, 2H), 6.10 (s, 1H), 5.01 (dt, *J* = 6.9, 1.3 Hz, 2H), 3.70 (tt, *J* = 10.9, 3.9 Hz, 1H), 1.90 (dd, *J* = 10.7, 3.8 Hz, 1H), 1.73 (s, 5H), 1.70−1.59 (m, 2H), 1.41−1.27 (m, 3H), 1.21 (s, 9H), 1.19−1.06 (m, 2H). ^{13}C NMR (126 MHz, CDCl₃) δ 172.82, 167.95, 151.29, 151.19, 149.55, 140.42, 137.86, 137.64, 130.88, 129.32, 125.77, 122.97, 119.77, 63.47, 48.78, 34.63, 32.90 (d, *J* = 10.4 Hz), 31.32, 25.57, 24.83, 24.77, 20.42. HRMS (ESI/Q-TOF) *m/z*: [M + Na]⁺ calculated for C₂₇H₃₅N₃NaO₂ 456.2621; found 456.2620.

N-(4-(*tert*-butyl)phenyl)-*N*-(2-(cyclohexylamino)-2-oxo-1-(pyridin-3-yl)ethyl)cyclopent-1-ene-1-carboxamide (11a). Compound was made and purified using general procedure A, pale yellow solid 80% yield, 333 mg. ^{1}H NMR (500 MHz, CDCl₃) δ 8.48 (d, *J* = 2.3 Hz, 1H), 8.46 (dd, *J* = 4.8, 1.7 Hz, 1H), 7.51 (dt, *J* = 8.0, 2.0 Hz, 1H), 7.21−7.16 (m, 2H), 7.08 (ddd, *J* = 7.9, 4.8, 0.8 Hz, 1H), 6.90 (d, *J* = 8.0 Hz, 2H), 6.28 (d, *J* = 8.0 Hz, 1H), 6.04 (s, 1H), 5.82 (d, *J* = 2.3 Hz, 1H), 3.89−3.78 (m, 1H), 2.19 (ddt, *J* = 7.7, 5.1, 2.5 Hz, 2H), 2.12 (tt, *J* = 6.7, 2.8 Hz, 2H), 2.02−1.93 (m, 1H), 1.92−1.84 (m, 1H), 1.73−1.54 (m, 4H), 1.44−1.29 (m, 2H), 1.25 (s, 9H), 1.23−1.07 (m, 3H). ^{13}C NMR (126 MHz, CDCl₃) δ 168.92, 168.16, 151.57, 151.22, 149.46, 140.13, 139.09, 137.96, 137.69, 130.98, 129.50, 125.81, 122.94, 63.92, 48.74, 34.69, 33.80, 33.22, 32.95, 32.92, 31.35, 25.60, 24.84, 24.79, 23.29. HRMS (ESI/Q-TOF) *m/z*: [M + Na]⁺ calculated for C₂₉H₃₇N₃NaO₂ 482.2778; found 482.2781.

N-(4-(*tert*-butyl)phenyl)-*N*-(2-(cyclohexylamino)-2-oxo-1-(pyridin-3-yl)ethyl)cyclohex-1-ene-1-carboxamide (12a). Compound was made and purified using general procedure A, white solid 37% yield, 157 mg. ^{1}H NMR (500 MHz, CDCl₃) δ 8.50 (d, *J* = 2.3 Hz, 1H), 8.47 (dd, *J* = 4.8, 1.6 Hz, 1H), 7.55 (dt, *J* = 8.0, 2.0 Hz, 1H), 7.18 (d, *J* = 8.8 Hz, 2H), 7.11 (ddd, *J* = 7.9, 4.8, 0.8 Hz, 1H), 6.88 (d, *J* = 8.1 Hz, 2H), 6.30 (d, *J* = 8.2 Hz, 1H), 6.00 (s, 1H), 5.84 (dt, *J* = 3.8, 2.0 Hz, 1H), 3.90−3.79 (m, 1H), 1.99−1.80 (m, 5H), 1.75−1.54 (m, 6H), 1.44−1.29 (m, 4H), 1.25 (s, 9H), 1.24−1.13 (m, 3H). ^{13}C NMR (126 MHz, CDCl₃) δ 173.52, 168.18, 151.11, 151.05, 149.50, 138.33, 137.79, 134.48, 133.17, 131.12, 129.08, 125.69, 123.02, 63.95, 48.72, 34.68, 33.01, 32.97, 31.37, 26.14, 25.64, 25.00, 24.85, 22.04, 21.45. HRMS (ESI/Q-TOF) *m/z*: [M + Na]⁺ calculated for C₃₀H₃₉N₃NaO₂ 496.2934; found 496.2931.

**N-(4-(*tert*-butyl)phenyl)-*N*-(2-(cyclohexylamino)-2-oxo-1-

(pyridin-3-yl)ethyl)but-2-ynamide (13a). Compound was made and purified using general procedure A, white solid 92% yield, 357 mg. ^{1}H NMR (500 MHz, CDCl₃) δ 8.44 (d, *J* = 4.9 Hz, 1H), 8.41 (d, *J* = 2.3 Hz, 1H), 7.44 (d, *J* = 8.1 Hz, 1H), 7.21 (d, *J* = 8.4 Hz, 2H), 7.05 (dd, *J* = 8.0, 4.8 Hz, 1H), 6.97 (d, *J* = 8.0 Hz, 2H), 6.20 (s, 1H), 6.03 (s, 1H), 3.80 (dtd, *J* = 10.8, 7.2, 4.0 Hz, 1H), 1.96 (dq, *J* = 13.2, 4.8 Hz, 1H), 1.84 (d, *J* = 16.6 Hz, 1H), 1.75−1.62 (m, 5H), 1.58 (dd, *J* = 13.1, 4.1 Hz, 1H), 1.42−1.26 (m, 2H), 1.25 (s, 9H), 1.25−1.05 (m, 3H). ^{13}C NMR (126 MHz, CDCl₃) δ 167.43, 155.41, 151.87, 151.20, 149.62, 138.15, 136.38, 130.34, 129.90, 125.70, 122.98, 92.12, 73.86, 62.23, 34.71, 32.87, 32.80, 31.31, 25.56, 24.85, 24.80. HRMS (ESI/Q-TOF) *m/z*: [M + Na]⁺ calculated for C₂₇H₃₃N₃NaO₂ 454.2465; found 454.2458.

2-(*N*-(4-(*tert*-butyl)phenyl)vinylsulfonamido)-*N*-cyclohexyl-2-(pyridin-3-yl)acetamide (14a). To a solution of **5a** (0.41 mmol, 150 mg) in DCM (4 mL) was added pyridine (0.56 mmol, 0.04 mL) and the solution cooled to 0 °C. 2-chloroethanesulfonyl chloride (0.49 mmol, 0.05 mL) was added dropwise and stirred for 1 h, after which pyridine (0.56 mmol, 0.04 mL) was added, and the solution was warmed to r.t. and stirred overnight. The reaction was monitored by TLC (1:1 DCM:EtOAc). The reaction was quenched with water and extracted with DCM (x2). The combined organic layers were washed with sat. NH₄Cl, sat. NaHCO₃ and brine, dried over Na₂SO₄, and concentrated in vacuo. The crude product was further purified by column chromatography (0−4% (MeOH + 1%NH₄OH)/DCM) to afford the pure product (66 mg, 35% yield) as a white powder. ^{1}H NMR (500 MHz, DMSO) δ 8.35 (dd, *J* = 4.9, 1.6 Hz, 1H), 8.31 (s, 0H), 8.10 (d, *J* = 7.6 Hz, 1H), 7.36 (dt, *J* = 8.0, 2.0 Hz, 1H), 7.17−7.09 (m, 4H), 6.98 (dd, *J* = 16.5, 9.9 Hz, 1H), 6.06 (d, *J* = 9.9 Hz, 1H), 5.98 (d, *J* = 16.5 Hz, 1H), 5.81 (s, 1H), 3.57 (tdt, *J* = 11.0, 7.6, 3.7 Hz, 1H), 1.79−1.72 (m, 1H), 1.67 (dt, *J* = 12.9, 4.0 Hz, 1H), 1.64−1.47 (m, 2H), 1.33−1.19 (m, 2H), 1.17 (s, 9H), 1.16−0.92 (m, 2H). ^{13}C NMR (126 MHz, DMSO) δ 167.43, 150.53, 150.51, 148.97, 136.88, 136.07, 133.56, 131.92, 131.00, 127.18, 124.92, 122.94, 63.05, 47.95, 34.19, 32.07, 31.88, 30.94, 25.09, 24.41, 24.31. HRMS (ESI/Q-TOF) *m/z*: [M + Na]⁺ calculated for C₂₅H₃₃N₃NaO₃S 478.2135; found 478.2127.

N-(4-(*tert*-butyl)phenyl)-*N*-(2-(cyclohexylamino)-2-oxo-1-(pyridin-3-yl)ethyl)-2-fluoroacetamide (15a). Compound was made and purified using general procedure A, pale yellow solid 70% yield, 270 mg. ^{1}H NMR (500 MHz, CDCl₃) δ 8.47 (dd, *J* = 4.9, 1.7 Hz, 1H), 8.43 (d, *J* = 2.3 Hz, 1H), 7.43 (dt, *J* = 7.9, 2.0 Hz, 1H), 7.24 (s, 2H), 7.06 (ddd, *J* = 8.0, 4.8, 0.8 Hz, 1H), 6.04 (s, 1H), 5.87 (d, *J* = 7.8 Hz, 1H), 4.64 (d, *J* = 3.1 Hz, 1H), 4.55 (d, *J* = 3.3 Hz, 1H), 3.86−3.75 (m, 1H), 2.02−1.95 (m, 1H), 1.89−1.81 (m, 1H), 1.74−1.55 (m, 3H), 1.44−1.28 (m, 2H), 1.25 (s, 9H), 1.22−1.02 (m, 3H). ^{13}C NMR (126 MHz, CDCl₃) δ 168.05, 167.89, 167.48, 153.00, 151.45, 149.99, 138.13, 133.76, 129.97, 129.82, 126.64, 123.12, 78.70 (d, *J* = 178.1 Hz), 62.38, 49.16, 34.84, 32.94 (d, *J* = 9.3 Hz), 31.31, 25.57, 24.90 (d, *J* = 6.9 Hz). HRMS (ESI/Q-TOF) *m/z*: [M + Na]⁺ calculated for C₂₅H₃₂FN₃NaO₂ 448.2371; found 448.2366.

N-(4-(*tert*-butyl)phenyl)-2-chloro-*N*-(2-(cyclohexylamino)-2-oxo-1-(pyridin-3-yl)ethyl) acetamide (16a). Compound was made and purified using general procedure A, yellow solid 93% yield, 370 mg. ^{1}H NMR (500 MHz, CDCl₃) δ 8.47 (dd, *J* = 4.8, 1.6 Hz, 1H), 8.43 (d, *J* = 2.3 Hz, 1H), 7.44 (dt, *J* = 7.9, 2.0 Hz, 1H), 7.26 (s, 3H), 7.07 (ddd, *J* = 7.8, 4.9, 0.8 Hz, 1H), 5.99 (s, 1H), 5.88 (s, 1H), 3.85 (s, 2H), 3.84−3.78 (m, 1H), 1.98 (dd, *J* = 12.6, 4.2 Hz, 1H), 1.85 (dd, *J* = 12.6, 4.2 Hz, 1H), 1.74−1.63 (m, 2H), 1.59 (dt, *J* = 12.8, 3.8 Hz, 1H), 1.43−1.28 (m, 2H), 1.26 (s, 9H), 1.22−1.03 (m, 3H). ^{13}C NMR (126 MHz, CDCl3) δ 167.43, 167.42, 152.83, 151.27, 149.75, 138.27, 135.35, 130.28, 129.73, 126.61, 123.16, 63.16, 49.11, 42.58, 34.84, 32.97, 32.90, 31.33, 25.57, 24.91, 24.85. HRMS (ESI/Q-TOF) *m/z*: [M + Na]⁺ calculated for C₂₅H₃₂ClN₃NaO₂ 464.2075; found 464.2087.

Ethyl (*E*)-4-((4-(*tert*-butyl)phenyl)(2-(cyclohexylamino)-2-oxo-1-(pyridin-3-yl)ethyl)amino)-4-oxobut-2-enoate (17a).

Compound was made and purified using general procedure A, white powder 52% yield, 170 mg. ^{1}H NMR (500 MHz, CDCl$_3$) δ 8.51–8.38 (m, 2H), 7.49 (dt, J = 8.1, 2.0 Hz, 1H), 7.23 (d, J = 8.1 Hz, 2H), 7.09 (dd, J = 8.0, 4.8 Hz, 1H), 6.85 (d, J = 15.3 Hz, 1H), 6.72 (d, J = 15.3 Hz, 1H), 6.24 (d, J = 8.1 Hz, 1H), 6.10 (s, 1H), 4.12 (q, J = 7.1 Hz, 2H), 3.80 (dtd, J = 10.8, 7.2, 4.0 Hz, 1H), 1.98–1.90 (m, 1H), 1.89–1.79 (m, 1H), 1.72–1.53 (m, 3H), 1.33 (ddd, J = 13.0, 10.0, 3.3 Hz, 1H), 1.25 (s, 9H), 1.20 (t, J = 7.1 Hz, 3H), 1.10 (ddt, J = 23.0, 15.4, 10.8 Hz, 1H). ^{13}C NMR (126 MHz, CDCl$_3$) δ 167.37, 165.46, 165.04, 152.42, 150.54, 148.89, 138.83, 135.41, 133.89, 132.15, 130.95, 129.77, 126.48, 123.26, 63.08, 61.13, 49.00, 34.77, 32.90, 32.84, 31.28, 25.53, 24.86, 24.80, 14.11. HRMS (ESI/Q-TOF) m/z: [M + Na]$^+$ calculated for C$_{29}$H$_{37}$N$_3$NaO$_4$ 514.2676; found 514.2691.

N-(4-(*tert*-butyl)phenyl)-N-(2-(cyclohexylamino)-2-oxo-1-(pyridin-3-yl)ethyl)-2-oxopropanamide (18a). To a solution of 4-*tert*-butylaniline (0.10 mL, 0.67 mmol, 1.0 eq.) in MeOH (2 mL) was added 3-pyridine carboxaldehyde (0.06 mL, 0.67 mmol, 1.0 eq.) and the solution stirred at room temperature for 30 min. The solution was cooled to 0 °C, and pyruvic acid (0.06 mL, 0.80 mmol, 1.2 eq.) and cyclohexyl isocyanide (0.10 mL, 0.80 mmol, 1.2 eq.) were added in quick succession. The solution was slowly warmed to room temperature and stirred overnight. The crude reaction mixture was evaporated in vacuo and purified by column chromatography (1:1 Hex:EtOAc) to afford the product (105 mg, 36%) as a white powder. ^{1}H NMR (500 MHz, CDCl$_3$) δ 8.69 (s, 1H), 8.56 (s, 1H), 7.84 (d, J = 8.0 Hz, 1H), 7.35 (d, J = 7.7 Hz, 1H), 7.23 (d, J = 8.8 Hz, 2H), 7.03 (d, J = 8.1 Hz, 2H), 6.49 (d, J = 8.0 Hz, 1H), 6.15 (s, 1H), 3.80 (tdd, J = 10.7, 6.7, 4.0 Hz, 1H), 2.19 (s, 3H), 1.97–1.79 (m, 2H), 1.69 (ddt, J = 17.1, 13.1, 4.0 Hz, 2H), 1.59 (dt, J = 12.8, 3.9 Hz, 1H), 1.41–1.25 (m, 2H), 1.24 (s, 9H), 1.16 (dtd, J = 16.2, 13.6, 12.7, 9.9 Hz, 2H). ^{13}C NMR (126 MHz, CDCl$_3$) δ 197.49, 168.14, 166.68, 152.69, 150.19, 148.63, 139.25, 134.15, 130.64, 129.82, 126.29, 123.61, 62.36, 49.22, 34.77, 32.85, 32.81, 31.26, 27.84, 25.51, 24.87, 24.81. HRMS (ESI/Q-TOF) m/z: [M + Na]$^+$ calculated for C$_{26}$H$_{33}$N$_3$NaO$_3$ 458.2412; found 458.2421.

Ethyl (4-(*tert*-butyl)phenyl)(2-(cyclohexylamino)-2-oxo-1-(pyridin-3-yl)ethyl)carbamate (19a). To a solution of **5a** (0.41 mmol, 150 mg) in DCM (8 mL) was added pyridine (0.82 mmol, 0.06 mL) and the solution was cooled to 0 °C. Ethyl chloroformate (0.49 mmol, 0.05 mL) was added dropwise and stirred at 0 °C for 1 h, then room temperature overnight. The reaction was quenched with water and extracted twice with DCM. The combined organic layers were washed with sat. NH$_4$Cl, sat. NaHCO$_3$ and brine, then dried over Na$_2$SO$_4$ and concentrated in vacuo. The crude residue was further purified by column chromatography (0–80% EtOAc/Hex) to afford the desired product (136 mg, 76% yield) as a white powder. ^{1}H NMR (500 MHz, CDCl$_3$) δ 8.55 (s, 1H), 8.51–8.46 (m, 1H), 7.66 (dt, J = 8.1, 1.9 Hz, 1H), 7.23 (td, J = 6.0, 5.5, 2.3 Hz, 3H), 6.97 (d, J = 8.5 Hz, 2H), 6.24 (d, J = 8.1 Hz, 1H), 5.72 (s, 1H), 4.15 (qd, J = 7.1, 2.7 Hz, 2H), 3.84 (dddd, J = 14.5, 10.5, 7.9, 3.9 Hz, 1H), 1.99–1.83 (m, 2H), 1.69 (tt, J = 12.5, 3.9 Hz, 2H), 1.60 (dt, J = 12.9, 3.9 Hz, 1H), 1.43–1.30 (m, 2H), 1.26 (s, 9H), 1.22–1.08 (m, 6H). ^{13}C NMR (126 MHz, CDCl3) δ 167.76, 156.29, 150.83, 148.98, 147.37, 139.54, 137.15, 132.52, 128.33, 126.00, 123.58, 64.95, 62.65, 48.91, 34.67, 32.97, 32.93, 31.38, 25.57, 24.84, 24.82, 14.64. HRMS (ESI/Q-TOF) m/z: [M + Na]$^+$ calculated for C$_{26}$H$_{35}$N$_3$NaO$_3$ 460.2571; found 460.2579.

N-(4-(*tert*-butyl)phenyl)-2-cyano-N-(2-(cyclohexylamino)-2-oxo-1-(pyridin-3-yl)ethyl)acetamide (20a). Compound was made and purified using general procedure B, white solid 84% yield, 328 mg. ^{1}H NMR (500 MHz, CDCl$_3$) δ 8.52–8.45 (m, 1H), 8.41 (s, 1H), 7.44–7.38 (m, 2H), 7.10–7.04 (m, 2H), 6.47 (s, 1H), 5.98 (d, J = 2.1 Hz, 1H), 5.68 (s, 1H), 3.86–3.75 (m, 1H), 3.27–3.20 (m, 2H), 1.97 (d, J = 12.6 Hz, 1H), 1.84 (d, J = 13.0 Hz, 2H), 1.68–1.56 (m, 2H), 1.40–1.28 (m, 2H), 1.25 (s, 9H), 1.23–0.99 (m, 4H). ^{13}C NMR

(126 MHz, CDCl$_3$) δ 166.87, 162.92, 152.91, 151.14, 149.87, 137.79, 135.02, 129.75, 129.52, 123.02, 113.69, 62.87, 49.04, 34.61, 32.70, 32.64, 31.04, 26.19, 25.28, 24.67, 24.60.

2-((4-(*tert*-butyl)phenyl)(cyanomethyl)amino)-N-cyclohexyl-2-(pyridin-3-yl)acetamide (21a). To a solution of 2-((4-(*tert*-butyl)phenyl)amino)acetonitrile (0.27 mmol, 50 mg) and 3-pyridinecarboxaldehyde (0.27 mmol, 0.03 mL) in MeOH (3 mL) was added cyclohexyl isocyanide (0.27 mmol, 0.04 mL) and phosphoric acid (0.05 mmol, 0.004 mL, 85%), and the solution stirred at room temperature overnight. The solvent was evaporated under a stream of air, and the crude reaction mixture was suspended in a small amount of EtOAc. Hexanes was added and the precipitate was collected by filtration and rinsed with hexanes and acetone. The precipitate was dried over vacuum to afford the desired product (74 mg, 68% yield) as a white powder. ^{1}H NMR (500 MHz, CDCl$_3$) δ 9.07 (s, 1H), 8.61 (s, 1H), 8.32 (d, J = 7.9 Hz, 1H), 7.61 (t, J = 6.6 Hz, 1H), 7.33 (d, J = 8.6 Hz, 2H), 7.08 (d, J = 8.7 Hz, 2H), 7.03 (d, J = 7.8 Hz, 1H), 5.57 (s, 1H), 4.16 (d, J = 17.9 Hz, 1H), 4.01 (d, J = 17.8 Hz, 1H), 1.98–1.67 (m, 2H), 1.68–1.49 (m, 4H), 1.45–1.28 (m, 1H), 1.27 (s, 9H), 1.24–0.64 (m, 3H). ^{13}C NMR (126 MHz, CDCl3) δ 166.94, 147.84, 143.94, 126.95, 125.47, 120.77, 115.57, 65.98, 48.79, 42.14, 34.47, 32.71, 32.32, 31.42, 31.21, 25.44, 24.68, 24.61.

N-(4-(*tert*-butyl)phenyl)-N-(2-(cyclohexylamino)-2-oxo-1-(pyridin-3-yl)ethyl)-3,3,3-trifluoro-2-oxopropanamide (22a). To a solution of 4-tBu-aniline (0.62 mmol, 0.1 mL) in MeOH was added 3-Py-carboxaldehyde (0.62 mmol, 0.06 mL) and stirred for 30 min. The solution was cooled to 0 °C and trifluoropyruvic acid (0.62 mmol, 100 mg) and cyclohexyl isocyanide (0.62 mmol, 0.08 mL) were added. The solution was slowly warmed to r.t. and stirred overnight. The solvent was evaporated under a stream of air, and the crude reaction mixture was suspended in a small amount of EtOAc. Hexanes was added and the precipitate was collected by filtration and rinsed with hexanes and acetone. The precipitate was dried over vacuum to afford the desired product (87 mg, 29% yield) as a white powder. ^{1}H NMR (500 MHz, CDCl$_3$) δ 8.62 (s, 1H), 8.55–8.51 (m, 1H), 7.60 (d, J = 7.9 Hz, 1H), 7.23 (d, J = 8.6 Hz, 3H), 7.03 (s, 2H), 6.10 (s, 2H), 3.82 (tdt, J = 10.9, 7.8, 3.9 Hz, 1H), 1.90 (dd, J = 49.5, 12.9 Hz, 2H), 1.75–1.54 (m, 4H), 1.43–1.27 (m, 1H), 1.23 (s, 9H), 1.21–1.02 (m, 3H). ^{13}C NMR (126 MHz, CDCl3) δ 165.76, 162.63, 153.82, 150.12, 148.74, 139.63, 132.24, 130.28, 130.01, 126.64, 123.76, 62.36, 49.38, 34.89, 32.81, 32.79, 31.33, 31.21, 31.17, 25.49, 24.88, 24.83. ^{19}F NMR (471 MHz, CDCl$_3$) δ −74.82.

N-(4-(*tert*-butyl)phenyl)-N-(2-(cyclohexylamino)-2-oxo-1-(pyridin-3-yl)ethyl)-4-hydroxybut-2-ynamide (23a). To a solution of 4-tBu-aniline (0.31 mmol, 0.05 mL) in MeOH was added 3-Py-carboxaldehyde (0.31 mmol, 0.03 mL) and stirred for 30 min. 4-hydroxy-butynoic acid (0.31 mmol, 31 mg) and cyclohexyl isocyanide (0.31 mmol, 0.04 mL) were added and the solution stirred at room temperature overnight. The solvent was evaporated under a stream of air, and the crude reaction mixture was suspended in a small amount of EtOAc. Hexanes was added and the precipitate was collected by filtration and further rinsed with hexanes. The precipitate was dried over vacuum to afford the desired product (60 mg, 43% yield) as a white powder. ^{1}H NMR (500 MHz, CDCl$_3$) δ 8.49 (d, J = 2.3 Hz, 1H), 8.44 (dd, J = 4.8, 1.7 Hz, 1H), 7.44 (dt, J = 8.0, 2.0 Hz, 1H), 7.22 (d, J = 8.8 Hz, 2H), 7.06 (dd, J = 8.0, 4.8 Hz, 1H), 7.03 (d, J = 7.9 Hz, 2H), 6.17 (d, J = 8.0 Hz, 1H), 6.07 (s, 1H), 4.05 (s, 2H), 3.84–3.73 (m, 1H), 2.45 (s, 1H), 1.96 (dd, J = 12.5, 4.1 Hz, 1H), 1.84 (dd, J = 12.1, 4.2 Hz, 1H), 1.74–1.53 (m, 2H), 1.43–1.27 (m, 3H), 1.25 (s, 9H), 1.23–1.00 (m, 3H). ^{13}C NMR (126 MHz, CDCl$_3$) δ 167.25, 154.75, 152.38, 151.32, 149.75, 138.19, 135.94, 130.27, 130.25, 125.80, 123.11, 92.47, 78.94, 62.16, 50.59, 49.09, 34.78, 32.88, 32.83, 31.36, 25.57, 24.92, 24.85. HRMS (ESI/Q-TOF) m/z: [M + H]$^+$ calculated for C$_{27}$H$_{33}$N$_3$O$_3$ 448.2595; found 448.2592.

N-cyclohexyl-2-(2-oxoazetidin-1-yl)-2-(pyridin-3-yl)

acetamide (24a). In a 6-dram vial equipped with a stir bar 3-Pyridinecarboxaldehyde (214 mg, 2.0 mmol, 1.0 eq.), glycinamide hydrochloride (221 mg, 2.0 mmol, 1.0 eq.), and triethylamine (202 mg, 2.0 mmol, 1.0 eq.), were mixed in methanol (5 mL). The obtained solution was stirred for 15 min at room temperature. Cyclohexyl isocyanide (218 mg, 2.0 mmol, 1.0 eq.), and acetic acid (120 mg, 2.0 mmol, 1.0 eq.) were then added to the reaction mixture and the walls of the vial were washed with additional MeOH (5 mL). The reaction mixture was stirred at room temperature overnight. The crude reaction mixture was evaporated in vacuo and redissolved in EtOAc (50 mL). The organic layer was extracted with water (3 x 100 mL). The obtained organic layer was dried over Na_2SO_4 and evaporated in vacuo. The obtained crude solid was triturated with hexanes (5 mL) and filtered. The obtained powder was further washed with hexanes (2 x 5 mL). The product was obtained as pale-yellow solid, 428 mg 79%. ^1H NMR (500 MHz, CDCl$_3$) δ 8.59 (s, 2H), 7.75 (dd, J = 8.0, 2.1 Hz, 1H), 7.32 (dd, J = 8.0, 4.9 Hz, 1H), 6.40 (d, J = 7.9 Hz, 1H), 5.34 (s, 0H), 3.76 (dtt, J = 11.4, 8.5, 4.0 Hz, 1H), 3.61 (td, J = 5.6, 2.8 Hz, 1H), 3.20 (td, J = 5.7, 2.8 Hz, 1H), 3.05−2.97 (m, 1H), 2.95−2.87 (m, 1H), 1.94−1.83 (m, 2H), 1.73−1.55 (m, 2H), 1.43−1.26 (m, 3H), 1.22−0.98 (m, 4H). ^{13}C NMR (126 MHz, CDCl$_3$) δ 168.10, 166.82, 150.04, 149.62, 135.82, 130.98, 123.90, 58.10, 48.97, 39.28, 36.53, 32.89, 32.85, 29.84, 25.52, 24.82, 24.78.

2-((cyanomethyl)amino)-N-cyclohexyl-2-(pyridin-3-yl)acetamide (25a). In a 6-dram vial equipped with a stir bar 3-pyridinecarboxaldehyde (107 mg,1.0 mmol, 1.0 eq.) and β-alanine (89 mg, 1.0 mmol, 1.0 eq.) were mixed together in MeOH (4 mL). The obtained solution was stirred for 30 min at room temperature. Cyclohexyl isocyanide (109 mg, 1.0 mmol, 1.0 eq.) was added to the reaction mixture and the walls of the vial were washed with 1 mL of MeOH. The obtained reaction mixture was stirred at room temperature overnight. The crude reaction mixture was evaporated in vacuo and redissolved in DCM. The obtained crude solution was deposited on silica. It was then purified using flash column chromatography using DCM/MeOH (gradient 0 → 5%) as eluent. The product was obtained as colorless oil, 156 mg 54%. ^1H NMR (500 MHz, CDCl$_3$) δ 8.65 (d, J = 2.4 Hz, 1H), 8.62 (dd, J = 4.8, 1.7 Hz, 1H), 7.75 (dt, J = 7.9, 2.0 Hz, 1H), 7.34 (dd, J = 7.9, 4.8 Hz, 1H), 6.02 (d, J = 8.4 Hz, 1H), 4.40 (s, 1H), 3.82−3.71 (m, 1H), 3.64 (d, J = 17.5 Hz, 1H), 3.45 (d, J = 17.3 Hz, 1H), 2.53 (s, 1H), 1.85 (ddd, J = 17.0, 12.4, 4.4 Hz, 2H), 1.64 (dtd, J = 25.9, 9.0, 4.7 Hz, 4H), 1.40−1.28 (m, 2H), 1.20−1.02 (m, 2H). ^{13}C NMR (126 MHz, CDCl$_3$) δ 168.45, 150.57, 149.43, 135.66, 133.25, 124.24, 116.87, 63.55, 48.67, 35.50, 33.06, 33.02, 25.49, 24.83. HRMS (ESI/Q-TOF) m/z: [M + Na]$^+$ calculated for $C_{15}H_{20}N_4NaO$ 295.1529; found 295.1523.

(E)-N-(4-(*tert*-butyl)phenyl)-N-(2-(*tert*-butylamino)-2-oxo-1-(pyridin-3-yl)ethyl)but-2-enamide (8b). Compound was made and purified using general procedure A, white solid 54% yield, 198 mg. ^1H NMR (500 MHz, CDCl$_3$) δ 8.48−8.41 (m, 2H), 7.43 (d, J = 8.0 Hz, 1H), 7.26 (d, J = 8.2 Hz, 2H), 7.05 (dd, J = 8.0, 4.8 Hz, 1H), 7.01−6.95 (m, 1H), 6.91 (s, 1H), 6.35 (s, 1H), 6.07 (s, 1H), 5.68 (dd, J = 15.1, 1.7 Hz, 1H), 1.75 (dd, J = 7.1, 1.7 Hz, 3H), 1.39 (s, 9H), 1.30 (s, 9H).^{13}C NMR (126 MHz, CDCl$_3$) δ 168.38, 166.89, 151.78, 151.38, 149.47, 142.97, 138.10, 136.53, 130.94, 129.85, 126.20, 122.77, 63.16, 51.73, 34.76, 31.38, 28.81, 18.21. HRMS (ESI/Q-TOF) m/z: [M + Na]$^+$ calculated for $C_{25}H_{33}N_3NaO_2$ 430.2438; found 430.2450.

N-(4-(*tert*-butyl)phenyl)-N-(2-(*tert*-butylamino)-2-oxo-1-(pyridin-3-yl)ethyl)but-2-ynamide (13b). Compound was made and purified using general procedure A, white solid 82% yield, 300 mg. ^1H NMR (500 MHz, CDCl$_3$) δ 8.45 (dd, J = 4.8, 1.5 Hz, 1H), 8.43 (d, J = 2.3 Hz, 1H), 7.43 (dt, J = 8.1, 2.0 Hz, 1H), 7.25−7.20 (m, 2H), 7.05 (dd, J = 8.0, 4.8 Hz, 1H), 6.97 (d, J = 8.0 Hz, 2H), 6.09 (s, 1H), 5.96 (s, 1H), 1.68 (s, 3H), 1.36 (s, 9H), 1.26 (s, 9H). ^{13}C NMR (126 MHz, CDCl$_3$) δ 167.54, 155.43, 151.94, 151.27, 149.67, 138.25, 136.37, 130.29, 129.91, 125.77, 122.95, 92.21, 73.90, 62.66, 51.98, 34.76, 31.35, 28.75. HRMS (ESI/Q-TOF) m/z: [M + Na]$^+$ calculated for $C_{25}H_{31}N_3NaO_2$ 428.2308; found 428.2307.

N-(4-(*tert*-butyl)phenyl)-N-(2-(*tert*-butylamino)-2-oxo-1-(pyridin-3-yl)ethyl)acrylamide (6b). Compound was made and purified using general procedure C, white solid 42% yield, 150 mg. ^1H NMR (500 MHz, CDCl$_3$) δ 8.46−8.42 (m, 2H), 7.43 (dt, J = 8.0, 2.0 Hz, 1H), 7.24 (d, J = 8.3 Hz, 2H), 7.04 (ddd, J = 8.0, 4.9, 0.9 Hz, 1H), 6.91 (s, 1H), 6.40 (dd, J = 16.8, 2.0 Hz, 1H), 6.20 (s, 1H), 6.06 (s, 1H), 5.98 (dd, J = 16.8, 10.3 Hz, 1H), 5.55 (dd, J = 10.3, 2.0 Hz, 1H), 1.37 (s, 9H), 1.26 (s, 9H). ^{13}C NMR (126 MHz, CDCl$_3$) δ 168.13, 166.58, 152.00, 151.38, 149.58, 138.15, 136.19, 130.77, 129.89, 128.77, 128.60, 126.25, 122.87, 63.18, 51.84, 34.77, 31.37, 28.80. HRMS (ESI/Q-TOF) m/z: [M + Na]$^+$ calculated for $C_{24}H_{31}N_3NaO_2$ 416.2308; found 416.2291.

N-(*tert*-butyl)-2-(N-(4-(*tert*-butyl)phenyl)acetamido)-2-(pyridin-3-yl)acetamide (4b). Compound was made and purified using general procedure A, white solid 84% yield, 290 mg. ^1H NMR (500 MHz, CDCl$_3$) δ 8.43 (dd, J = 4.8, 1.6 Hz, 1H), 8.40 (s, 1H), 7.37 (d, J = 8.1 Hz, 1H), 7.22 (d, J = 8.2 Hz, 2H), 7.01 (dd, J = 7.6, 5.3 Hz, 1H), 6.91 (s, 1H), 6.04 (s, 1H), 5.98 (s, 1H), 1.87 (s, 3H), 1.36 (s, 9H), 1.25 (s, 9H). ^{13}C NMR (126 MHz, CDCl$_3$) δ 171.75, 168.32, 151.86, 151.45, 149.59, 138.13, 137.31, 130.88, 129.65, 126.24, 122.84, 62.64, 51.80, 34.72, 31.36, 28.79, 23.36. HRMS (ESI/Q-TOF) m/z: [M + Na]$^+$ calculated for $C_{23}H_{31}N_3NaO_2$ 404.2308; found 404.2307.

N-(4-(*tert*-butyl)phenyl)-N-(2-(cyclopentylamino)-2-oxo-1-(pyridin-3-yl)ethyl)but-2-ynamide (13c). Compound was made and purified using general procedure A, white solid 94% yield, 354 mg. ^1H NMR (500 MHz, CDCl$_3$) δ 8.46 (dd, J = 4.9, 1.6 Hz, 1H), 8.44 (d, J = 2.3 Hz, 1H), 7.50−7.44 (m, 1H), 7.23 (d, J = 8.8 Hz, 2H), 7.07 (dd, J = 8.0, 4.8 Hz, 1H), 6.97 (d, J = 8.0 Hz, 2H), 6.20 (s, 1H), 6.02 (s, 1H), 4.23 (h, J = 6.8 Hz, 1H), 2.02 (dd, J = 13.0, 6.2 Hz, 1H), 1.95 (q, J = 2.7 Hz, 1H), 1.68 (s, 3H), 1.64−1.56 (m, 4H), 1.49−1.42 (m, 1H), 1.39−1.34 (m, 1H), 1.26 (s, 9H). ^{13}C NMR (126 MHz, CDCl$_3$) δ 167.92, 155.47, 151.97, 151.06, 149.54, 138.34, 136.39, 130.32, 129.87, 125.79, 123.06, 92.26, 73.85, 62.23, 51.89, 34.76, 33.08, 33.01, 31.34, 23.87, 23.84, 4.06. HRMS (ESI/Q-TOF) m/z: [M + H]$^+$ calculated for $C_{26}H_{32}N_3O_2$ 418.24890; found 418.24854.

N-(2-(benzylamino)-2-oxo-1-(pyridin-3-yl)ethyl)-N-(4-(*tert*-butyl)phenyl)but-2-ynamide (13d). Compound was made and purified using general procedure A, pale yellow solid 86% yield, 340 mg. ^1H NMR (500 MHz, CDCl$_3$) δ 8.43 (d, J = 4.7 Hz, 1H), 8.40 (t, J = 1.6 Hz, 2H), 7.45 (d, J = 7.8 Hz, 1H), 7.33−7.16 (m, 6H), 7.05 (dd, J = 8.0, 4.8 Hz, 1H), 6.94 (d, J = 8.1 Hz, 2H), 6.66 (d, J = 8.5 Hz, 1H), 6.05 (s, 1H), 4.55−4.43 (m, 2H), 1.66 (s, 3H), 1.25 (s, 9H). ^{13}C NMR (126 MHz, CDCl$_3$) δ 168.38, 155.47, 151.96, 151.08, 149.59, 138.41, 137.91, 136.33, 130.18, 129.93, 128.85, 127.84, 127.64, 125.78, 123.11, 92.27, 73.83, 62.35, 44.02, 34.74, 31.65, 31.33, 4.04. HRMS (ESI/Q-TOF) m/z: [M + H]$^+$ calculated for $C_{28}H_{30}N_3O_2$ 440.23325; found 440.23303.

N-(4-(*tert*-butyl)phenyl)-2-chloro-N-(2-(cyclopentylamino)-2-oxo-1-(pyridin-3-yl)ethyl)acetamide (16b). Compound was made and purified using general procedure A, pale yellow solid 88% yield, 340 mg. ^1H NMR (500 MHz, CDCl$_3$) δ 8.46 (dd, J = 4.9, 1.7 Hz, 1H), 8.42 (d, J = 2.3 Hz, 1H), 7.44 (dd, J = 8.0, 2.1 Hz, 1H), 7.26 (s, 3H), 7.06 (dd, J = 8.0, 4.8 Hz, 1H), 6.06 (d, J = 7.3 Hz, 1H), 5.99 (s, 1H), 4.23 (h, J = 6.8 Hz, 1H), 3.85 (s, 2H), 2.10−1.99 (m, 1H), 1.98−1.90 (m, 1H), 1.70−1.52 (m, 4H), 1.51−1.40 (m, 1H), 1.33 (dq, J = 13.6, 6.8, 5.8 Hz, 1H), 1.25 (s, 9H). ^{13}C NMR (126 MHz, CDCl$_3$) δ 167.93, 167.42, 152.82, 151.20, 149.68, 138.30, 135.29, 130.25, 129.75, 126.59, 123.16, 63.03, 51.94, 42.61, 34.83, 33.08, 33.03, 31.32, 23.88, 23.86. HRMS (ESI/Q-TOF) m/z: [M + H]$^+$ calculated for $C_{24}H_{31}N_3O_2Cl$ 428.20993; found 428.21001.

N-benzyl-2-(N-(4-(*tert*-butyl)phenyl)-2-chloroacetamido)-2-(pyridin-3-yl)acetamide (16c). Compound was made and purified using general procedure A, yellow solid 91% yield, 370 mg. ^1H NMR

(500 MHz, CDCl$_3$) δ 8.45 (dd, J = 4.8, 1.6 Hz, 1H), 8.40 (d, J = 2.3 Hz, 1H), 7.43 (dt, J = 8.0, 2.1 Hz, 1H), 7.35–7.13 (m, 9H), 7.04 (ddd, J = 8.1, 4.9, 0.9 Hz, 1H), 6.55 (s, 1H), 6.06 (s, 1H), 4.49 (qd, J = 14.8, 5.8 Hz, 2H), 3.85 (d, J = 1.5 Hz, 2H), 1.25 (s, 9H). ^{13}C NMR (126 MHz, CDCl$_3$) δ 168.45, 167.46, 152.84, 151.36, 149.93, 138.24, 137.84, 135.18, 129.95, 129.79, 128.86, 127.83, 127.70, 126.59, 123.14, 63.10, 44.07, 42.67, 34.82, 31.31. HRMS (ESI/Q-TOF) m/z: [M + H]$^+$ calculated for C$_{26}$H$_{29}$N$_3$O$_2$Cl 450.19428; found 450.19392.

N-(4-(*tert*-butyl)phenyl)-N-(2-(cyclopentylamino)-2-oxo-1-(pyridin-3-yl)ethyl)cyclopent-1-ene-1-carboxamide (11b). Compound was made and purified using general procedure B, white solid 67% yield, 270 mg. ^{1}H NMR (500 MHz, CDCl$_3$) δ 8.51 (d, J = 2.3 Hz, 1H), 8.49 (dd, J = 4.8, 1.7 Hz, 1H), 7.54 (dt, J = 8.0, 2.0 Hz, 1H), 7.25–7.19 (m, 2H), 7.11 (ddd, J = 8.0, 4.8, 0.8 Hz, 1H), 6.92 (d, J = 8.0 Hz, 2H), 6.35 (d, J = 7.4 Hz, 1H), 6.05 (s, 1H), 5.85 (p, J = 2.2 Hz, 1H), 4.28 (q, J = 6.7 Hz, 1H), 2.22 (ddd, J = 7.6, 6.1, 2.5 Hz, 2H), 2.15 (tt, J = 6.4, 2.2 Hz, 2H), 2.10–1.93 (m, 2H), 1.65–1.64 (m, 6H), 1.53–1.35 (m, 2H), 1.28 (s, 9H). ^{13}C NMR (126 MHz, CDCl$_3$) δ 168.81, 168.55, 151.49, 151.12, 149.40, 140.09, 138.96, 137.84, 137.57, 130.79, 129.37, 125.73, 122.83, 63.78, 51.62, 34.60, 33.71, 33.13, 33.01, 32.97, 31.25, 23.73, 23.71, 23.18. HRMS (ESI/Q-TOF) m/z: [M + H]$^+$ calculated for C$_{28}$H$_{36}$N$_3$O$_2$ 446.28020; found 446.28024.

N-[2-(4-methoxy) ethyl] formamide (26b). Compound was made and purified using general procedure D. Light yellow liquid with 95% yield, 852.0 mg. Rf = 0.07 (1:1 EtOAc:hexanes). ^{1}H NMR (500 MHz, CDCl$_3$) mixture of rotamers is observed, major rotamer is given: δ 8.10 (d, J = 1.7 Hz, 1H), 7.12 (d, J = 8.6 Hz, 2H), 6.85 (d, J = 8.7 Hz, 2H), 5.92 (bs, 1H), 3.79 (s, 3H), 3.52 (q, J = 6.2 Hz, 2H), 2.78 (t, J = 7.1 Hz, 2H). ^{13}C NMR (126 MHz, CDCl$_3$) mixture of rotamers is observed, major rotamer is given: δ 164.55, 161.26, 158.35, 129.70, 114.09, 55.28, 39.40, 34.60. HRMS (ESI) m/z: [M + Na]+ calculated for C$_{10}$H$_{13}$NNaO$_2$ 202.0838; found 202.0841.

N-[2-(3-chlorophenyl) ethyl] formamide (26c). Compound was made and purified using general procedure D. Light yellow liquid with 98% yield, 899.3 mg. Rf = 0.12 (1:1 EtOAc:hexanes). ^{1}H NMR (500 MHz, CDCl$_3$) mixture of rotamers is observed, major rotamer is given: δ 8.09 (d, J = 1.8 Hz, 1H), 7.31–7.15 (m, 3H), 7.09 (dt, J = 7.2, 1.5 Hz, 1H), 6.10 (bs, 1H), 3.53 (q, J = 6.8 Hz, 2H), 2.82 (t, J = 7.0 Hz, 2H). ^{13}C NMR (126 MHz, CDCl$_3$) mixture of rotamers is observed, major rotamer is given: δ 161.35, 140.67, 134.36, 129.95, 128.87, 126.98, 126.82, 38.64, 35.20. HRMS (ESI) m/z: [M + Na]+ calculated for C$_9$H$_{10}$ClNNaO 206.0343; found 206.0346.

N-[2-(3-methoxy) ethyl] formamide (26d). Compound was made and purified using general procedure D. Light yellow liquid with 40% yield, 331.0 mg. Rf = 0.18 (2:1 EtOAc:hexanes). ^{1}H NMR (500 MHz, CDCl$_3$) mixture of rotamers is observed, major rotamer is given: δ 8.15 (d, J = 1.7 Hz, 1H), 7.27–7.24 (m, 1H), 6.82–6.79 (m, 2H), 6.78–6.75 (m, 1H), 5.64 (bs, 1H), 3.82 (s, 3H), 3.59 (q, J = 6.8 Hz, 2H), 2.84 (t, J = 6.9 Hz, 2H). ^{13}C NMR (126 MHz, CDCl$_3$) mixture of rotamers is observed, major rotamer is given: δ 161.12, 159.89, 140.09, 129.75, 121.05, 114.54, 111.93, 55.21, 39.05, 35.54. HRMS (ESI) m/z: [M + Na]+ calculated for C$_{10}$H$_{13}$NNaO$_2$ 202.0838; found 202.0831.

N-(3-phenylpropyl)formamide (26e). Compound was made and purified using general procedure D. Colourless liquid with 99% yield, 803 mg. Rf = 0.31 (4:1 EtOAc:hexanes). ^{1}H NMR (500 MHz, CDCl$_3$) mixture of rotamers is observed, major rotamer is given: δ 8.15 (s, 1H), 7.33–7.28 (m, 2H), 7.23–7.17 (m, 3H), 6.07 (bs, 1H), 3.32 (q, J = 7.2 Hz, 2H), 2.67 (t, J = 7.2 Hz, 2H), 1.89 (p, J = 7.2 Hz, 2H). ^{13}C NMR (126 MHz, CDCl$_3$) mixture of rotamers is observed, major rotamer is given: δ 161.43, 141.23, 128.51, 128.38, 126.09, 37.80, 33.17, 31.10. HRMS (APCI) m/z: [M + H]+ calculated for C$_{10}$H$_{14}$NO 164.1070; found 164.1070.

N-(1-benzylpiperidin-4-yl)formamide (26f). Compound was made and purified using general procedure D. Orange viscous liquid with more than 99% yield, 1270 mg. Rf = 0.05 (4:1 EtOAc:hexanes). 1H NMR (500 MHz, CDCl$_3$) mixture of rotamers is observed, major rotamer is given: δ 8.12 (s, 1H), 7.35–7.30 (m, 4H), 7.28–7.25 (m,1H), 5.71 (bs, 1H), 3.94–3.87 (m, 1H), 3.51 (s, 2H), 2.83 (d, J = 12.2 Hz, 2H), 2.14 (t, J = 11.4 Hz, 2H), 1.93 (d, J = 12.7 Hz, 2H), 1.51 (dtd, J = 12.7, 11.0, 3.8 Hz, 2H).). ^{13}C NMR (126 MHz, CDCl$_3$) mixture of rotamers is observed, major rotamer is given: δ 160.55, 138.18, 129.13, 128.26, 127.12, 63.00, 52.11, 45.42, 32.13. HRMS (ESI) m/z: [M + H]+ calculated for C$_{13}$H$_{19}$N$_2$O 219.1492; found 219.1491.

(S)−N-(1-phenylethyl)formamide (26g). Compound was made and purified using general procedure D. Light yellow liquid with more than 99% yield, 763.7 mg. Rf = 0.27 (2:1 EtOAc:hexanes). ^{1}H NMR (500 MHz, CDCl$_3$) mixture of rotamers is observed, major rotamer is given: δ 8.15 (s, 1H), 7.40−7.25 (m, 5H), 6.17 (s, 1H), 5.21 (p, J = 7.1 Hz, 1H), 1.52 (dd, J = 7.0, 1.6 Hz, 3H). ^{13}C NMR (126 MHz, CDCl$_3$) mixture of rotamers is observed, major rotamer is given: δ 160.34, 142.63, 128.74, 127.53, 126.16, 47.61, 21.76. HRMS (ESI) m/z: [M + Na]+ calculated for C$_9$H$_{11}$NNaO 172.0733; found 172.0735.

1-(2-isocyanoethyl)-4-methoxybenzene (27b). Compound was made and purified using general procedure E. Dark red liquid with 73% yield, 228.6 mg. Rf = 0.87 (3:1 Et$_2$O:DCM). ^{1}H NMR (500 MHz, CDCl$_3$): δ 7.17 (d, J = 8.7 Hz, 2H), 6.90 (d, J = 8.6 Hz, 2H), 3.82 (s, 3H), 3.59 (tt, J = 7.1, 1.8 Hz, 2H), 2.95 (tt, J = 7.1, 2.1 Hz, 2H). ^{13}C NMR (126 MHz, CDCl$_3$): δ 158.83, 156.43 (t, J = 5.4 Hz), 129.74, 128.72, 114.20, 55.30, 43.28 (t, J = 6.3 Hz), 34.88. HRMS (ESI) m/z: [M + Na]+ calculated for C$_{10}$H$_{11}$NNaO 184.0733; found 184.0730.

1-chloro-3-(2-isocyanoethyl)benzene (27c). Compound was made and purified using general procedure E. Dark red liquid with 83% yield, 273 mg. Rf = 0.84 (3:1 Et$_2$O:DCM). ^{1}H NMR (500 MHz, CDCl$_3$): δ 7.32−7.27 (m, 2H), 7.25 (s, 1H), 7.15−7.11 (m, 1H),f 3.62 (tt, J = 7.0, 1.9 Hz, 2H), 2.96 (tt, J = 7.0, 2.1 Hz, 2H). ^{13}C NMR (126 MHz, CDCl$_3$): δ 157.14 (t, J = 5.4 Hz), 138.54, 134.61, 130.10, 128.81, 127.58, 126.96, 42.67 (t, J = 6.6 Hz), 35.23. HRMS (ESI) m/z: [M + Na]+ calculated for C$_9$H$_8$ClNNa 188.0237; found 188.0232.

1-(2-isocyanoethyl)-3-methoxybenzene (27d). Compound was made and purified using general procedure E. Orange liquid with 79% yield, 256 mg. Rf = 0.95 (2:1 EtOAc:hexanes). ^{1}H NMR (500 MHz, CDCl$_3$): δ 7.28 (t, J = 8.0 Hz, 1H), 6.86−6.83 (m, 2H), 6.79 (t, J = 2.1 Hz, 1H), 3.83 (s, 3H), 3.63 (tt, J = 7.2, 1.9 Hz, 2H), 2.99 (tt, J = 7.1, 2.0 Hz, 2H). ^{13}C NMR (126 MHz, CDCl$_3$): δ 159.89,156.62 (t, J = 5.3 Hz), 138.19, 129.84, 120.94, 114.52, 112.56, 55.24, 42.89 (t, J = 6.6 Hz), 35.74. HRMS (ESI) m/z: [M + Na]+ calculated for C$_{10}$H$_{11}$NNaO 184.0733; found 184.0730.

(3-isocyanopropyl)benzene (27e). Compound was made and purified using general procedure E. Orange liquid with 71% yield, 196 mg. Rf = 0.89 (1:1 EtOAc:hexanes). ^{1}H NMR (500 MHz, CDCl$_3$): δ 7.35−7.32 (m, 2H), 7.27−7.21 (m, 3H), 3.39 (tt, J = 6.5, 1.8 Hz 2H), 2.82 (t, J = 7.4 Hz, 2H), 2.07−1.98 (m, 2H). ^{13}C NMR (126 MHz, CDCl$_3$) δ 156.28 (t, J = 5.6 Hz), 139.82, 128.67, 128.49, 126.46, 40.70 (t, J = 6.3 Hz), 32.20, 30.56. HRMS (APCI) m/z: [M + H]+ calculated for C$_{10}$H$_{12}$N 146.0964; found 146.0967.

1-benzyl-4-isocyanopiperidine (27f). Compound was made and purified using general procedure E. Orange viscous liquid with 50% yield, 300 mg (3 mmol 2 g used). Rf = 0.74 (3:1 Et$_2$O:DCM). ^{1}H NMR (500 MHz, CDCl$_3$): δ 7.47−7.21 (m, 5H), 3.68 (s, 1H), 3.53 (s, 2H), 2.67 (s, 2H), 2.35 (s, 2H), 2.01−1.95 (m, 2H), 1.93−1.83 (m, 2H). ^{13}C NMR (126 MHz, CDCl$_3$) δ 155.19 (t, J = 5.5 Hz), 138.12, 129.01, 128.31, 127.18, 62.98, 49.74, 31.91. HRMS (ESI) m/z: [M + H]+ calculated for C$_{13}$H$_{17}$N$_2$ 201.1386; found 201.1389.

(S)-(1-isocyanoethyl)benzene (27g). Compound was made and purified using general procedure E. Dark red liquid with 74% yield, 198.5 mg. Rf = 0.92 (1:1 EtOAc:hexanes). ^{1}H NMR (500 MHz, CDCl$_3$): δ 7.48−7.33 (m, 5H), 4.85 (qt, J = 6.9, 1.9 Hz, 1H), 1.71 (dt, J = 6.9, 2.2 Hz 3H). ^{13}C NMR (126 MHz, CDCl$_3$): δ 156.37 (t, J = 4.9 Hz), 138.57, 128.96, 128.31, 125.41, 53.88, 53.83 (t, J = 6.1 Hz),

53.78, 25.15. HRMS (APCI) m/z: [M + H]+ calculated for $C_9H_{10}N$ 132.0808; found 132.0810.

2-((4-(*tert*-butyl)phenyl)amino)-*N*-(4-methoxyphenethyl)-2-(pyridin-3-yl)acetamide (28b). Compound was made and purified using general procedure F. White solid with 42% yield, 176 mg. $Rf = 0.2$ (2:1 EtOAc:hexanes). ^{1}H NMR (500 MHz, CDCl$_3$): δ 8.66 (d, $J = 2.3$ Hz, 1H), 8.60 (dd, $J = 4.9$, 1.6 Hz, 1H), 7.60 (dt, $J = 7.9$, 1.8 Hz, 1H), 7.27 (d, $J = 8.6$ Hz, 2H), 6.93 (d, $J = 8.5$ Hz, 2H), 6.84 (t, $J = 6.2$ Hz, 1H), 6.77 (d, $J = 8.5$ Hz, 2H), 6.60 (d, $J = 8.6$ Hz, 2H), 4.74 (d, $J = 2.3$ Hz, 1H), 4.28 (s, 1H), 3.80 (s, 3H), 3.56 (ddt, $J = 46.9$, 13.6, 6.9 Hz, 2H), 2.73 (ddt, $J = 59.3$, 14.1, 6.7 Hz, 2H), 1.31 (s, 9H). ^{13}C NMR (126 MHz, CDCl$_3$): δ 170.25, 158.27, 149.90, 149.08, 143.78, 142.65, 134.86, 134.70, 130.38, 129.71, 126.25, 123.94, 114.05, 113.67, 62.23, 55.26, 40.66, 34.72, 34.03, 31.49. HRMS (ESI) m/z: [M + Na]+ calculated for $C_{26}H_{31}N_3NaO_2$ 440.2308; found 440.2324.

2-((4-(*tert*-butyl)phenyl)amino)-*N*-(3-chlorophenethyl)-2-(pyridin-3-yl)acetamide (28c). Compound was made and purified using general procedure F. Off-white solid with 45% yield, 165 mg. $Rf = 0.25$ (1:1 EtOAc:hexanes). ^{1}H NMR (500 MHz, CDCl$_3$): δ 8.64 (d, $J = 20.0$ Hz, 1H), 7.63 (dt, $J = 7.9$, 2.0 Hz, 1H), 7.32−7.30 (m,1H), 7.27 (d, $J = 8.7$ Hz, 2H), 7.21−7.19 (m, 1H), 7.15 (t, $J = 7.7$ Hz, 1H), 7.09 (t, $J = 1.9$ Hz, 1H), 6.92−6.87 (m, 2H), 6.60 (d, $J = 8.6$ Hz, 2H), 4.74 (d, $J = 2.3$ Hz, 1H), 4.46 (s, 1H), 3.59 (ddt, $J = 45.0$, 14.0, 6.8 Hz, 2H), 2.79 (ddt, $J = 31.0$, 13.2, 6.6 Hz, 2H), 1.31 (s, 9H). ^{13}C NMR (126 MHz, CDCl$_3$): δ 170.47, 150.00, 149.03, 143.74, 142.78, 140.53, 134.78, 134.56, 134.39, 129.89, 128.82, 126.94, 126.82, 126.31, 124.01, 113.67, 62.35, 40.28, 35.27, 34.04, 31.48. HRMS (ESI) m/z: [M + Na]+ calculated for $C_{25}H_{28}ClN_3NaO$ 444.1813; found 444.1800.

2-((4-(*tert*-butyl)phenyl)amino)-*N*-(3-methoxyphenethyl)-2-(pyridin-3-yl)acetamide (28d). Compound was made and purified using general procedure F. White solid with 48% yield, 202 mg. $Rf = 0.23$ (2:1 EtOAc:hexanes). ^{1}H NMR (500 MHz, CDCl$_3$): δ 8.64 (d, $J = 3.3$ Hz, 1H), 8.60 (dd, $J = 4.8$, 1.6 Hz, 1H), 7.61 (dt, $J = 7.9$, 2.0 Hz, 1H), 7.30−7.24 (m, 2H), 7.15 (t, $J = 7.8$ Hz, 1H), 6.87 (t, $J = 5.9$ Hz, 1H), 6.77 (ddd, $J = 8.3$, 2.6, 1.0 Hz, 1H), 6.67 (t, $J = 5.9$ Hz, 1H), 6.61−6.58 (m, 3H), 4.74 (d, $J = 2.6$ Hz, 1H), 4.29 (d, $J = 2.5$ Hz, 1H), 3.77 (s, 3H), 3.60 (q, $J = 6.7$ Hz, 2H), 2.79 (ddt, $J = 49.2$, 14.0, 6.9 Hz, 1H), 1.31 (s, 9H). ^{13}C NMR (126 MHz, CDCl$_3$): δ 170.34, 159.85, 149.90, 149.08, 143.83, 142.63, 140.01, 134.83, 134.69, 129.64, 126.26, 123.97, 121.08, 114.24, 113.67, 112.05, 62.31, 55.15, 40.40, 35.61, 34.02, 31.48. HRMS (ESI) m/z: [M + Na]+ calculated for $C_{26}H_{31}N_3NaO_2$ 440.2308; found 440.2294.

2-((4-(*tert*-butyl)phenyl)amino)-*N*-(3-phenylpropyl)-2-(pyridin-3-yl)acetamide (28e). Compound was made and purified using general procedure F. Pale yellow solid with 26% yield, 105 mg. $Rf = 0.16$ (1:1 EtOAc:hexanes). ^{1}H NMR (500 MHz, CDCl$_3$) δ 8.71 (d, $J = 2.3$ Hz, 1H), 8.62 (dd, $J = 4.8$, 1.6 Hz, 1H), 7.75 (dt, $J = 7.9$, 2.0 Hz, 1H), 7.33 (dd, $J = 7.8$, 4.7 Hz, 1H), 7.28−7.25 (m, 3H), 7.22−7.19 (m, 1H), 7.11 (d, $J = 6.7$ Hz, 2H), 6.89 (t, $J = 6.1$ Hz, 1H), 6.64 (d, $J = 8.6$ Hz, 1H), 4.76 (s, 1H), 4.32 (s, 1H), 3.36 (q, $J = 7.2$ Hz, 2H), 2.59 (td, $J = 8.3$, 7.6, 2.4 Hz, 2H), 1.88−1.81 (m, 2H), 1.30 (s, 9H). ^{13}C NMR (126 MHz, CDCl$_3$) δ 170.35, 149.93, 148.96, 143.76, 142.70, 141.20, 134.96, 134.82, 128.50, 128.34, 126.30, 126.06, 124.00, 113.67, 62.29, 39.19, 34.02, 33.20, 31.47, 31.13. HRMS (ESI) m/z: [M + H]+ calculated for $C_{26}H_{32}N_3O$ 402.2540; found 402.2535.

***N*-(1-benzylpiperidin-4-yl)-2-((4-(*tert*-butyl)phenyl)amino)-2-(pyridin-3-yl)acetamide (28f).** Compound was made and purified using general procedure F. Pale yellow solid with 25% yield, 346 mg (3 mmol 3 g used). $Rf = 0.31$ (5% MeOH in DCM). ^{1}H NMR (500 MHz, CDCl$_3$) δ 8.71 (d, $J = 2.4$ Hz, 1H), 8.61 (dd, $J = 4.8$, 1.6 Hz, 1H), 7.75 (dt, $J = 7.9$, 2.0 Hz, 1H), 7.36−7.29 (m, 4H), 7.28−7.22 (m, 3H), 6.78 (d, $J = 8.3$ Hz, 1H), 6.62 (d, $J = 8.7$ Hz, 2H), 4.75 (d, $J = 2.5$ Hz, 1H), 4.27 (d, $J = 2.6$ Hz, 1H), 3.92−3.77 (m, 1H), 3.48 (s, 2H), 2.77 (dd, $J = 24.3$, 11.3 Hz, 2H), 2.13 (dq, $J = 11.3$, 2.1 Hz, 2H), 1.90 (dddd, $J = 16.2$, 11.7, 4.0, 2.0 Hz, 2H), 1.70 (bs, 1H), 1.51 (qd,

$J = 11.3$, 4.0 Hz, 1H), 1.41 (qd, $J = 11.1$, 4.0 Hz, 1H), 1.30 (s, 9H). ^{13}C NMR (126 MHz, CDCl$_3$) δ 169.70, 149.94, 149.00, 143.76, 142.74, 134.93, 134.77, 129.06, 128.23, 127.07, 126.25, 123.97, 113.71, 62.99, 62.47, 52.11, 52.00, 46.66, 34.02, 32.02, 31.77, 31.47. HRMS (ESI) m/z: [M + H]+ calculated for $C_{29}H_{37}N_4O$ 457.2962; found 457.1959.

2-((4-(*tert*-butyl)phenyl)amino)-*N*-((S)-1-phenylethyl)-2-(pyridin-3-yl)acetamide (28g). Compound was made and purified using general procedure F. Pale yellow solid with 40% yield, 157 mg. $Rf = 0.16$ (1:1 EtOAc:hexanes). ^{1}H NMR (500 MHz, CDCl$_3$) two diastereomers were observed, both diastereomers are described: δ 8.73 (s, 1H), 8.66 (s, 1H), 8.61 (d, $J = 5.2$ Hz, 1H), 8.58 (d, $J = 4.9$ Hz, 1H), 7.77 (dt, $J = 7.9$, 2.0 Hz, 1H), 7.69 (dt, $J = 7.9$, 2.0 Hz, 1H), 7.35−7.11 (m, 20H), 6.64 (d, $J = 8.7$ Hz, 2H), 6.58 (d, $J = 8.7$ Hz, 2H), 5.26−5.11 (m, 2H), 4.80 (dd, $J = 3.9$, 2.3 Hz, 2H), 4.41 (s, 1H), 4.35 (s, 1H), 1.51 (d, $J = 7.0$ Hz, 3H), 1.46 (d, $J = 6.9$ Hz, 3H), 1.31 (s, 9H), 1.30 (s, 9H). ^{13}C NMR (126 MHz, CDCl$_3$) two diastereomers were observed, both diastereomers are described: δ 169.64, 169.55, 149.90, 149.84, 148.98, 148.92, 143.86, 143.54, 142.60, 135.04, 134.95, 134.83, 134.74, 128.78, 128.50, 127.58, 127.31, 126.27, 126.17, 126.00, 124.00, 123.98, 113.84, 113.74, 62.44, 62.15, 48.80, 34.03, 34.01, 31.50, 31.48, 21.86, 21.23, 14.22. HRMS (ESI) m/z: [M + Na]+ calculated for $C_{25}H_{29}N_3NaO$ 410.2203; found 410.2199.

2-(*N*-(4-(*tert*-butyl)phenyl)vinylsulfonamido)-*N*-(4-methoxyphenethyl)-2-(pyridin-3-yl)acetamide (14b). Compound was made and purified using general procedure G. White solid with 66% yield, 61 mg. $Rf = 0.38$ (1:1 EtOAc:DCM). ^{1}H NMR (500 MHz, CDCl$_3$): δ 8.49 (dd, $J = 4.7$, 1.6 Hz, 1H), 8.35 (d, $J = 2.3$ Hz, 1H), 7.22−7.18 (m, 3H), 7.08−7.04 (m, 3H), 6.94 (d, $J = 8.6$ Hz, 2H), 6.83 (d, $J = 8.7$ Hz, 2H), 6.11 (d, $J = 16.6$ Hz, 1H), 6.02 (t, $J = 5.8$ Hz, 1H), 5.94 (d, $J = 9.9$ Hz, 1H), 5.80 (s, 1H), 3.80 (s, 3H), 3.59 (ddt, $J = 29.2$, 13.2, 6.5 Hz, 2H), 2.87−2.74 (m, 2H), 1.26 (s, 9H). ^{13}C NMR (126 MHz, CDCl$_3$) δ 170.34, 159.85, 149.90, 149.08, 143.83, 142.63, 140.01, 134.83, 134.69, 129.64, 126.26, 123.97, 121.08, 114.24, 113.67, 112.05, 62.31, 55.15, 40.40, 35.61, 34.02, 31.48. HRMS (ESI) m/z: [M + Na]+ calculated for $C_{28}H_{33}N_3NaO_4S$ 530.2084; found 530.2087.

2-(*N*-(4-(*tert*-butyl)phenyl)vinylsulfonamido)-*N*-(3-chlorophenethyl)-2-(pyridin-3-yl)acetamide (14c). Compound was made and purified using general procedure G. White solid with 45% yield, 46 mg. $Rf = 0.38$ (1:1 EtOAc:DCM). ^{1}H NMR (500 MHz, CDCl$_3$): δ 8.50 (dd, $J = 4.7$, 1.7 Hz, 1H), 8.35 (d, $J = 2.3$ Hz, 1H), 7.27−7.18 (m, 4H), 7.16 (s, 1H), 7.11−7.03 (m, 2H), 6.95 (d, $J = 8.6$ Hz, 2H), 6.82 (dd, $J = 16.6$, 9.9 Hz, 1H), 6.12 (d, $J = 16.6$ Hz, 1H), 6.03 (t, $J = 5.8$ Hz, 1H), 5.95 (d, $J = 9.9$ Hz, 1H), 5.80 (s, 1H), 3.62 (ddt, $J = 62.7$, 13.5, 6.6 Hz, 2H), 2.86 (t, $J = 6.9$ Hz, 2H), 1.27 (s, 9H). ^{13}C NMR (126 MHz, CDCl$_3$): δ 168.80, 152.28, 151.22, 150.04, 140.44, 137.86, 135.54, 134.44, 133.10, 131.41, 130.20, 130.00, 128.89, 127.59, 127.02, 126.91, 126.05, 123.02z, 65.52, 40.93, 35.12, 34.63, 31.19. HRMS (ESI) m/z: [M + Na]+ calculated for $C_{27}H_{30}ClN_3NaO_3S$ 534.1589; found 534.1584.

2-(*N*-(4-(*tert*-butyl)phenyl)vinylsulfonamido)-*N*-(3-methoxyphenethyl)-2-(pyridin-3-yl)acetamide (14d). Compound was made and purified using general procedure G. White solid with 73% yield, 96 mg. $Rf = 0.36$ (1:1 EtOAc:DCM). ^{1}H NMR (500 MHz, CDCl$_3$): δ 8.47 (d, $J = 4.8$ Hz, 1H), 8.30 (s, 1H), 7.25−7.13 (m, 3H), 7.05 (dd, $J = 8.0$, 4.8 Hz, 1H), 6.95 (d, $J = 8.6$ Hz, 2H), 6.86−6.68 (m, 4H), 6.12 (s, 1H), 6.10 (d, $J = 16.5$ Hz, 1H), 5.94 (d, $J = 9.9$ Hz, 1H), 5.80 (s, 1H), 3.79 (s, 3H), 3.62 (ddt, $J = 40.3$, 13.1, 6.4 Hz, 2H), 2.84 (td, $J = 6.8$, 4.7 Hz, 2H), 1.26 (s, 9H). ^{13}C NMR (126 MHz, CDCl$_3$) δ 168.66, 159.89, 152.19, 151.25, 149.93, 139.91, 137.90, 135.59, 133.12, 131.45, 130.27, 129.75, 127.50, 125.99, 122.98, 121.04, 114.37, 112.14, 65.49, 55.18, 41.07, 35.44, 34.61, 31.19. HRMS (ESI) m/z: [M + Na]+ calculated for $C_{28}H_{33}N_3NaO_4S$ 530.2084; found 530.2101.

2-(*N*-(4-(*tert*-butyl)phenyl)vinylsulfonamido)-*N*-(3-phenylpropyl)-2-(pyridin-3-yl)acetamide (14e). Compound was made and purified using general procedure G. White solid with 80%

yield, 103.0 mg. Rf = 0.50 (1:1 EtOAc:DCM). ^{1}H NMR (500 MHz, CDCl$_3$): δ 8.52 (d, J = 4.2 Hz, 1H), 8.39 (s, 1H), 7.34 (dt, J = 8.0, 2.0 Hz, 1H), 7.31−7.26 (m, 3H), 7.22 (d, J = 8.5 Hz, 2H), 7.17 (d, J = 6.9 Hz, 2H),7.12 (dd, J = 8.0, 4.8 Hz, 1H), 7.04 (d, J = 8.6 Hz, 2H), 6.84 (dd, J = 16.6, 9.9 Hz, 1H), 6.12 (d, J = 16.5 Hz, 1H), 6.02 (s, 1H), 5.95 (d, J = 9.9 Hz, 1H), 5.82 (s, 1H), 3.38 (dt, J = 7.3, 5.4 Hz, 2H), 2.67 (td, J = 7.4, 1.3 Hz, 2H), 1.89 (p, J = 7.4 Hz, 2H), 1.26 (s, 9H). ^{13}C NMR (126 MHz, CDCl$_3$) δ 168.64, 152.27, 151.26, 150.03, 141.06, 138.01, 135.58, 133.12, 131.45, 130.30, 128.54, 128.34, 127.54, 126.13, 126.04, 123.06, 65.45, 39.83, 34.62, 33.23, 31.18, 30.99. HRMS (ESI) m/z: [M + H]+ calculated for C$_{28}$H$_{34}$N$_3$O$_3$S 493.2315; found 492.2313.

N-(1-benzylpiperidin-4-yl)-2-(N-(4-(tert-butyl)phenyl)vinyl-sulfonamido)-2-(pyridin-3-yl)acetamide (14f). Compound was made and purified using general procedure G. Pale yellow solid with 42% yield, 116.5 mg. Rf = 0.24 (5% MeOH in DCM). ^{1}H NMR (500 MHz, CDCl$_3$): δ 8.51 (dd, J = 4.9, 1.6 Hz, 1H), 8.39 (d, J = 2.3 Hz, 1H), 7.35−7.30 (m, 4H), 7.31−7.24 (m, 1H), 7.21 (d, J = 8.6 Hz, 2H), 7.11 (dd, J = 8.0, 4.8 Hz, 1H), 7.03 (d, J = 8.6 Hz, 2H), 6.82 (dd, J = 16.5, 9.9 Hz, 1H), 6.12 (d, J = 16.6 Hz, 1H), 6.00 (d, J = 7.9 Hz, 1H), 5.94 (d, J = 9.9 Hz, 1H), 5.85 (s, 1H), 3.93−3.85 (m, 1H), 3.52 (s, 2H), 2.82 (q, J = 11.0 Hz, 2H), 2.17 (q, J = 11.8 Hz, 2H), 2.03−1.95 (m, 1H), 1.95−1.88 (m, 1H), 1.52 (dqd, J = 41.1, 11.0, 3.8 Hz, 2H), 1.25 (s, 9H). ^{13}C NMR (126 MHz, CDCl$_3$) δ 167.96, 152.26, 151.28, 150.01, 137.98, 135.57, 133.06, 131.46, 130.29, 129.05, 128.27, 127.51, 127.12, 126.01, 123.03, 65.29, 62.92, 52.00, 47.46, 34.62, 31.90, 31.81, 31.18. HRMS (ESI) m/z: [M + H]+ calculated for C$_{31}$H$_{39}$N$_4$O$_3$S 547.2737; found 547.2736.

(S)- and (R)-2-(N-(4-(tert-butyl)phenyl)vinylsulfonamido)-N-((S)-1-phenylethyl)-2-(pyridin-3-yl)acetamide (14g and 14h). Compound was made and purified using general procedure G. White solid with 75% yield, 276.8 mg. Rf = 0.63 (1:1 EtOAc:DCM). The diastereomer was separated by reverse-phase HPLC using the ZORBAX Rx-C18 Semi-Preparative column with 50% ACN in water with 3 mL/min flow rate. The absolute stereochemistry was inferred based on previously published crystal structures and the structure-activity relationship between different diastereomers. **14g:** ^{1}H NMR (500 MHz, CDCl$_3$) δ 8.51 (dd, J = 4.8, 1.6 Hz, 1H), 8.42 (d, J = 2.2 Hz, 1H), 7.43−7.31 (m, 5H), 7.16 (d, J = 8.6 Hz, 2H), 7.11 (dd, J = 8.0, 4.8 Hz, 1H), 6.98−6.88 (m, 2H), 6.69 (dd, J = 16.5, 9.9 Hz, 1H), 6.38 (d, J = 8.1 Hz, 1H), 6.08 (d, J = 16.6 Hz, 1H), 5.88 (d, J = 10.0 Hz, 1H), 5.86 (s, 1H), 5.17 (p, J = 7.1 Hz, 1H), 1.51 (d, J = 7.0 Hz, 3H), 1.24 (s, 9H). ^{13}C NMR (126 MHz, CDCl$_3$) δ 167.64, 152.21, 151.21, 150.03, 142.49, 138.09, 135.43, 132.87, 131.44, 130.12, 128.87, 127.69, 127.56, 126.21, 125.96, 123.01, 65.03, 49.79, 34.60, 31.17, 21.68. HRMS (ESI) m/z: [M + Na]+ calculated for C$_{27}$H$_{31}$N$_3$NaO$_3$S 500.1978; found 500.1968. **14h:** ^{1}H NMR (500 MHz, CDCl$_3$) δ 8.49 (dd, J = 4.7, 1.7 Hz, 1H), 8.39 (d, J = 2.3 Hz, 1H), 7.35−7.30 (m, 2H), 7.25 (ddd, J = 11.8, 7.8, 1.7 Hz, 3H), 7.19 (d, J = 8.6 Hz, 2H), 7.09−7.04 (m, 1H), 7.04−6.98 (m, 2H), 6.82 (dd, J = 16.5, 9.9 Hz, 1H), 6.34 (d, J = 7.7 Hz, 1H), 6.12 (d, J = 16.5 Hz, 1H), 5.94 (d, J = 9.9 Hz, 1H), 5.90 (s, 1H), 5.18 (p, J = 7.1 Hz, 1H), 1.57 (d, J = 6.9 Hz, 3H), 1.25 (s, 8H). ^{13}C NMR (126 MHz, CDCl$_3$) δ 167.78, 152.24, 151.29, 150.02, 142.55, 138.05, 135.56, 132.90, 131.54, 130.00, 128.74, 127.54, 125.99, 125.97, 122.94, 65.11, 49.83, 34.61, 31.18, 22.00. HRMS (ESI) m/z: [M + Na]+ calculated for C$_{27}$H$_{31}$N$_3$NaO$_3$S 500.1978; found 500.1982.

N-(4-(tert-butyl)phenyl)-N-(2-(cyclohexylamino)-2-oxo-1-(thiophen-3-yl)ethyl)cyclopent-1-ene-1-carboxamide (11c). Compound was made and purified using general procedure B, off white solid 79% yield, 330 mg. ^{1}H NMR (500 MHz, CDCl$_3$) δ 7.27−7.24 (m, 1H), 7.20−7.12 (m, 3H), 6.94−6.87 (m, 3H), 6.09 (d, J = 8.1 Hz, 1H), 6.06 (s, 1H), 5.81 (q, J = 2.2 Hz, 1H), 3.87−3.76 (m, 1H), 2.22−2.06 (m, 4H), 2.01−1.84 (m, 2H), 1.71−1.53 (m, 5H), 1.42−1.28 (m, 2H), 1.26 (s, 9H), 1.15 (ddt, J = 16.1, 12.0, 8.0 Hz, 3H). ^{13}C NMR (126 MHz, CDCl$_3$) δ 168.73, 168.53, 151.12, 139.46, 139.40, 138.34, 135.52, 129.16, 129.08, 126.40, 125.51, 125.33, 61.62, 48.59, 34.68, 33.83, 33.19, 32.97, 32.93, 31.42, 25.67, 24.88, 24.83, 23.36.

HRMS (ESI/Q-TOF) m/z: [M + Na]+ calculated for C$_{28}$H$_{36}$N$_2$NaO$_2$S 487.2390; found 487.2404.

N-(4-(tert-butyl)phenyl)-N-(2-(cyclohexylamino)-2-oxo-1-(quinolin-3-yl)ethyl)cyclopent-1-ene-1-carboxamide (11d). Compound was made and purified using general procedure B, pale yellow solid 59% yield, 270 mg. ^{1}H NMR (500 MHz, CDCl$_3$) δ 8.73 (d, J = 2.1 Hz, 1H), 8.03 (d, J = 8.4 Hz, 1H), 8.00 (s, 1H), 7.74−7.66 (m, 1H), 7.65−7.61 (m, 1H), 7.52−7.45 (m, 1H), 7.13 (d, J = 8.2 Hz, 2H), 6.39 (s, 2H), 6.27 (s, 1H), 5.86 (p, J = 2.3 Hz, 1H), 3.93−3.82 (m, 1H), 2.23−2.09 (m, 4H), 2.00 (dd, J = 12.2, 4.1 Hz, 2H), 1.89 (dd, J = 12.8, 4.2 Hz, 1H), 1.66 (p, J = 7.7 Hz, 5H), 1.36 (ddd, J = 16.2, 13.1, 11.4 Hz, 2H), 1.19 (s, 9H), 1.18−1.08 (m, 3H). ^{13}C NMR (126 MHz, CDCl$_3$) δ 169.02, 168.29, 151.91, 151.58, 147.65, 140.28, 139.13, 138.06, 137.59, 130.00, 129.59, 129.15, 128.23, 127.98, 127.47, 126.87, 125.83, 63.71, 48.83, 34.69, 33.87, 33.26, 33.02, 32.98, 31.31, 25.62, 24.90, 24.85, 23.32. HRMS (ESI/Q-TOF) m/z: [M + Na]+ calculated for C$_{33}$H$_{39}$N$_3$NaO$_2$ 532.2934; found 532.2946.

N-(1-(benzo[b]thiophen-3-yl)-2-(cyclohexylamino)-2-oxoethyl)-N-(4-(tert-butyl)phenyl)cyclopent-1-ene-1-carboxamide (11e). Compound was made and purified using general procedure B, pale yellow solid 26% yield, 120 mg. ^{1}H NMR (500 MHz, CDCl$_3$) δ 7.83 (d, J = 7.6 Hz, 1H), 7.78−7.72 (m, 1H), 7.53 (s, 1H), 7.37 (p, J = 7.0 Hz, 2H), 7.03 (d, J = 8.2 Hz, 2H), 6.69 (d, J = 19.7 Hz, 3H), 6.20 (d, J = 8.2 Hz, 1H), 5.84−5.79 (m, 1H), 2.17−2.00 (m, 4H), 1.97−1.90 (m, 2H), 1.65 (pt, J = 14.3, 6.5 Hz, 5H), 1.36 (ddt, J = 15.3, 11.9, 6.0 Hz, 3H), 1.19 (s, 12H). ^{13}C NMR (126 MHz, CDCl$_3$) δ 169.16, 168.29, 151.15, 139.68, 139.60, 139.30, 138.74, 137.04, 129.40, 129.26, 129.10, 125.16, 124.61, 124.59, 122.92, 121.61, 57.25, 48.65, 34.61, 33.87, 33.18, 33.04, 32.98, 31.36, 25.65, 24.94, 24.89, 23.36. HRMS (ESI/Q-TOF) m/z: [M + Na]+ calculated for C$_{32}$H$_{38}$N$_2$NaO$_2$S 537.2546; found 537.2549.

N-(4-(tert-butyl)phenyl)-N-(2-(cyclohexylamino)-2-oxo-1-(pyridin-4-yl)ethyl)cyclopent-1-ene-1-carboxamide (11f). Compound was made and purified using general procedure B, white solid 71% yield, 90 mg. ^{1}H NMR (500 MHz, CDCl$_3$) δ 8.49 (d, J = 6.2 Hz, 2H), 7.30−7.19 (m, 4H), 6.97 (d, J = 8.1 Hz, 2H), 6.45 (d, J = 8.1 Hz, 1H), 5.88 (p, J = 2.2 Hz, 1H), 5.82 (s, 1H), 3.89−3.78 (m, 1H), 2.21 (ddt, J = 7.6, 5.0, 2.6 Hz, 2H), 2.12 (dtt, J = 9.9, 5.0, 2.2 Hz, 2H), 1.98−1.84 (m, 3H), 1.67 (p, J = 7.4 Hz, 4H), 1.43−1.29 (m, 2H), 1.26 (s, 9H), 1.19 (dddd, J = 26.8, 22.7, 10.8, 4.5 Hz, 3H). ^{13}C NMR (126 MHz, CDCl$_3$) δ 169.03, 167.76, 151.65, 149.80, 144.29, 140.77, 139.08, 138.60, 128.71, 126.05, 124.23, 67.01, 48.74, 34.76, 33.69, 33.27, 32.92, 32.88, 31.39, 25.62, 24.80, 23.34. HRMS (ESI/Q-TOF) m/z: [M + H]+ calculated for C$_{29}$H$_{38}$N$_3$O$_2$ 460.29585; found 460.29546.

N-(4-(tert-butyl)phenyl)-N-(2-(cyclohexylamino)-2-oxo-1-(pyrimidin-5-yl)ethyl)cyclopent-1-ene-1-carboxamide (11g). Compound was made and purified using general procedure B, off white solid 29% yield, 120 mg. ^{1}H NMR (500 MHz, CDCl$_3$) δ 9.06 (s, 1H), 8.55 (s, 2H), 7.25 (d, J = 8.9 Hz, 2H), 6.85 (dd, J = 15.8, 5.0 Hz, 2H), 6.62 (d, J = 8.1 Hz, 1H), 6.18 (s, 1H), 5.84 (td, J = 2.7, 1.3 Hz, 1H), 3.89−3.78 (m, 1H), 2.55 (dd, J = 25.2, 2.4 Hz, 2H), 2.20 (ddd, J = 7.8, 6.0, 2.5 Hz, 2H), 2.12 (ddd, J = 10.3, 5.6, 2.3 Hz, 2H), 2.01−1.86 (m, 1H), 1.76−1.57 (m, 5H), 1.46−1.31 (m, 2H), 1.27 (s, 9H), 1.26−1.14 (m, 3H). ^{13}C NMR (101 MHz, CDCl$_3$) δ 169.14, 167.31, 158.59, 158.11, 152.37, 145.94, 141.02, 138.68, 136.78, 129.38, 128.84, 126.31, 61.37, 48.85, 34.82, 33.84, 33.70, 33.32, 32.99, 32.91, 31.36, 31.32, 25.60, 24.79, 23.31, 23.29. HRMS (ESI/Q-TOF) m/z: [M + Na]+ calculated for C$_{28}$H$_{36}$N$_4$NaO$_2$ 483.2730; found 483.2746.

N-(4-(tert-butyl)phenyl)-N-(2-(cyclohexylamino)-1-(iso-quinolin-4-yl)-2-oxoethyl)cyclopent-1-ene-1-carboxamide (11h). Compound was made and purified using general procedure A, off white solid 78% yield, 358 mg. ^{1}H NMR (500 MHz, CDCl$_3$) δ 9.08 (d, J = 1.9 Hz, 1H), 8.28 (s, 1H), 8.01 (d, J = 8.5 Hz, 1H), 7.95 (d, J = 8.1 Hz, 1H), 7.77 (dd, J = 8.5, 6.9 Hz, 1H), 7.66−7.59 (m, 1H), 7.06

(s, 1H), 6.93 (d, J = 8.1 Hz, 2H), 6.78 (s, 1H), 5.81 (q, J = 2.1 Hz, 1H), 5.67 (s, 1H), 3.91 (dt, J = 7.5, 3.5 Hz, 1H), 2.21–2.09 (m, 4H), 1.97 (d, J = 16.2 Hz, 2H), 1.72–1.62 (m, 5H), 1.34 (tdd, J = 12.3, 8.3, 3.8 Hz, 2H), 1.13 (d, J = 0.9 Hz, 12H). ^{13}C NMR (126 MHz, CDCl$_3$) δ 168.96, 168.39, 153.31, 151.05, 145.51, 139.71, 139.19, 136.80, 135.07, 131.47, 129.61, 128.57, 128.14, 127.44, 125.06, 124.84, 122.71, 58.84, 49.11, 34.52, 33.87, 33.23, 33.04, 33.00, 31.28, 25.61, 25.00, 24.89, 23.34. HRMS (ESI-Q-TOF) m/z: [M + Na]$^+$ calculated for C$_{33}$H$_{39}$N$_3$NaO$_2$ 532.2934; found 532.2932.

N-(4-(*tert*-butyl)phenyl)-N-(2-(cyclohexylamino)-1-(1*H*-imidazole-5-yl)-2-oxoethyl)cyclopent-1-ene-1-carboxamide (11i). Compound was made and purified using general procedure B, off white solid 37% yield, 150 mg. ^{1}H NMR (500 MHz, CDCl$_3$) δ 7.61 (d, J = 1.0 Hz, 1H), 7.28 (d, J = 8.6 Hz, 2H), 7.11 (s, 1H), 7.00 (d, J = 8.2 Hz, 2H), 6.81 (d, J = 2.5 Hz, 1H), 5.86 (p, J = 2.3 Hz, 1H), 5.75 (s, 1H), 3.79 (td, J = 6.3, 3.4 Hz, 1H), 2.60 (ddd, J = 10.0, 4.9, 2.3 Hz, 2H), 2.52 (ddt, J = 7.7, 5.2, 2.6 Hz, 2H), 2.21 (ddt, J = 7.6, 5.0, 2.5 Hz, 2H), 1.85 (d, J = 14.6 Hz, 2H), 1.73–1.65 (m, 4H), 1.37–1.22 (m, 15H). ^{13}C NMR (101 MHz, CDCl$_3$) δ 169.46, 167.62, 158.91, 158.43, 152.68, 146.26, 141.34, 139.00, 137.10, 129.70, 129.15, 126.63, 61.69, 49.16, 35.14, 34.15, 34.02, 33.64, 33.31, 33.22, 31.67, 31.64, 25.92, 25.11, 23.63, 23.60. HRMS (ESI-Q-TOF) m/z: [M + H]$^+$ calculated for C$_{27}$H$_{37}$N$_4$O$_2$ 449.29110; found 449.29124.

(E)-N-(4-(*tert*-butyl)phenyl)-N-(2-(cyclohexylamino)-2-oxo-1-(pyridin-4-yl)ethyl)but-2-enamide (8c). Compound was made and purified using general procedure A, white solid 74% yield, 287 mg. ^{1}H NMR (500 MHz, CDCl$_3$) δ 8.49–8.45 (m, 2H), 7.28 (d, J = 8.9 Hz, 2H), 7.19–7.12 (m, 2H), 7.03–6.92 (m, 3H), 6.47 (d, J = 7.9 Hz, 1H), 5.84 (s, 1H), 5.70 (dd, J = 15.0, 1.8 Hz, 1H), 4.03–3.75 (m, 1H), 1.95 (dd, J = 12.3, 4.3 Hz, 1H), 1.91–1.85 (m, 1H), 1.78–1.74 (m, 3H), 1.70–1.64 (m, 2H), 1.58 (dt, J = 12.9, 3.9 Hz, 1H), 1.37–1.31 (m, 2H), 1.29 (s, 9H), 1.25–1.08 (m, 3H). ^{13}C NMR (126 MHz, CDCl$_3$) δ 167.84, 167.10, 151.87, 149.73, 144.20, 143.48, 137.54, 129.06, 126.42, 124.35, 122.64, 66.12, 48.75, 34.80, 32.89, 31.39, 25.62, 24.83, 24.80, 18.25. HRMS (ESI-Q-TOF) m/z: [M + Na]$^+$ calculated for C$_{27}$H$_{35}$N$_3$NaO$_2$ 456.2621; found 456.2614.

N-(4-(*tert*-butyl)phenyl)-2-chloro-N-(2-(cyclohexylamino)-2-oxo-1-(thiophen-3-yl)ethyl)acetamide (16d). Compound was made and purified using general procedure A, white solid 87% yield, 352 mg. ^{1}H NMR (500 MHz, CDCl$_3$) δ 7.28 (s, 2H), 7.25–7.21 (m, 1H), 7.17 (dd, J = 5.0, 3.0 Hz, 1H), 6.84 (dd, J = 5.0, 1.3 Hz, 1H), 6.01 (s, 1H), 5.79 (d, J = 8.2 Hz, 1H), 3.87 (s, 2H), 3.82 (ddt, J = 14.7, 6.7, 3.9 Hz, 1H), 1.98–1.92 (m, 1H), 1.91–1.85 (m, 1H), 1.74–1.60 (m, 3H), 1.38 (dqd, J = 8.3, 3.3, 1.6 Hz, 2H), 1.30 (s, 9H), 1.23–1.05 (m, 3H). ^{13}C NMR (126 MHz, CDCl$_3$) δ 167.83, 166.99, 152.39, 136.30, 134.59, 129.25, 128.85, 126.93, 126.34, 125.82, 61.28, 48.89, 42.69, 34.81, 32.95 (d, J = 10.4 Hz), 31.57, 31.38, 25.62, 24.90, 24.84. HRMS (ESI-Q-TOF) m/z: [M + H]$^+$ calculated for C$_{24}$H$_{32}$N$_2$O$_2$ClS 447.18675; found 447.18675.

N-(4-(*tert*-butyl)phenyl)-2-chloro-N-(2-(cyclohexylamino)-2-oxo-1-(pyridin-4-yl)ethyl)acetamide (16e). Compound was made and purified using general procedure A, white solid 94% yield, 375 mg. ^{1}H NMR (500 MHz, CDCl$_3$) δ 8.47 (d, J = 6.1 Hz, 2H), 7.26 (s, 2H), 7.16–7.11 (m, 2H), 5.88 (d, J = 8.0 Hz, 1H), 5.83 (s, 1H), 3.87 (d, J = 1.9 Hz, 2H), 3.85–3.77 (m, 1H), 2.00–1.94 (m, 1H), 1.86 (dd, J = 12.9, 4.0 Hz, 1H), 1.75–1.53 (m, 3H), 1.41–1.28 (m, 2H), 1.26 (s, 9H), 1.23–1.03 (m, 3H). ^{13}C NMR (126 MHz, CDCl$_3$) δ 167.57, 166.93, 152.92, 149.88, 143.19, 135.93, 129.26, 126.68, 124.90, 65.47, 49.11, 42.49, 34.87, 32.90, 32.85, 31.33, 25.56, 24.88, 24.82. HRMS (ESI-Q-TOF) m/z: [M + H]$^+$ calculated for C$_{25}$H$_{33}$N$_3$O$_2$Cl 442.22558; found 442.22525.

N-(4-(*tert*-butyl)phenyl)-2-chloro-N-(2-(cyclohexylamino)-1-(5-methylpyrazin-2-yl)-2-oxoethyl)acetamide (16f). Compound was made and purified using general procedure B, pale yellow solid 34% yield, 140 mg. ^{1}H NMR (500 MHz, CDCl$_3$) δ 8.62 (s,

1H), 8.39 (s, 1H), 7.37 (d, J = 8.2 Hz, 2H), 7.29–7.06 (m, 2H), 5.88 (s, 1H), 3.89 (q, J = 13.6 Hz, 2H), 3.82–3.72 (m, 1H), 1.92–1.85 (m, 3H), 1.77–1.53 (m, 5H), 1.32 (s, 13H), 1.22–1.12 (m, 2H). ^{13}C NMR (126 MHz, CDCl$_3$) δ 167.11, 165.73, 153.11, 152.59, 147.62, 144.81, 142.87, 136.87, 128.87, 126.66, 65.99, 48.50, 42.31, 34.75, 32.59, 32.49, 31.60, 31.24, 25.48, 24.57, 24.50, 22.66, 21.31, 14.13. HRMS (ESI-Q-TOF) m/z: [M + H]$^+$ calculated for C$_{25}$H$_{34}$N$_4$O$_2$Cl 457.23648; found 457.23621.

N-(4-(*tert*-butyl)phenyl)-N-(2-(cyclohexylamino)-1-(iso-quinolin-4-yl)-2-oxoethyl)but-2-ynamide (13e). Compound was made and purified using general procedure A, pale white solid 90% yield, 392 mg. ^{1}H NMR (500 MHz, CDCl$_3$) δ 9.11 (d, J = 0.7 Hz, 1H), 8.24 (s, 1H), 8.00–7.94 (m, 2H), 7.82–7.73 (m, 1H), 7.65 (ddd, J = 7.9, 6.9, 1.0 Hz, 1H), 7.00 (d, J = 8.1 Hz, 2H), 6.95 (s, 1H), 6.86 (s, 2H), 5.62 (d, J = 8.1 Hz, 1H), 3.89 (dtd, J = 10.8, 7.8, 7.2, 3.9 Hz, 1H), 2.01–1.94 (m, 1H), 1.93 (s, 1H), 1.65 (s, 6H), 1.31 (d, J = 18.7 Hz, 2H), 1.15 (s, 9H), 1.10–0.97 (m, 3H). ^{13}C NMR (126 MHz, CDCl3) δ 167.30, 155.31, 153.07, 151.22, 144.79, 135.59, 134.71, 131.56, 129.62, 128.48, 127.90, 127.41, 124.89, 124.21, 122.31, 91.66, 73.65, 57.76, 48.95, 34.33, 32.74, 32.68, 30.99, 25.32, 24.73, 24.63, 3.79, 3.63. HRMS (ESI-Q-TOF) m/z: [M + H]$^+$ calculated for C$_{31}$H$_{36}$N$_3$O$_2$ 482.28020; found 482.28025.

N-(4-(*tert*-butyl)phenyl)-N-(2-(cyclohexylamino)-2-oxo-1-(quinolin-3-yl)ethyl)but-2-ynamide (13f). Compound was made and purified using general procedure A, pale white solid 69% yield, 298 mg. ^{1}H NMR (500 MHz, CDCl$_3$) δ 8.70 (d, J = 2.2 Hz, 1H), 8.07 (dd, J = 8.4, 1.0 Hz, 1H), 8.00 (d, J = 2.4 Hz, 1H), 7.73–7.70 (m, 1H), 7.65 (dd, J = 8.2, 1.4 Hz, 1H), 7.52 (ddd, J = 8.1, 6.8, 1.2 Hz, 1H), 7.21 (d, J = 8.8 Hz, 2H), 7.01 (d, J = 8.0 Hz, 2H), 6.27 (s, 1H), 6.23–6.18 (m, 1H), 3.95–3.83 (m, 1H), 2.05–1.99 (m, 1H), 1.92–1.84 (m, 1H), 1.78–1.58 (m, 6H), 1.47–1.35 (m, 3H), 1.23 (s, 9H), 1.21–1.10 (m, 3H). ^{13}C NMR (126 MHz, CDCl3) δ 167.79, 155.80, 152.21, 151.92, 147.77, 138.75, 136.61, 130.53, 130.17, 129.23, 128.49, 127.69, 127.51, 127.29, 126.06, 92.59, 74.16, 49.31, 35.00, 33.22, 33.15, 31.54, 25.85, 25.15, 25.11, 23.05, 14.51, 4.35. HRMS (ESI-Q-TOF) m/z: [M + H]$^+$ calculated for C$_{31}$H$_{36}$N$_3$O$_2$ 482.28020; found 482.28007.

N-(1-(benzo[*d*]thiazol-2-yl)-2-(cyclohexylamino)-2-oxoethyl)-N-(4-(*tert*-butyl)phenyl)but-2-ynamide (13g). Compound was made and purified using general procedure A, pale white solid 91% yield, 398 mg. ^{1}H NMR (500 MHz, CDCl$_3$) δ 9.61 (d, J = 7.9 Hz, 1H), 8.11–8.00 (m, 1H), 7.95–7.84 (m, 1H), 7.56–7.51 (m, 1H), 7.47 (d, J = 1.2 Hz, 1H), 7.46–7.35 (m, 2H), 7.29–7.22 (m, 2H), 6.15 (d, J = 1.6 Hz, 1H), 4.04–3.94 (m, 1H), 1.99 (d, J = 1.6 Hz, 3H), 1.91–1.64 (m, 4H), 1.55–1.34 (m, 6H), 1.24 (s, 9H). ^{13}C NMR (126 MHz, CDCl$_3$) δ 171.84, 169.60, 163.31, 158.61, 152.14, 148.14, 135.47, 134.80, 126.83, 126.70, 126.56, 126.18, 124.24, 123.56, 122.32, 121.64, 121.47, 50.84, 49.26, 34.67, 32.77, 32.67, 31.72, 31.59, 31.37, 25.94, 25.14, 24.84, 24.68, 24.60, 13.39, 4.08. HRMS (ESI-Q-TOF) m/z: [M + H]$^+$ calculated for C$_{29}$H$_{34}$N$_3$O$_2$S 488.23662; found 488.23672.

N-(1-(benzo[*b*]thiophen-3-yl)-2-(cyclohexylamino)-2-oxoethyl)-N-(4-(*tert*-butyl)phenyl)but-2-ynamide (13h). Compound was made and purified using general procedure A, grey solid 92% yield, 402 mg. ^{1}H NMR (500 MHz, CDCl$_3$) δ 7.86–7.82 (m, 1H), 7.77–7.71 (m, 1H), 7.50 (s, 1H), 7.45–7.34 (m, 2H), 7.14–7.08 (m, 2H), 6.82 (s, 2H), 6.65 (s, 1H), 6.04 (d, J = 8.2 Hz, 1H), 3.88 (dddd, J = 14.5, 10.5, 7.9, 3.9 Hz, 1H), 2.01–1.91 (m, 1H), 1.92–1.87 (m, 1H), 1.79–1.60 (m, 6H), 1.47–1.28 (m, 3H), 1.23 (s, 9H), 1.21–1.07 (m, 2H). ^{13}C NMR (126 MHz, CDCl$_3$) δ 167.45, 155.48, 151.34, 139.47, 138.29, 136.01, 129.42, 129.35, 128.26, 125.05, 124.60, 124.58, 122.81, 121.41, 91.83, 73.83, 56.30, 48.74, 34.53, 32.83, 32.79, 31.19, 25.49, 24.79, 24.75, 3.93. HRMS (ESI-Q-TOF) m/z: [M + H]$^+$ calculated for C$_{30}$H$_{35}$N$_2$O$_2$S 487.24138; found 487.24187.

N-(4-(*tert*-butyl)phenyl)-N-(1-(cyclohexylamino)-3-(2,5-dioxoimidazolidin-1-yl)-1-oxopropan-2-yl)but-2-ynamide (13i). To a solution of 4-tBu-aniline (0.56 mmol, 0.09 mL) in MeOH was

added 2-(2,4-dioxoimidazolidin-1-yl)acetaldehyde (0.56 mmol, 80 mg) and stirred for 30 min. Butynoic acid (0.56 mmol, 47 mg) and cyclohexyl isocyanide (0.56 mmol, 0.07 mL) were added and the solution stirred at room temperature overnight. The resulting white precipitate was collected by filtration and rinsed with hexanes. The precipitate was dried over vacuum to afford the desired product (58 mg, 22% yield) as a white precipitate. ^{1}H NMR (400 MHz, CDCl$_3$) δ 8.35 (s, 1H), 7.39 (d, J = 8.5 Hz, 2H), 7.18 (d, J = 8.5 Hz, 2H), 6.87 (d, J = 8.0 Hz, 1H), 5.24 (dd, J = 9.3, 5.3 Hz, 1H), 4.07 (d, J = 18.0 Hz, 1H), 3.77 (d, J = 18.0 Hz, 1H), 3.70 (dd, J = 14.0, 5.3 Hz, 1H), 3.28 (dd, J = 13.9, 9.4 Hz, 1H), 1.89 (t, J = 16.9 Hz, 2H), 1.70 (s, 5H), 1.65−1.54 (m, 0H), 1.44−1.28 (m, 11H), 1.22 (q, J = 10.5 Hz, 4H). ^{13}C NMR (126 MHz, CDCl$_3$) δ 170.49, 168.02, 156.59, 155.84, 152.37, 135.31, 128.88, 126.21, 93.11, 73.57, 56.15, 52.78, 48.72, 42.35, 34.89, 32.75, 32.71, 31.38, 25.59, 24.78, 24.74, 4.08. HRMS (ESI/Q-TOF) m/z: [M + Na]$^+$ calculated for C$_{26}$H$_{34}$N$_4$O$_4$ 489.2472; found 489.2475.

N-(4-(*tert*-butyl)phenyl)-N-(2-(cyclohexylamino)-2-oxo-1-(1*H*-pyrazol-4-yl)ethyl)propiolamide (13j). 1*H*-pyrazole-4-carbaldehyde (100 mg, 1.04 mmol) and 4-*tert*-butylaniline (0.17 mL, 1.04 mmol) were stirred in MeOH (4.16 mL) and for 30 min at rt. A white precipitate was observed. But-2-ynoic acid (87.4 mg, 1.04 mmol) and cyclohexyl isocyanide (0.12 mL, 0.936 mmol) were added and the solution stirred at rt overnight. Upon addition of the isocyanide, the white precipitate dissolved. A stream of air was used to evaporate the MeOH. EtOAc was added to dissolve the impurities and the mixture was sonicated. The product was finally triturated with hexanes and EtOAc. Vacuum filtration was used to collect the precipitate. The white powder precipitate was dried using the vacuum filtration and the product (186 mg, 47% yield) was obtained. *Rf* (5% (MeOH + 1% NH$_4$OH) in DCM): 0.45. ^{1}H NMR (500 MHz, CDCl$_3$) δ 8.63−8.39 (m, 2H), 7.50 (s, 2H), 7.28 (s, 1H), 7.00−6.93 (m, 2H), 6.38 (d, J = 8.1 Hz, 1H), 6.09 (s, 1H), 3.78 (tdd, J = 10.4, 7.1, 4.0 Hz, 1H), 1.96−1.82 (m, 2H), 1.69 (d, J = 8.5 Hz, 4H), 1.59 (dq, J = 13.0, 4.0 Hz, 1H), 1.41−1.31 (m, 1H), 1.28 (s, 9H), 1.24−1.12 (m, 2H). ^{13}C NMR (126 MHz, CDCl$_3$) δ 167.63, 155.30, 151.92, 136.43, 134.76, 129.41, 126.03, 125.75, 114.45, 92.11, 73.85, 55.72, 48.82, 34.78, 32.86, 32.80, 31.37, 25.61, 24.80, 4.07. HRMS (ESI/Q-TOF) m/z: [M+Na]¬+ calculated for C$_{25}$H$_{32}$N$_4$NaO$_2$ 443.2417, found 443.2426.

N-(2-(cyclohexylamino)-2-oxo-1-(pyridin-3-yl)ethyl)-2-oxo-N-(*m*-tolyl)propanamide (18b). Compound was prepared according to the procedure for **6m**. Pale yellow solid, 134 mg, 37% yield. ^{1}H NMR (500 MHz, CDCl$_3$) δ 8.63 (d, J = 5.7 Hz, 2H), 7.69 (dd, J = 5.8, 3.8 Hz, 1H), 7.30 (dd, J = 8.0, 4.8 Hz, 1H), 7.25−7.14 (m, 2H), 7.07 (s, 1H), 7.02 (s, 1H), 6.22 (d, J = 8.0 Hz, 1H), 6.14 (s, 1H), 4.06−3.86 (m, 1H), 2.35 (s, 3H), 2.32 (s, 3H), 2.13−1.94 (m, 3H), 1.88−1.68 (m, 2H), 1.55−1.40 (m, 2H), 1.37−1.16 (m, 3H). ^{13}C NMR (126 MHz, CDCl$_3$) δ 197.36, 168.01, 166.76, 150.59, 149.11, 139.55, 138.91, 136.94, 130.81, 130.27, 130.10, 129.10, 127.29, 123.56, 62.46, 49.25, 32.88, 32.84, 27.84, 25.51, 24.88, 24.81, 21.22. HRMS (ESI/Q-TOF) m/z: [M + Na]$^+$ calculated for C$_{23}$H$_{27}$N$_3$O$_3$ 416.1945; found 416.1952.

N-(2-(cyclohexylamino)-2-oxo-1-(pyridin-3-yl)ethyl)-N-(4-methoxyphenyl)but-2-ynamide (13k). Compound was made and purified using general procedure A, grey solid 83% yield, 302 mg. ^{1}H NMR (500 MHz, CDCl$_3$) δ 8.50 (dd, J = 4.8, 1.7 Hz, 1H), 8.45 (d, J = 2.3 Hz, 1H), 7.48 (d, J = 8.0 Hz, 1H), 7.12 (ddd, J = 8.0, 4.9, 0.9 Hz, 1H), 6.98 (s, 2H), 6.79−6.70 (m, 2H), 6.10 (s, 1H), 6.00 (d, J = 8.0 Hz, 1H), 3.88−3.81 (m, 1H), 3.79 (s, 3H), 1.94−1.84 (m, 2H), 1.74 (s, 4H), 1.61 (s, 1H), 1.42−1.11 (m, 6H). ^{13}C NMR (126 MHz, CDCl$_3$) δ 167.75, 159.81, 155.97, 151.57, 149.93, 138.74, 132.10, 130.52, 123.44, 114.20, 92.59, 61.98, 55.74, 49.28, 33.21, 33.14, 25.85, 25.10, 4.39. HRMS (ESI/Q-TOF) m/z: [M + H]$^+$ calculated for C$_{24}$H$_{28}$N$_3$O$_3$ 406.21252; found 406.21250.

N-(2-(cyclohexylamino)-2-oxo-1-(pyridin-3-yl)ethyl)but-2-

ynamide (13l). Compound was made and purified using general procedure C, white solid 57% yield, 153 mg. ^{1}H NMR (500 MHz, CDCl$_3$) δ 8.58 (dd, J = 2.4, 0.9 Hz, 1H), 8.50 (dd, J = 4.8, 1.6 Hz, 1H), 7.77−7.72 (m, 1H), 7.62 (d, J = 7.5 Hz, 1H), 7.32−7.20 (m, 2H), 5.65 (d, J = 7.5 Hz, 1H), 3.74−3.63 (m, 1H), 1.93 (s, 3H), 1.75−1.64 (m, 3H), 1.63−1.52 (m, 2H), 1.36−1.16 (m, 2H), 1.14−0.98 (m, 3H). ^{13}C NMR (126 MHz, CDCl$_3$) δ 167.88, 153.20, 149.46, 148.97, 135.07, 134.31, 124.12, 85.46, 74.64, 54.99, 49.14, 32.84, 32.68, 25.70, 25.02, 24.90, 3.98.

N-(3-acetamidophenyl)-N-(2-(cyclohexylamino)-2-oxo-1-(pyridin-3-yl)ethyl)but-2-ynamide (13m). Compound was made and purified using general procedure A, white solid 82% yield, 320 mg. ^{1}H NMR (500 MHz, CDCl$_3$) δ 8.42 (s, 2H), 7.96 (s, 1H), 7.83−7.76 (m, 1H), 7.49 (dt, J = 7.9, 2.1 Hz, 2H), 7.17−7.04 (m, 2H), 6.74 (d, J = 7.8 Hz, 1H), 6.34 (d, J = 8.1 Hz, 1H), 6.03 (s, 1H), 3.78−3.68 (m, 1H), 2.13 (s, 3H), 1.92 (d, J = 12.2 Hz, 1H), 1.82 (s, 1H), 1.69 (s, 3H), 1.63−1.51 (m, 2H), 1.33−1.22 (m, 2H), 1.11 (dtd, J = 35.2, 11.2, 3.6 Hz, 3H). ^{13}C NMR (126 MHz, CDCl$_3$) δ 168.57, 167.51, 155.06, 151.09, 149.64, 139.27, 138.81, 137.84, 130.10, 129.22, 125.98, 123.24, 121.38, 119.91, 92.30, 77.29, 77.04, 76.79, 73.69, 62.29, 49.04, 32.69, 25.40, 24.76, 24.71, 24.54, 3.99. HRMS (ESI/Q-TOF) m/z: [M + H]$^+$ calculated for C$_{25}$H$_{29}$N$_4$O$_3$ 433.22342; found 433.22345.

N-(4-acetamidophenyl)-N-(2-(cyclohexylamino)-2-oxo-1-(pyridin-3-yl)ethyl)but-2-ynamide (13n). Compound was made and purified using general procedure A, light brown solid 89% yield, 345 mg. ^{1}H NMR (500 MHz, CDCl$_3$) δ 8.48−8.44 (m, 1H), 8.41 (s, 1H), 7.50 (dt, J = 7.6, 1.9 Hz, 1H), 7.43 (d, J = 8.4 Hz, 2H), 7.14 (dd, J = 8.0, 4.8 Hz, 1H), 7.03 (d, J = 7.5 Hz, 2H), 6.24 (s, 1H), 6.09 (s, 1H), 3.81 (dp, J = 11.0, 4.0, 3.6 Hz, 1H), 2.15−2.12 (m, 3H), 2.01−1.91 (m, 1H), 1.89−1.82 (m, 1H), 1.78−1.64 (m, 4H), 1.64−1.52 (m, 1H), 1.45−1.05 (m, 6H). ^{13}C NMR (126 MHz, CDCl$_3$) δ 168.74, 167.40, 155.36, 151.06, 149.50, 138.70, 138.23, 134.05, 131.10, 130.16, 123.29, 119.30, 92.50, 77.30, 77.05, 76.79, 73.67, 61.88, 49.01, 32.77, 32.71, 25.42, 24.75, 24.70, 24.57, 4.00. HRMS (ESI/Q-TOF) m/z: [M + H]$^+$ calculated for C$_{25}$H$_{29}$N$_4$O$_3$ 433.22342; found 433.22352.

N-(2-(cyclohexylamino)-2-oxo-1-(pyridin-3-yl)ethyl)-N-(4-fluorophenyl)but-2-ynamide (13o). Compound was made and purified using general procedure A, light brown solid 88% yield, 311 mg. ^{1}H NMR (500 MHz, CDCl$_3$) δ 8.49 (dd, J = 4.8, 1.6 Hz, 1H), 8.44 (d, J = 2.3 Hz, 1H), 7.46 (dt, J = 8.0, 2.0 Hz, 1H), 7.11 (dt, J = 10.7, 5.3 Hz, 2H), 6.91 (t, J = 8.6 Hz, 2H), 6.10 (s, 1H), 6.02 (s, 1H), 3.82 (dtd, J = 10.8, 7.3, 4.0 Hz, 1H), 2.04−1.93 (m, 1H), 1.89−1.82 (m, 1H), 1.72 (s, 3H), 1.67−1.56 (m, 2H), 1.45−1.29 (m, 2H), 1.27−1.04 (m, 3H). ^{13}C NMR (126 MHz, CDCl$_3$) δ 167.24, 163.25, 161.27, 155.15, 151.13, 149.73, 138.05, 134.72, 134.69, 132.76, 132.69, 130.05, 123.21, 115.69, 115.51, 92.45, 73.58, 61.42, 49.01, 32.78, 32.72, 25.43, 24.77, 24.71, 3.89.

N-(2-(cyclohexylamino)-2-oxo-1-(pyridin-3-yl)ethyl)-N-(4-(difluoromethoxy)phenyl)but-2-ynamide (13p). Compound was made and purified using general procedure A, light brown solid 89% yield, 355 mg. ^{1}H NMR (500 MHz, CDCl$_3$) δ 8.51 (dd, J = 4.8, 1.6 Hz, 1H), 8.46 (d, J = 2.3 Hz, 1H), 7.50 (dt, J = 8.0, 2.0 Hz, 1H), 7.20−7.10 (m, 2H), 7.03−6.93 (m, 2H), 6.50 (t, J = 73.4 Hz, 1H), 6.10 (s, 1H), 5.93 (d, J = 8.1 Hz, 1H), 3.83 (dtd, J = 10.8, 7.7, 7.3, 4.0 Hz, 1H), 1.98 (s, 1H), 1.87 (dd, J = 12.1, 4.0 Hz, 1H), 1.76−1.71 (m, 4H), 1.70−1.57 (m, 2H), 1.45−1.28 (m, 2H), 1.24−1.03 (m, 3H). ^{13}C NMR (126 MHz, CDCl$_3$) δ 167.53, 155.46, 151.37, 150.03, 138.52, 132.78, 130.44, 123.65, 119.71, 115.88, 92.99, 73.95, 61.89, 49.41, 33.17, 33.11, 25.81, 25.14, 25.09, 4.30, 4.16. ^{19}F NMR (471 MHz, CDCl$_3$) δ −81.48 (d, J = 73.5 Hz). HRMS (ESI/Q-TOF) m/z: [M + H]$^+$ calculated for C$_{24}$H$_{26}$N$_3$O$_3$F$_2$ 442.19367; found 442.19361.

N-benzyl-N-(2-(cyclohexylamino)-2-oxo-1-(pyridin-3-yl)ethyl)propiolamide (13q). Pyridine-3-carboxaldehyde (0.09 mL, 0.93 mmol) and benzylamine (0.10 mL, 0.93 mmol) were stirred in MeOH (3.7 mL) and for 30 min at rt. 2-Butynoic acid (78.5 mg,

0.93 mmol) and cyclohexyl isocyanide (0.10 mL, 0.84 mmol) were added and the solution stirred at rt overnight. The reaction was concentrated in vacuo and the crude product was dissolved in EtOAc washed with water and brine. The resulting aqueous phases were extracted three times for residual compound. The combined organic phases were washed with brine and dried over Na_2SO_4. The crude product was purified using column chromatography with a gradient of mixture of (MeOH + 1% NH_4OH) and DCM (0% → 5%). The reaction was further purified using column chromatography with a gradient of EtOAc in hexanes (0% → 100%). White powder (114 mg, 35% yield). *Rf* (5% (MeOH + 1% NH_4OH) in DCM) = 0.39. ^{1}H NMR (500 MHz, CDCl$_3$) δ 8.57−8.49 (m, 0.4H), 8.43 (t, J = 2.9 Hz, 1.6H), 7.75 (dt, J = 8.1, 1.9 Hz, 0.8H), 7.64 (d, J = 7.9 Hz, 0.2H), 7.25−7.16 (m, 3H), 7.11 (dd, J = 7.4, 2.0 Hz, 1.4H), 7.03 (dd, J = 6.7, 2.8 Hz, 0.3H), 6.14 (s, 0.3H), 6.02 (d, J = 8.0 Hz, 0.7H), 5.73 (d, J = 8.1 Hz, 0.3H), 5.64 (s, 0.7H), 5.06 (d, J = 16.2 Hz, 0.7H), 4.79 (d, J = 16.2 Hz, 0.7H), 4.58 (d, J = 15.3 Hz, 0.3H), 4.52 (d, J = 15.3 Hz, 0.3H), 3.75−3.64 (m, 1H), 2.04 (d, J = 9.0 Hz, 0.7H), 1.98 (s, 2.1H), 1.85−1.77 (m, 2H), 1.71−1.52 (m, 4H), 1.37−1.23 (m, 2H), 1.21−0.98 (m, 2H). ^{13}C NMR (126 MHz, CDCl$_3$, *: major isomer) δ 167.05, 166.83*, 156.12, 150.98*, 150.72, 149.83*, 149.60, 137.46*, 137.30*, 137.19, 136.84, 130.54*, 130.44, 128.92*, 128.67, 128.25*, 127.75*, 127.70, 127.43, 123.43*, 123.26, 92.78, 91.19, 73.52, 73.15, 64.66*, 60.61, 52.48, 48.81, 47.03*, 32.78, 32.72, 32.66, 25.57, 25.46, 24.80, 24.76, 4.39*, 4.27. HRMS (ESI/Q-TOF) *m/z*: [M+Na]$^+$ calculated for $C_{24}H_{27}N_3NaO_2$ 412.1995, found 412.1995.

5.1.1. *In vitro assays*

Protein production. The DNA sequence encoding 3CL SARS-CoV-2 protease (GI: 1831502838) was synthetized (optimized for expression in *Escherichia coli*) and cloned into a pGEX-6-1 vector between BamHI and XhoI restriction sites, by GenScript (Piscataway, NJ, USA), based on Zhang et al. methodology. [25]. The protein sequence was preceded by an N-terminal GST sequence and the HRV3C PreScission protease site (SAVLQ↓SGFRK). Autocleavage activity of the enzyme leaves its *N*-terminus starting with the serine after the QS cleavage site (Q↓S). At the C-terminus, based on Xue et al. [73], and Zhang et al. [25], the protein was designed to end at the last glutamine comprising the natural C-terminus of the enzyme, followed by a glycine, a proline residue and six histidine residues. The protein this has a 6-His purification tag that can be cleaved using a modified-PreScission protease approach (SGVTFQ↓GP).

E. coli BL21 (DE3) cells were transformed using the plasmid described above and the CaCl$_2$ method [74] and colonies were selected on LB-agar-ampicillin plates. A single colony was picked and grew over night in LB media and then used to inoculate a 400 mL LB culture. This was grown at 37 °C, 250 rpm, until an optical density at 600 nm of 0.7 (O.D.600) was reached and then induced for 18 h at 16 °C (250 rpm) by adding 0.25 mM IPTG. The bacterial pellet was collected after 4000 rpm centrifugation and resuspended in 30 mL of 50 mM Tris-HCl pH 8.0, 150 mM NaCl (resuspension buffer). An Ultrasonic Cell Disruption Sonifier 450 (Branson) was used to sonicate the cells (on ice) with 6 pulses of 2 min (Output Control 7 and 50% Duty Cycle).

Buffer A (50 mM Tris-HCl pH 8.0, 150 mM NaCl, 20 mM imidazole) and Buffer B (50 mM Tris-HCl, 150 mM NaCl, 500 mM imidazole) were used for purifying 3CL^{pro} after the clarified supernatant (14,000 rpm centrifugation) was loaded into a 1 mL HisTrap FF (GE Healthcare, IL, USA). 5 mL fractions were collected by washing with single column volumes of increasing imidazole concentration (0, 5, 10, 15, 20, 25, 30, 35, 40, 45 and 50% Buffer B).

After running SDS-PAGE for confirmation (Mini-PROTEAN® TGX™ Precast Gels, Bio-Rad), two sets of fractions were pooled independently. One of them contained 3CL^{pro} with a high molecular weight contaminant (5 and 10% Buffer B) while the other contained only the pure enzyme (15, 20 and 25% buffer B). Imidazole was eliminated from pooled fractions by multiple washes with resuspension buffer using 10K cut-off Amicon® Ultra-15 Centrifugal Filter Units (Millipore Sigma, Burlington, MA, USA). Absorbance at 280 nm was recorded for the pure sample and the protein concentration was estimated to be 8.5 μM (around 0.3 g/L). Based on SDS-PAGE results, the same concentration was assumed for the other sample. These samples were aliquoted and stored at −20 Celsius degrees. In all the experiments (unless specified) the pure preparation was used. See Fig. S1 for more information.

Bulk amount of 3CL^{pro} for crystallization was purified from cell pellets resuspended in a buffer (50 mM Tris, 150 mM NaCl, 20 mM imidazole, pH 8.0). Cell lysate was subsequently centrifuged at 15,000g at 4 °C for 20 min. The supernatant was further loaded on a HisTrap HP column (Cytiva) and then purified using a second buffer (50 mM Tris, 150 mM NaCl, 500 mM imidazole, pH 8.0) on an AKTA Avant purification system (Cytiva). The fractions were pooled, the his-tag removed with Pierce HRV 3C protease (Thermo Scientific) at 4 °C for 24 h and dialyzed in buffer A with TCEP at 0.5 mM. The unlabeled protein was loaded again on a HisTrap HP column (Cytiva), the flow-through was collected and dialyzed in a third buffer (20 mM Tris, 100 mM NaCl, 0.5 mM TCEP, pH 8.0). A second step of purification was carried out on a HiTrap Q FF column using the third buffer (20 mM Tris, 100 mM NaCl, 0.5 mM TCEP, pH 8.0) The fractions were pooled and concentrated to 12 mg/mL.

Detection of inhibitors by fluorescence spectrophotometry. For all inhibition experiments, reactions were performed in 50 μL assay with 11.76 μM fluorescence substrate DABCYL-KTSAVLQSGFRKME-EDANS from BPS Biosciences (San Diego, CA, USA), which has been previously used for assaying 3CL proteases [75].

38 μL of enzyme (diluted in a 3CL^{pro} Protease Assay Buffer from BPS Bioscience supplemented with 1 mM DTT) were incubated for 30 min at room temperature with 2 μL of 1.25 mM compounds (diluted in DMSO; Sigma). In both cases, screenings (duplicates) and IC$_{50}$ experiments (duplicates and triplicates), 10 μL of diluted substrate (58.8 μM) were added and reactions monitored by following the fluorescence as a function of time (excitation at 360 nm, emission at 460 nm) using a Synergy™ H4 Hybrid Multi-Mode Microplate Reader (Winooski, VT, USA). Controls were (i) no inhibition: 2 μL of DMSO, (ii) positive inhibition: 2 μL **GC376** (500 μM, BPS Bioscience) diluted in distilled water and (iii) blank: 38 μL of the 3CL^{pro} Protease Assay Buffer with 1 mM DTT was added instead of the enzyme, together with 2 μL of DMSO. In all cases the compounds were added as DMSO solutions and their final concentration in the reactions was 50 μM. The reactions ran for at least 1 h, and the linear initial slopes of the progress curves were used to calculate the reaction initial velocity in Relative Fluorescent Units in time (RFU per minute). GraphPad software was used to determine IC$_{50}$ values.

Liquid chromatography-mass spectrometry (LC-MS). Stored-frozen protein samples were buffer exchanged with 5 mM Tris-HCl pH 8.0, 15 mM NaCl buffer using 4K cut-off Amicon® small Centrifugal Filter Units (Millipore Sigma, Burlington, MA, USA) and prepared at 0.1−0.2 mg/mL 96 μL of this solution was mixed with 4 μL of 2.5 mM **16a** or **14a**. Pure DMSO was used as a negative control. Protein samples were analyzed by LC-MS using a Dionex Ultimate 3000 UHPLC coupled to a Bruker Maxis Impact Q-TOF in positive ESI mode. Samples were separated on an Agilent PLRP-S column (1000 Å, 5 μM, 2.1 × 50 mm) heated to 80 °C at a flow rate of 0.5 ml/min using a gradient of 80% mobile phase A (0.1% formic acid in H_2O) and 20% mobile phase B (0.1% formic acid in ACN) for 2 min, ramped to 60% mobile phase A and 40% mobile phase B in 5 min, and 10% mobile phase A and 90% mobile phase B in 5 min. The data was processed and spectra deconvoluted using the Bruker DataAnalysis software version 4.2.

Isothermal Titration Calorimetry (ITC). All ITC experiments were performed on an ITC200 instrument (Malvern Panalytical Ltd, UK) in high-feedback mode with a 1s signal averaging window, a stirring rate of 750 rpm, pre-injection delay of 120 s, and a reference power of 7. A small first injection of 0.2 μL was followed by a 1.5 μL injection with a wait period of 1400 s. The sample cell contained 0.5 mg/mL of the peptide Cbz-TSAVLQSGFRK (CanPeptide, Montreal, QC, Canada) with either 16.7 μM inhibitor no inhibitor, while the injection syringe contained 54.6 μM 3CL^{pro}. All syringe and sample cell components were dissolved in 3CL^{pro} Protease Assay Buffer from BPS Bioscience.

Cathepsin L fluorescence assays: Cathepsin L activity was measured by Cathepsin L Inhibitor Screening Assay Kit (BPS Bioscience, USA). 3CL^{pro} inhibitor concentrations were tested from 0.1 to 100 μM, following the kit's instructions. E−64 protease inhibitor at 10 μM was used such as positive control. The percentage of inhibition for each molecule was calculated based on slope values versus a blank condition experiment without inhibitor. All the samples were processed in duplicate in a Synergy™ H4 Hybrid Multi-Mode Microplate Reader (Winooski, VT, USA) (excitation at 360 nm, emission at 460 nm) in 100 μL assays. 10 min of incubation at room temperature (inhibitors and enzyme).

Protein crystallization and structure solution. The enzyme was buffer exchanged into 20 mM Tris pH8, 100 mM NaCl, 1 mM DTT and concentrated to 5 mg/ml, and was then incubated with 450 μM of compound **16a** for 1 h at room temperature. Following incubation, the sample was filtered using a 0.22 μm filter and used for crystallization trials. Crystals were grown using the sitting drop method at 22 °C. 200 nL enzyme was mixed with 200 nL well solution (30% PEG2000 MME, 0.2 M Potassium thiocyanate) and allowed to equilibrate against 50 μL well solution. The crystals were cryo-protected using well solution supplemented with 20% ethylene glycol and flash frozen in liquid nitrogen. Data was collected at the Canadian Light Source CMCF-BM beamline and processed in space group C 1 2 1. The structure was solved in PHASER [76] with a previously published structure of the enzyme (6WTK) [26] as a search model. Restraints for the covalently bonded inhibitor were generated using AceDRG [77] in CCP4i2 [78], and the model was refined with REFMAC5 [79] and Coot [80].

Declaration of competing interest

The authors declare that they have no known competing financial interests or personal relationships that could have appeared to influence the work reported in this paper.

Acknowledgment

Appendix A. Supplementary data

Supplementary data to this article can be found online at https://doi.org/10.1016/j.ejmech.2021.114046.

References

[1] https://www.who.int/.
[2] https://www.ecdc.europa.eu/en/publications-data/distribution-confirmed-cases-mers-cov-place-infection-and-month-onset-march-2012.
[3] K. Schlottau, M. Rissmann, A. Graaf, J. Schön, J. Sehl, C. Wylezich, D. Höper, T.C. Mettenleiter, A. Balkema-Buschmann, T. Harder, C. Grund, D. Hoffmann, A. Breithaupt, M. Beer, SARS-CoV-2 in fruit bats, ferrets, pigs, and chickens: an experimental transmission study, Lancet Micr 1 (2020) E218−E225.
[4] Z. Shi, Z. Hu, A review of studies on animal reservoirs of the SARS coronavirus, Virus Res. 133 (2008) 74−87.
[5] E. Abdollahi, D. Champredon, J.M. Langley, A.P. Galvani, S.M. Moghadas, Temporal estimates of case-fatality rate for COVID-19 outbreaks in Canada and the United States, Can. Med. Assoc. J. 192 (2020) E666−E670.
[6] https://www.imperial.ac.uk/mrc-global-infectious-disease-analysis/news−wuhan-coronavirus/.
[7] W.H. Organization, WHO Coronavirus Disease, COVID-19) Dashboard, 2020.
[8] C. Modi, V. Böhm, S. Ferraro, G. Stein, U. Seljak, Estimating COVID-19 mortality in Italy early in the COVID-19 pandemic, Nat. Commun. 12 (2021) 2729.
[9] K. Stankiewicz, Pfizer's CEO Says Covid Vaccine Effectiveness Drops to 84% after Six Months, 2021.
[10] H. Ledford, Six months of COVID vaccines: what 1.7 billion doses have taught scientists, Nature 594 (2021) 164−167.
[11] L. Dai, G.F. Gao, Viral targets for vaccines against COVID-19, Nat. Rev. Immunol. 21 (2021) 73−82.
[12] G. Chodick, L. Tene, R.S. Rotem, T. Patalon, S. Gazit, A. Ben-Tov, C. Weil, I. Goldshtein, G. Twig, D. Cohen, K. Muhsen, The effectiveness of the two-dose BNT162b2 vaccine: analysis of real-world data, Clin. Infect. Dis. (2021).
[13] Merck Merck, Ridgeback's Molnupiravir, An Oral COVID-19 Antiviral Medicine, Receives First Authorization in the World, 2021.
[14] R. Cannalire, C. Cerchia, A.R. Beccari, F.S. Di Leva, V. Summa, Targeting SARS-CoV-2 proteases and polymerase for COVID-19 treatment: state of the art and future opportunities, J. Med. Chem. (2020).
[15] P. Zhou, X.-L. Yang, X.-G. Wang, B. Hu, L. Zhang, W. Zhang, H.-R. Si, Y. Zhu, B. Li, C.-L. Huang, H.-D. Chen, J. Chen, Y. Luo, H. Guo, R.-D. Jiang, M.-Q. Liu, Y. Chen, X.-R. Shen, X. Wang, X.-S. Zheng, K. Zhao, Q.-J. Chen, F. Deng, L.-L. Liu, B. Yan, F.-X. Zhan, Y.-Y. Wang, G.-F. Xiao, Z.-L. Shi, A pneumonia outbreak associated with a new coronavirus of probable bat origin, Nature 579 (2020) 270−273.
[16] A. Wu, Y. Peng, B. Huang, X. Ding, X. Wang, P. Niu, J. Meng, Z. Zhu, Z. Zhang, J. Wang, J. Sheng, L. Quan, Z. Xia, W. Tan, G. Cheng, T. Jiang, Genome Composition and Divergence of the Novel Coronavirus (2019-nCoV) Originating in China, Cell Host & Microbe, 2020.
[17] A.D. Rathnayake, Y. Kim, C.S. Dampalla, H.N. Nguyen, A.-R.M. Jesri, M.M. Kashipathy, G.H. Lushington, K.P. Battaile, S. Lovell, K.-O. Chang, W.C. Groutas, Structure-guided optimization of dipeptidyl inhibitors of norovirus 3CL protease, J. Med. Chem. (2020).
[18] C.-J. Kuo, J.-J. Shie, J.-M. Fang, G.-R. Yen, J.T.A. Hsu, H.-G. Liu, S.-N. Tseng, S.-C. Chang, C.-Y. Lee, S.-R. Shih, P.-H. Liang, Design, synthesis, and evaluation of 3C protease inhibitors as anti-enterovirus 71 agents, Bioorg. Med. Chem. 16 (2008) 7388−7398.
[19] P.S. Dragovich, T.J. Prins, R. Zhou, S.E. Webber, J.T. Marakovits, S.A. Fuhrman, A.K. Patick, D.A. Matthews, C.A. Lee, C.E. Ford, B.J. Burke, P.A. Rejto, T.F. Hendrickson, T. Tuntland, E.L. Brown, J.W. Meador, R.A. Ferre, J.E.V. Harr, M.B. Kosa, S.T. Worland, Structure-based design, synthesis, and biological evaluation of irreversible human Rhinovirus 3C protease inhibitors. 4. Incorporation of P1 lactam moieties as l-glutamine replacements, J. Med. Chem. 42 (1999) 1213−1224.
[20] Z. Jin, X. Du, Y. Xu, Y. Deng, M. Liu, Y. Zhao, B. Zhang, X. Li, L. Zhang, C. Peng, Y. Duan, J. Yu, L. Wang, K. Yang, F. Liu, R. Jiang, X. Yang, T. You, X. Liu, X. Yang, F. Bai, H. Liu, X. Liu, L.W. Guddat, W. Xu, G. Xiao, C. Qin, Z. Shi, H. Jiang, Z. Rao, H. Yang, Structure of Mpro from SARS-CoV-2 and discovery of its inhibitors, Nature 582 (2020) 289−293.
[21] H.-x. Su, S. Yao, W.-f. Zhao, M.-j. Li, J. Liu, W.-j. Shang, H. Xie, C.-q. Ke, H.-c. Hu, M.-n. Gao, K.-q. Yu, H. Liu, J.-s. Shen, W. Tang, L.-k. Zhang, G.-f. Xiao, L. Ni, D.-w. Wang, J.-p. Zuo, H.-l. Jiang, F. Bai, Y. Wu, Y. Ye, Y.-c. Xu, Anti-SARS-CoV-2 activities in vitro of Shuanghuanglian preparations and bioactive ingredients, Acta Pharmacol. Sin. 41 (2020) 1167−1177.
[22] D.W. Kneller, S. Galanie, G. Phillips, H.M. O'Neill, L. Coates, A. Kovalevsky, Malleability of the SARS-CoV-2 3CL Mpro active-site cavity facilitates binding of clinical antivirals, Structure 28 (2020) 1313−1320, e1313.
[23] D.W. Kneller, G. Phillips, H.M. O'Neill, R. Jedrzejczak, L. Stols, P. Langan, A. Joachimiak, L. Coates, A. Kovalevsky, Structural plasticity of SARS-CoV-2 3CL Mpro active site cavity revealed by room temperature X-ray crystallography, Nat. Commun. 11 (2020) 3202.
[24] T. Pillaiyar, M. Manickam, V. Namasivayam, Y. Hayashi, S.-H. Jung, An overview of severe acute respiratory syndrome−coronavirus (SARS-CoV) 3CL protease inhibitors: peptidomimetics and small molecule chemotherapy, J. Med. Chem. 59 (2016) 6595−6628.
[25] L. Zhang, D. Lin, X. Sun, U. Curth, C. Drosten, L. Sauerhering, S. Becker, K. Rox, R. Hilgenfeld, Crystal structure of SARS-CoV-2 main protease provides a basis for design of improved α-ketoamide inhibitors, Science 368 (2020) 409−412.
[26] W. Vuong, M.B. Khan, C. Fischer, E. Arutyunova, T. Lamer, J. Shields, H.A. Saffran, R.T. McKay, M.J. van Belkum, M.A. Joyce, H.S. Young, D.L. Tyrrell, J.C. Vederas, M.J. Lemieux, Feline coronavirus drug inhibits the main protease of SARS-CoV-2 and blocks virus replication, Nat. Commun. 11 (2020) 4282.
[28] K. Anand, J. Ziebuhr, P. Wadhwani, J.R. Mesters, R. Hilgenfeld, Coronavirus main proteinase (3CLpro) structure: basis for design of anti-SARS drugs, Science 300 (2003) 1763−1767.
[29] C. Liu, Q. Zhou, Y. Li, L.V. Garner, S.P. Watkins, L.J. Carter, J. Smoot, A.C. Gregg, A.D. Daniels, S. Jervey, D. Albaiu, Research and development on therapeutic agents and vaccines for COVID-19 and related human coronavirus diseases, ACS Cent. Sci. 6 (2020) 315−331.
[30] M. Westberg, Y. Su, X. Zou, L. Ning, B. Hurst, B. Tarbet, M.Z. Lin, Rational Design of a New Class of Protease Inhibitors for the Potential Treatment of

Coronavirus Diseases, bioRxiv, 2020, 2020.2009.2015.275891.

[31] S. Iketani, F. Forouhar, H. Liu, S.J. Hong, F.-Y. Lin, M.S. Nair, A. Zask, Y. Huang, L. Xing, B.R. Stockwell, A. Chavez, D.D. Ho, Lead compounds for the development of SARS-CoV-2 3CL protease inhibitors, Nat. Commun. 12 (2021), 2016.

[32] B. Boras, R.M. Jones, B.J. Anson, D. Arenson, L. Aschenbrenner, M.A. Bakowski, N. Beutler, J. Binder, E. Chen, H. Eng, J. Hammond, R. Hoffman, E.P. Kadar, R. Kania, E. Kimoto, M.G. Kirkpatrick, L. Lanyon, E.K. Lendy, J.R. Lillis, S.A. Luthra, C. Ma, S. Noell, R.S. Obach, M.N. O' Brien, R. O'Connor, K. Ogilvie, D. Owen, M. Pettersson, M.R. Reese, T.F. Rogers, M.I. Rossulek, J.G. Sathish, C. Steppan, M. Ticehurst, L.W. Updyke, Y. Zhu, J. Wang, A.K. Chatterjee, A.D. Mesecar, A.S. Anderson, C. Allerton, Discovery of a Novel Inhibitor of Coronavirus 3CL Protease as a Clinical Candidate for the Potential Treatment of COVID-19, bioRxiv, 2021, 2020.2009.2012.293498.

[33] R. Hoffman, R.S. Kania, M.A. Brothers, J.F. Davies, R.A. Ferre, K.S. Gajiwala, M. He, R.J. Hogan, K. Kozminski, L.Y. Li, J.W. Lockner, J. Lou, M.T. Marra, L.J.J. Mitchell, B.W. Murraya, J.A. Nieman, S. Noell, S.P. Planken, T. Rowe, K. Ryan, G.J.I. Smith, J.E. Solowiej, C.M. Steppan, B. Taggart, The discovery of ketone-based covalent inhibitors of coronavirus 3CL proteases for the potential therapeutic treatment of COVID-19, ChemRxiv (2020), https://doi.org/10.26434/chemrxiv.12631496.v1.

[34] R.L. Hoffman, R.S. Kania, M.A. Brothers, J.F. Davies, R.A. Ferre, K.S. Gajiwala, M. He, R.J. Hogan, K. Kozminski, L.Y. Li, J.W. Lockner, J. Lou, M.T. Marra, L.J. Mitchell, B.W. Murray, J.A. Nieman, S. Noell, S.P. Planken, T. Rowe, K. Ryan, G.J. Smith, J.E. Solowiej, C.M. Steppan, B. Taggart, Discovery of ketone-based covalent inhibitors of coronavirus 3CL proteases for the potential therapeutic treatment of COVID-19, J. Med. Chem. 63 (2020) 12725−12747.

[35] Study of PF-07321332 in Healthy Participants — NCT04756531, 2021.

[36] D.R. Owen, C.M.N. Allerton, A.S. Anderson, L. Aschenbrenner, M. Avery, S. Berritt, B. Boras, R.D. Cardin, A. Carlo, K.J. Coffman, A. Dantonio, L. Di, H. Eng, R. Ferre, K.S. Gajiwala, S.A. Gibson, S.E. Greasley, B.L. Hurst, E.P. Kadar, A.S. Kalgutkar, J.C. Lee, J. Lee, W. Liu, S.W. Mason, S. Noell, J.J. Novak, R.S. Obach, K. Ogilvie, N.C. Patel, M. Pettersson, D.K. Rai, M.R. Reese, M.F. Sammons, J.G. Sathish, R.S.P. Singh, C.M. Steppan, A.E. Stewart, J.B. Tuttle, L. Updyke, P.R. Verhoest, L. Wei, Q. Yang, Y. Zhu, An oral SARS-CoV-2 Mpro inhibitor clinical candidate for the treatment of COVID-19, Science, 0 eabl4784.

[37] Pfizer, Pfizer's Novel COVID-19 Oral Antiviral Treatment Candidate Reduced Risk of Hospitalization O Death by 89% in Iterim Analysis of Phase 2/3 EPIC-HR Study, 2021.

[38] B. Bai, A. Belovodskiy, M. Hena, A.S. Kandadai, M.A. Joyce, H.A. Saffran, J.A. Shields, M.B. Khan, E. Arutyunova, J. Lu, S.K. Bajwa, D. Hockman, C. Fischer, T. Lamer, W. Vuong, M.J. van Belkum, Z. Gu, F. Lin, Y. Du, J. Xu, M. Rahim, H.S. Young, J.C. Vederas, D.L. Tyrrell, M.J. Lemieux, J.A. Nieman, Peptidomimetic α-acyloxymethylketone warheads with six-membered lactam P1 glutamine mimic: SARS-CoV-2 3CL protease inhibition, coronavirus antiviral activity, and in vitro biological stability, J. Med. Chem. (2021).

[39] B. Bai, E. Arutyunova, M.B. Khan, J. Lu, M.A. Joyce, H.A. Saffran, J.A. Shields, A.S. Kandadai, A. Belovodskiy, M. Hena, W. Vuong, T. Lamer, H.S. Young, J.C. Vederas, D.L. Tyrrell, M.J. Lemieux, J.A. Nieman, Peptidomimetic nitrile warheads as SARS-CoV-2 3CL protease inhibitors, RSC Med. Chem. 12 (2021) 1722−1730.

[40] L. Zhang, D. Lin, Y. Kusov, Y. Nian, Q. Ma, J. Wang, A. von Brunn, P. Leyssen, K. Lanko, J. Neyts, A. de Wilde, E.J. Snijder, H. Liu, R. Hilgenfeld, α-Ketoamides as broad-spectrum inhibitors of coronavirus and enterovirus replication: structure-based design, synthesis, and activity assessment, J. Med. Chem. 63 (2020) 4562−4578.

[41] Y. Kim, H. Liu, A.C. Galasiti Kankanamalage, S. Weerasekara, D.H. Hua, W.C. Groutas, K.-O. Chang, N.C. Pedersen, Reversal of the progression of fatal coronavirus infection in cats by a broad-spectrum coronavirus protease inhibitor, PLoS Pathog. 12 (2016), e1005531.

[42] W. Vuong, C. Fischer, M.B. Khan, M.J. van Belkum, T. Lamer, K.D. Willoughby, J. Lu, E. Arutyunova, M.A. Joyce, H.A. Saffran, J.A. Shields, H.S. Young, J.A. Nieman, D.L. Tyrrell, M.J. Lemieux, J.C. Vederas, Improved SARS-CoV-2 Mpro inhibitors based on feline antiviral drug GC376: structural enhancements, increased solubility, and micellar studies, Eur. J. Med. Chem. 222 (2021) 113584.

[43] L.-R. Chen, Y.-C. Wang, Y.W. Lin, S.-Y. Chou, S.-F. Chen, L.T. Liu, Y.-T. Wu, C.-J. Kuo, T.S.-S. Chen, S.-H. Juang, Synthesis and evaluation of isatin derivatives as effective SARS coronavirus 3CL protease inhibitors, Bioorg. Med. Chem. Lett 15 (2005) 3058−3062.

[44] J. Zhang, C. Huitema, C. Niu, J. Yin, M.N.G. James, L.D. Eltis, J.C. Vederas, Aryl methylene ketones and fluorinated methylene ketones as reversible inhibitors for severe acute respiratory syndrome (SARS) 3C-like proteinase, Bioorg. Chem. 36 (2008) 229−240.

[45] C.-H. Zhang, E.A. Stone, M. Deshmukh, J.A. Ippolito, M.M. Ghahremanpour, J. Tirado-Rives, K.A. Spasov, S. Zhang, Y. Takeo, S.N. Kudalkar, Z. Liang, F. Isaacs, B. Lindenbach, S.J. Miller, K.S. Anderson, W.L. Jorgensen, Potent noncovalent inhibitors of the main protease of SARS-CoV-2 from molecular sculpting of the drug Perampanel guided by free energy perturbation calculations, ACS Cent. Sci. (2021).

[46] N. Drayman, K.A. Jones, S.-A. Azizi, H.M. Froggatt, K. Tan, N.I. Maltseva, S. Chen, V. Nicolaescu, S. Dvorkin, K. Furlong, R.S. Kathayat, M.R. Firpo, V. Mastrodomenico, E.A. Bruce, M.M. Schmidt, R. Jedrzejczak, M.Á. Muñoz-Alía, B. Schuster, V. Nair, J.W. Botten, C.B. Brooke, S.C. Baker, B.C. Mounce, N.S. Heaton, B.C. Dickinson, A. Jaochimiak, G. Randall, S. Tay, Drug Repurposing Screen Identifies Masitinib as a 3CLpro Inhibitor that Blocks

[47] Replication of SARS-CoV-2 in Vitro, bioRxiv, 2020, 2020.2008.2031.274639.

[47] W. Zhu, M. Xu, C.Z. Chen, H. Guo, M. Shen, X. Hu, P. Shinn, C. Klumpp-Thomas, S.G. Michael, W. Zheng, Identification of SARS-CoV-2 3CL protease inhibitors by a quantitative high-throughput screening, ACS Pharmacol. Transl. Sci. (2020).

[48] S. De Cesco, J. Kurian, C. Dufresne, A. Mittermaier, N. Moitessier, Covalent inhibitors design and discovery, Eur. J. Med. Chem. 138 (2017) 96−114.

[49] S. Zhou, E. Chan, W. Duan, M. Huang, Y.Z. Chen, Drug Bioactivation, Covalent Binding to Target Proteins and Toxicity Relevance, Drug Metab. Rev., 2005, pp. 41−213.

[50] L. Guterman, Covalent drugs form long-lived ties, C&EN 89 (2011) 19−26.

[51] B. Tang, F. He, D. Liu, M. Fang, Z. Wu, D. Xu, AI-aided Design of Novel Targeted Covalent Inhibitors against SARS-CoV-2, bioRxiv, 2020, 2020.2003.2003.972133.

[52] D.D. Nguyen, K. Gao, J. Chen, R. Wang, G.-W. Wei, Potentially Highly Potent Drugs for 2019-nCoV, bioRxiv, 2020, 2020.2002.2005.936013.

[53] R. Roy, M.F. Sk, N.A. Jonniya, S. Poddar, P. Kar, Finding Potent Inhibitors against SARS-CoV-2 Main Protease through Virtual Screening, ADMET, and Molecular Dynamic Simulation Studies, ChemRxiv, Preprint, 2020.

[54] G. Mariaule, S. De Cesco, F. Airaghi, J. Kurian, P. Schiavini, S. Rocheleau, I. Huskić, K. Auclair, A. Mittermaier, N. Moitessier, 3-Oxo-hexahydro-1H-isoindole-4-carboxylic acid as a drug chiral bicyclic scaffold: structure-based design and preparation of conformationally constrained covalent and noncovalent prolyl oligopeptidase inhibitors, J. Med. Chem. 59 (2016) 4221−4234.

[55] J. Plescia, C. Dufresne, N. Janmamode, A.S. Wahba, A.K. Mittermaier, N. Moitessier, Discovery of covalent prolyl oligopeptidase boronic ester inhibitors, Eur. J. Med. Chem. 185 (2020) 111783.

[56] J. Jacobs, V. Grum-Tokars, Y. Zhou, M. Turlington, S.A. Saldanha, P. Chase, A. Eggler, E.S. Dawson, Y.M. Baez-Santos, S. Tomar, A.M. Mielech, S.C. Baker, C.W. Lindsley, P. Hodder, A. Mesecar, S.R. Stauffer, Discovery, synthesis, and structure-based optimization of a series of N-(tert-Butyl)-2-(N-arylamido)-2-(pyridin-3-yl) acetamides (ML188) as potent noncovalent small molecule inhibitors of the severe acute respiratory syndrome coronavirus (SARS-CoV) 3CL protease, J. Med. Chem. 56 (2013) 534−546.

[57] D. Zaidman, P. Gehrtz, M. Filep, D. Fearon, J. Prilusky, S. Duberstein, G. Cohen, D. Owen, E. Resnick, C. Strain-Damerell, P. Lukacik, H. Barr, M.A. Walsh, F. von Delft, N. London, An Automatic Pipeline for the Design of Irreversible Derivatives Identifies a Potent SARS-CoV-2 Mpro Inhibitor, bioRxiv, 2020, 2020.2009.2021.299776.

[58] A.D. Mesecar, Structure of COVID-19 Main Protease Bound to Potent Broad-Spectrum Non-covalent Inhibitor X77, 2020, https://doi.org/10.2210/pdb2216W2263/pdb.

[59] N. Moitessier, J. Pottel, E. Therrien, P. Englebienne, Z. Liu, A. Tomberg, C.R. Corbeil, Medicinal chemistry projects requiring imaginative structure-based drug design methods, Acc. Chem. Res. 49 (2016) 1646−1657.

[60] D. Behnke, R. Taube, K. Illgen, S. Nerdinger, E. Herdtweck, Substituted 2-(Cyanomethyl-amino)-acetamides by a novel three-component reaction, Synlett (2004) 688−692, 2004.

[61] S. Gedey, J. Van der Eycken, F. Fülöp, Liquid-phase combinatorial synthesis of alicyclic β-lactams via Ugi four-component reaction, Org. Lett. 4 (2002) 1967−1969.

[62] K.P. Dhake, P.J. Tambade, R.S. Singhal, B.M. Bhanage, An efficient, catalyst- and solvent-freeN-formylation of aromatic and aliphatic amines, Green Chem. Lett. Rev. 4 (2011) 151−157.

[63] P. Patil, M. Ahmadian-Moghaddam, A. Dömling, Isocyanide 2.0, Green Chem. 22 (2020) 6902−6911.

[64] S.E. St John, A.D. Mesecar, Broad Spectrum Non-covalent Coronavirus Protease Inhibitors, USA, 2018.

[65] L. Petri, A. Egyed, D. Bajusz, T. Imre, A. Hetényi, T. Martinek, P. Ábrányi-Balogh, G.M. Keserű, An electrophilic warhead library for mapping the reactivity and accessibility of tractable cysteines in protein kinases, Eur. J. Med. Chem. 207 (2020) 112836.

[66] M. Turlington, A. Chun, S. Tomar, A. Eggler, V. Grum-Tokars, J. Jacobs, J.S. Daniels, E. Dawson, A. Saldanha, P. Chase, Y.M. Baez-Santos, C.W. Lindsley, P. Hodder, A.D. Mesecar, S.R. Stauffer, Discovery of N-(benzo[1,2,3]triazol-1-yl)-N-(benzyl)acetamido)phenyl) carboxamides as severe acute respiratory syndrome coronavirus (SARS-CoV) 3CLpro inhibitors: identification of ML300 and noncovalent nanomolar inhibitors with an induced-fit binding, Bioorg. Med. Chem. Lett 23 (2013) 6172−6177.

[67] J.M. Di Trani, S. De Cesco, R. O'Leary, J. Plescia, C.J. do Nascimento, N. Moitessier, A.K. Mittermaier, Rapid measurement of inhibitor binding kinetics by isothermal titration calorimetry, Nat. Commun. 9 (2018) 893.

[68] P.R. Bevington, D.K. Robinson, Data Reduction and ErrorAnalysis for the Physical Sciences, WCB/McGraw-Hill, New York, 1992.

[69] N. Kitamura, M.D. Sacco, C. Ma, Y. Hu, J.A. Townsend, X. Meng, F. Zhang, X. Zhang, M. Ba, T. Szeto, A. Kukuljac, M.T. Marty, D. Schultz, S. Cherry, Y. Xiang, Y. Chen, J. Wang, Expedited approach toward the rational design of noncovalent SARS-CoV-2 main protease inhibitors, J. Med. Chem. (2021).

[70] K. Steuten, H. Kim, J.C. Widen, B.M. Babin, O. Onguka, S. Lovell, O. Bolgi, B. Cerikan, C.J. Neufeldt, M. Cortese, R.K. Muir, J.M. Bennett, R. Geiss-Friedlander, C. Peters, R. Bartenschlager, M. Bogyo, Challenges for targeting SARS-CoV-2 proteases as a therapeutic strategy for COVID-19, ACS Infect. Dis. (2021).

[71] M.-M. Zhao, W.-L. Yang, F.-Y. Yang, L. Zhang, W.-J. Huang, W. Hou, C.-F. Fan, R.-H. Jin, Y.-M. Feng, Y.-C. Wang, J.-K. Yang, Cathepsin L plays a key role in SARS-CoV-2 infection in humans and humanized mice and is a promising

target for new drug development, Signal Transduct. Target. Ther. 6 (2021) 134.

[72] V.O. Rogachev, P. Metz, Thermal and high pressure intramolecular Diels−Alder reaction of vinylsulfonamides, Nat. Protoc. 1 (2006) 3076−3087.

[73] X. Xue, H. Yang, W. Shen, Q. Zhao, J. Li, K. Yang, C. Chen, Y. Jin, M. Bartlam, Z. Rao, Production of authentic SARS-CoV Mpro with enhanced activity: application as a novel tag-cleavage endopeptidase for protein overproduction, J. Mol. Biol. 366 (2007) 965−975.

[74] D. Hanahan, Studies on transformation of Escherichia coli with plasmids, J. Mol. Biol. 166 (1983) 557−580.

[75] S. Chen, L.-l. Chen, H.-b. Luo, T. Sun, J. Chen, F. Ye, J.-h. Cai, J.-k. Shen, X. Shen, H.-l. Jiang, Enzymatic activity characterization of SARS coronavirus 3C-like protease by fluorescence resonance energy transfer technique, Acta Pharmacol. Sin. 26 (2005) 99−106.

[76] A.J. McCoy, R.W. Grosse-Kunstleve, P.D. Adams, M.D. Winn, L.C. Storoni, R.J. Read, Phaser crystallographic software, J. Appl. Crystallogr. 40 (2007)

[77] F. Long, R.A. Nicholls, P. Emsley, S. Graæulis, A. Merkys, A. Vaitkus, G.N. Murshudov, Validation and extraction of molecular-geometry information from small-molecule databases, Acta Crystallogr. D Struct. Biol. 73 (2017) 103−111.

[78] L. Potterton, J. Agirre, C. Ballard, K. Cowtan, E. Dodson, P.R. Evans, H.T. Jenkins, R. Keegan, E. Krissinel, K. Stevenson, A. Lebedev, S.J. McNicholas, R.A. Nicholls, M. Noble, N.S. Pannu, C. Roth, G. Sheldrick, P. Skubak, J. Turkenburg, V. Uski, F. von Delft, D. Waterman, K. Wilson, M. Winn, M. Wojdyr, CCP4i2: the new graphical user interface to the CCP4 program suite, Acta Crystallogr. D Struct. Biol. 74 (2018) 68−84.

[79] P. Skubák, G.N. Murshudov, N.S. Pannu, Direct incorporation of experimental phase information in model refinement, Acta Crystallogr. D Biol. Crystallogr. 60 (2004) 2196−2201.

[80] P. Emsley, K. Cotwan, Coot: model-building tools for molecular graphics, Acta Crystallogr. D Biol. Crystallogr. 60 (2004) 2126−2132.

658−674.